

See discussions, stats, and author profiles for this publication at: <https://www.researchgate.net/publication/355955587>

Past Antarctic ice sheet dynamics (PAIS) and implications for future sea-level change

Chapter · January 2022

DOI: 10.1016/B978-0-12-819109-5.00010-4

CITATIONS

13

READS

450

16 authors, including:



Florence Colleoni

National Institute of Oceanography and Applied Geophysics - OGS

82 PUBLICATIONS 1,065 CITATIONS

SEE PROFILE



Laura De Santis

National Institute of Oceanography and Applied Geophysics - OGS

151 PUBLICATIONS 2,269 CITATIONS

SEE PROFILE



Carlota Escutia

Spanish National Research Council

543 PUBLICATIONS 4,554 CITATIONS

SEE PROFILE



Paolo Stocchi

Italian National Research Council

58 PUBLICATIONS 1,420 CITATIONS

SEE PROFILE

Past Antarctic Ice Sheet (PAIS) dynamics and implications for future sea-level change

Florence Colleoni, Laura De Santis, Tim Naish, Rob DeConto, Carlota Escutia, Paolo Stocchi, Gabriel Uenzelmann-Neben, Katharina Hochmuth, Claus-Dieter Hillenbrand, Tina, van De Flierdt, Lara Perez, German Leitchenkov, Francesca Sangiorgi, Stewart Jamieson, Mike Bentley, David Wilson, and the PAIS community ([see list of co-authors before the references](#))

The legacy of the Scientific Committee on Antarctic Research’s (SCAR) PAIS strategic research programme includes not only breakthrough scientific discoveries, but it is also the story of a long-standing deep collaboration amongst different multi-disciplinary researchers from many nations, to share scientific infrastructure and data, facilities, and numerical models, in order to address high priority questions regarding the evolution and behaviour of the Antarctic ice sheets (AIS). The PAIS research philosophy is based on data-data and data-model integration and intercomparison, and the development of “ice-to-abys” data transects and paleo-environmental, extending from the ice sheet interior to the deep sea. PAIS strives to improve understanding of AIS dynamics and to reduce uncertainty in model simulations of future ice loss and global sea level change, by studying warm periods of the geological past that are relevant to future climate scenarios. The multi-disciplinary approach fostered by PAIS represents its greatest strength. Eight years after the start of this program, PAIS achievements have been high-profile and impactful, both in terms of field campaigns that collected unique data sets and samples, and in terms of scientific advances concerning past AIS dynamics, that have measurably improved understanding of ice sheet sensitivity in response to global warming. Here, we provide an overview and synthesis of the new knowledge generated by the PAIS Programme and its implications for anticipating and managing the impacts of global sea-level rise.

1. Research focus of the PAIS programme

Ice sheet and sea-level reconstructions from the past “warmer-than-present” climates of the last 34 million years provide powerful insights into the long-term response of the polar ice sheets to climate changes projected for the twenty-first century. Proximal geological evidence shows the onset of large-scale Antarctic glaciations occurred around the Eocene/Oligocene Transition at approximately 34 Ma (EOT, e.g. **Barrett et al., 1989; Hambrey et al., 1991; Coxall et al., 2005; Escutia et al., 2011; Passchier et al., 2013; Galeotti et al., 2016; Passchier et al., 2016**). Since then, AIS evolution and variability, recorded in the direct geological archives have been widely compared with benthic oxygen isotope proxy record of deep-water temperature and global ice volume from far-field deep ocean locations (e.g. **Zachos et al., 2001; De Vleeschouwer et al., 2017**). Together, they reveal fluctuations in ice volume and extent that can be explained by changes in atmospheric CO₂ and astronomical forcing (**Naish et al., 2001; Pälike et al., 2006; Naish et al., 2009a; Patterson et al., 2014; Hansen et al., 2015; Galeotti et al., 2016; Levy et al., 2019**). Looking at the broad picture, the EOT really marked the transition into an ice-house and cool-house world (**Miller et al., 1991; 2020b; Westerhold et al., 2020**). As the initial cryosphere evolved, only one pole, the South Pole, hosted a continental-size ice sheet. Geological evidence from the Arctic revealed that small ice-sheets or ice caps may have formed in the Northern high latitudes as early as the Eocene (e.g. **Eldrett et al 2007; Tripathi & Darby, 2018**). Then, along with the gradual decrease in atmospheric CO₂ (**Figure 1a**), Greenland glaciated from the Late Miocene, rapidly followed by episodic and extensive glaciations of most of the high-latitude Arctic margins, after the onset of Northern Hemisphere glaciations 2.7 Ma (e.g. **Thiede et al., 2011**).

54 During the past 34 million years, changes in global climate and polar ice volume have been
55 paced by orbital forcing – the Milankovitch cycles. These regular glacial-interglacial cycles,
56 which are amplified by internal Earth system feedbacks, occur on a background of secular
57 change over millions of years driven by global plate tectonics and the carbon cycle (**Figure 1**).
58 Rapid stepwise transitions between climate states (e.g. EOT) correspond to thresholds in the
59 Earth system often linked to a combination of tectonic reorganisation, atmospheric
60 greenhouse gas composition and extreme astronomical forcing (**Zachos et al., 2001, 2008;**
61 **Levy et al., 2019**). Our knowledge of the evolution of the AIS and its influence on global
62 climate is now widely documented by proximal ice and sediment core records (e.g. **EPICA**
63 **Community Members, 2006; Bereiter et al., 2015; Barrett, 2007; McKay et al., 2016;**
64 **Escutia et al., 2019; Levy et al., 2019**).

66 The circum-Antarctic seismic stratigraphic records of the continental margins reveal erosive
67 unconformities indicative of at least six main periods of massive Antarctic ice sheet (AIS)
68 advances (e.g. **Steinhauff and Webb 1987; Larter et al., 1997; Cooper et al., 1999, 2011;**
69 **Brancolini et al., 1995a, 1995b; De Santis et al., 1999; Donda et al., 2007; Kristoffersen**
70 **and Jokat, 2008; Bart & DeSantis, 2012; Gohl et al., 2013; Lindeque et al. 2016; Gulick**
71 **et al., 2017**). Not all the unconformities have been dated but **Hochmuth et al., (2019, 2020)**
72 recently provided the first attempt of pan-Antarctic correlation of the various regional seismic
73 unconformities (**Figure 1b**). These seismic unconformities likely correspond to: early Antarctic
74 glaciations after the EOT (e.g. **Galeotti et al., 2016**), a transient glaciation at Oligocene-
75 Miocene boundary ~23-21 Ma (e.g. **Naish et al., 2001**; summarised in **Wilson and Luyendyk,**
76 **2009**), ice sheet re-advance at the end of the Mid-Miocene Climatic Optimum (MCO) about
77 15.8-14.2 Ma (e.g. **Levy et al., 2016**), the cooling and expansion of the East Antarctic Ice
78 Sheet (EAIS) at the Middle Miocene Climate Transition (MMCT) ~13.8 Ma (e.g. **Lewis et al.,**
79 **2007; 2008; Levy et al., 2016; Pierce et al., 2017**), cooling after a period of warmth known
80 as the Late Miocene Cooling ~ 8 - 5 Ma (LMC) (**McKay et al., 2009; Herbert et al., 2016;**
81 **Gulick et al., 2017**), and cooling and expansion of marine-based ice during the Plio-
82 Pleistocene Transition (PPT) 3-2.5 Ma (**Naish et al., 2009a; McKay et al., 2012a; Patterson**
83 **et al., 2014**) and possibly to the Mid-Pleistocene Transition ~1 Ma (e.g. **O'Brien et al., 2007**).
84 These periods evidenced by positive excursions in the deep sea benthic $\delta^{18}\text{O}$ isotope records
85 (**Figure 1a**) correspond to episodes of global cooling and ice volume growth periods, generally
86 associated with a decline in atmospheric CO_2 below a threshold (**Figure 1b**) for triggering the
87 expansion of terrestrial or marine-based ice and/or the onset of perennial sea-ice.

89 Between these cooling periods, multi-proxy global climatic reconstructions and proximal
90 Antarctic geological climate and ice sheet reconstructions provide evidence for intense and
91 brief warm periods during which:

- 92 - atmospheric CO_2 levels, surface temperatures and global sea level rose well above
93 present-day levels during the MCO (17-15 Ma) and the middle Pliocene Warm Period
94 (mPWP, 3.3 -3 Ma) (e.g. **Miller et al., 2020b** for a review); both periods were
95 characterised by CO_2 concentrations higher than 400 ppm and up to 800ppm for some
96 specific intervals of the MCO (see **Figure 1a** and references therein).
- 97 - atmospheric CO_2 levels were near pre-industrial levels, i.e. lower than 300 ppm, but
98 were associated with warmer global surface temperatures and higher sea-levels than
99 today during the “super interglacials” of the Pleistocene. This was likely driven by
100 astronomical forcing. Examples include marine isotope stage (MIS) 31 (1.081-1.062
101 Ma), and specific warm Late Pleistocene interglacials such as MIS 11 (425-395 ka)
102 and MIS 5e (130-116 ka) (e.g. **Dutton et al., 2015; Miller et al., 2020b**).

104 These past warm periods are policy-relevant as they provide accessible examples of how the
105 AIS responded to warmer-than-present global temperatures, comparable to those projected
106 for the coming decades to centuries (**IPCC AR5, 2013; IPCC SCROCC, 2019**). However,
107 using these past warm periods to inform our understanding of the AIS sensitivity under
108 different atmospheric CO_2 levels remains a challenge, in part because Earth system boundary

109 conditions were subtly different than today, and the duration and intensity of these past warm
110 periods was highly variable (e.g. **Dutton et al., 2015; DeConto and Pollard, 2016; Colleoni**
111 **et al., 2018a; Bracegirdle et al., 2019; Noble et al., 2020**).

112
113 For example, the duration of those past warm periods differs, from about ~ 2 million years for
114 the MCO, approximately 300 thousand years for the mPWP to a few millennia for some
115 Pleistocene interglacials. Thus, an approach focusing on specific MCO and mPWP glacial-
116 interglacial cycles and interglacials (with similarities to our present interglacial) is being
117 developed. For example, the Pliocene Model Intercomparison Project community is focussing
118 its ongoing mPWP model-data comparison on the M2-KM5c (3.264-3.205 Ma) and KM5c-KM2
119 (3.205-3.130 Ma) intervals (**Figure 1b**) (**Haywood et al., 2016**). By using more appropriate
120 forcing and boundary conditions for climate model simulations, discrepancies between models
121 and data generally decrease (e.g. **Otto-Bliesner et al, 2017**).

122
123 In most simulations of future ice sheets evolution, model projections typically extend only until
124 the policy horizon of 2100 CE (Common Era). However, some ice sheet models have run
125 projections out as far as 2500 CE (e.g. **Golledge et al., 2015, DeConto and Pollard, 2016;**
126 **Clark et al., 2016**). The recent IPCC special report on “**Ocean and Cryosphere in a**
127 **Changing Climate**” (**IPCC SROCC, 2019**) utilises these projections and the results of a
128 structured expert judgement approach (**Bamber et al., 2019**) to present projections to 2300
129 CE, that to some extent account for the long-term thermo-dynamical response of the
130 Greenland and Antarctic ice sheets and related instabilities (e.g. **Golledge et al., 2015,**
131 **DeConto and Pollard, 2016**). Paleoclimatic changes are often considered at timescales of
132 tens of millennia to millennia and, in few archives, at sub-millennial timescale. At such
133 timescales, past reconstructions can inform long-term projections over a few millennia (e.g.
134 **Golledge et al., 2020** for a review), but some refinements at sub-millennial timescales to
135 investigate some abrupt events of the near past are necessary to reconcile with the
136 projections.

137
138 **During** past warm periods, global paleogeography, paleotopography and/or paleobathymetry
139 can differ substantially from today. Periods prior to the Plio-Pleistocene Transition (3.0-2.5 Ma)
140 were characterised by a very different continental and oceanic configuration that yielded
141 changes in the proportion of emerged lands and their locations. This affected surface
142 elevation, oceanic gateways and bathymetry, which in turn impacted on ocean and
143 atmospheric circulation (e.g. **Dowsett et al., 2016; Herold et al. 2008; Kennedy et al., 2015,**
144 **von der Heydt et al., 2016, Huang et al., 2017**), on global mean sea level changes (e.g.
145 **Miller et al. 2020b**) and on heat transport compared to modern conditions. The Antarctic
146 continent and its surface elevation have also evolved throughout the Cenozoic, with important
147 consequences for ice sheet behaviour (e.g. **Colleoni et al., 2018b; Paxman et al., 2020**).
148 Thus, direct comparison between the past and future AIS sensitivity to high levels of
149 atmospheric greenhouse gases is not straightforward.

150
151 Most of the efforts of the PAIS programme, and its predecessor, the Antarctic Climate
152 Evolution (ACE) programme, focused on the past warm periods (e.g. MCO, mPWP, warm
153 interglacials of the Pleistocene) (**Figure 1**). More specifically, ice sheets and climate
154 simulations of the MCO emerged during the PAIS programme lifetime. Within its programme,
155 PAIS promoted collaborative work within six specific sub-committees that addressed the
156 following topics for almost all of the warm periods listed above:

- 157 - Palaeoclimate Records from the Antarctic Margin and Southern Ocean (PRAMSO)
- 158 - Palaeotopographic-Palaeobathymetric Reconstructions
- 159 - Subglacial Geophysics
- 160 - Ice Cores and Marine Core Synthesis
- 161 - Recent Ice Sheet Reconstruction
- 162 - Deep-Time Ice Sheet Reconstructions

163 Scientific advances related to each of these topics are extensively described in the previous
164 chapters of this book. Many research projects that were initiated within the ACE programme
165 concluded during the PAIS programme. Many of their findings continues to have a significant
166 impact on the community of Antarctic researchers and well beyond. In the following sections,
167 we highlight some of the key findings that have advanced our understanding of the Antarctic
168 Ice Sheet dynamics, instabilities and thresholds during past warm periods. We conclude with
169 a discussion of the PAIS legacy, and highlight emerging issues, knowledge gaps, needs and
170 challenges to be addressed within the next decade by the observational and modelling
171 communities.

173 **2. Importance of evolving topography, bathymetry, erosion and** 174 **pinning points**

175
176 Ice-sheet-ocean-bedrock interactions are of major importance for understanding the dynamics
177 of the AIS (Mengel et al. 2014; Bart et al., 2016, Colleoni et al., 2018a; Whitehouse et al.
178 2019; Paxman et al., 2020). Surface and basal boundary conditions determine the
179 characteristics and regime of the ice flow. At the base of a terrestrial or marine-based ice
180 sheet, the geothermal heat flux, the morphology as well as the nature of the bed (hard rock or
181 soft sediments), affect the sliding of the ice, generate heat and yield basal meltwater. When
182 the ice sheet advances, it erodes its bed and carries sediment. Eroded material is released
183 into ice shelf cavities and onto the continental shelf at the grounding zone where the ice sheet
184 floats, disconnecting from its bed. Some of this glacial detritus finds its way via glacial
185 troughs and via channels across the continental slope and rise, and ultimately to the abyssal
186 plain. Some eroded material is also carried by icebergs and deposited offshore as Iceberg
187 Rafted Debris (IBRD). These sediments preserved in a wide range of marine environments
188 provide a valuable archive of past ice sheet dynamics and coeval oceanic and atmospheric
189 conditions.

190
191 The AIS substantially expanded 34 Ma and since that time has advanced and retreated
192 numerous times (see Galeotti et al., this volume). As a result, the morphology of the bed below
193 the ice sheet constantly evolved. Seismic stratigraphic records from the Antarctic continental
194 margins (e.g. Cooper et al., 1991; Eitrem et al., 1995; De Santis et al.; 1999; Whitehead
195 et al., 2006; Gohl et al., 2013; Huang and Jokat., 2016), clearly show that the shallow
196 continental shelves have been prograding northward through time. Sediment isopach
197 (thickness) reconstructions indicate that much of the sediments have accumulated, and
198 accreted along the Antarctic continental slope and rise (see references in Hochmuth and
199 Gohl 2019; Hochmuth et al. 2020 for circum-Antarctic review and reconstructions), implying
200 that a large volume of material has been eroded and removed from inland regions since the
201 onset of continental glaciation (e.g. Wilson et al., 2012; Paxman et al., 2019; Hochmuth et
202 al., 2020).

203
204 The most recent circum-Antarctic reconstructions show that the morphology of the bed has
205 evolved substantially over the past 34 million years (Figure 2). At the EOT, most of the West
206 and East Antarctic sectors that are currently below sea level were instead above sea level
207 (Wilson et al., 2012; Paxman et al., 2019) (Figure 2). With time, tectonic subsidence and
208 erosion caused those sectors to have deepened below sea level. These reconstructions have
209 significant implications for the understanding of the evolution of the AIS and for its ice flow. It
210 is, indeed, much easier to grow an ice sheet on terrestrial surface than on a submarine bed.
211 On such a restored and emergent topography, simulated Antarctic glaciations at the EOT
212 produce a total ice volume greater than today and similar to that of the Last Glacial Maximum
213 (LGM, ~21 ka) (Wilson et al., 2013; Ladant et al., 2014), even though atmospheric CO₂ levels
214 were much higher than today, ranging from around 780 to 560 ppm (Figure 1a). At the EOT,
215 the ice sheet did not expand across the continental shelves, because the ocean temperatures
216 were too warm (e.g. DeConto et al., 2007; Bijl et al., 2018). In fact, geological evidence from

217 the Antarctic Peninsula documents a faunal turnover from species adapted to temperate
218 waters (+5°C) to species adapted to cold waters through the EOT (Kriwet et al., 2016, Buono
219 et al., 2019).

220
221 Continental shelf evolution was critical for advances of the AIS across the marine realm after
222 the EOT (e.g. Paxman et al., 2020). The evolution of the shallow continental shelves around
223 Antarctica was connected to the evolution of the topography in the continent's interior. Various
224 reconstructions (Cooper et al., 1991; Eitrem et al., 1995; Brancolini 1995a,1995b; Huang
225 and Jokat, 2016; Paxman et al., 2019; Hochmuth et al., 2020) suggest that in most of the
226 sectors, the continental shelf edge was located further south than today (Figure 2) and then
227 prograded seaward over time (e.g. Cooper et al., 1991, De Santis et al., 1999, Huang et al.,
228 2014). The stratigraphic records combined with existing Antarctic deep drilling sites suggest
229 that the majority of the continental margin expansion occurred prior to the Pliocene (De Santis
230 et al., 1995, 1999, Hochmuth and Gohl 2019), although in some sectors (e.g Amundsen Sea,
231 Gohl et al., 2013; Prydz Bay, O'Brien et al., 2007; Wilkes Land, Escutia et al., 2011),
232 progradation of the margin was still important throughout the Pliocene. The Middle to Late
233 Miocene is a period of transition during which the Antarctic ice sheet margin advanced into a
234 cooling ocean, grounding on the continental shelf. This is also when prominent marine-based
235 sectors of the AIS developed (e.g., Uenzelmann-Neben, 2019), especially in West Antarctica
236 (Bart et al., 2003). Numerical ice sheet simulations using new Antarctic Mid-Miocene
237 paleogeographies, showed that during this period, the AIS became increasingly sensitive to
238 oceanic conditions (Colleoni et al., 2018b), resulting in large glacial-interglacial changes in
239 ice volume (Gasson et al., 2016). From the Pliocene onward, the Antarctic continental margin
240 evolved very little. Erosion of the continental interior appears to have been less influential on
241 the ice sheet since the Pliocene than during the earlier Oligocene and Miocene. The terrestrial
242 ice sheet became more stable (Passchier et al., 2011; McKay et al., 2012a; Gulick et al.,
243 2017, Kim et al., 2018). However, fluctuations of marine- based ice in deep subglacial basins
244 still occurred, especially when atmospheric CO₂ was between 400-300ppm, during the early
245 and middle Pliocene between 5 and 3 Ma (Naish et al., 2009a; Pollard and DeConto, 2009;
246 Cook et al., 2013; Cook et al., 2014; Patterson et al., 2014; Reinardy et al., 2015; Hansen
247 et al., 2015; Bertram et al., 2018; Blackburn et al., 2020). The relative stability of the
248 terrestrial AIS is further supported by a recent study of cosmogenic nuclide concentrations
249 (e.g. in-situ ¹⁰Be) in a sediment core from the Ross Sea (ANDRILL Site AND-1B) and implying
250 minimal retreat of the EAIS onto land during the last 8 million years (Shakun et al., 2018).

251
252 Another important aspect of the continental margin evolution is that its orientation or slope
253 gradually changed from seaward dipping until the Early Pliocene, to landward dipping as it is
254 now (Cooper et al., 1991; De Santis et al., 1999) (Figure 3a). This change in the bed
255 morphology was caused by the numerous ice sheet advances and retreats and associated
256 erosion and deposition of sediments from the bed. In turn, changes in the bed morphology
257 then feedback on the ice sheet dynamics. Thus, since the Pliocene, the bed of the AIS marine-
258 based sectors generally has been characterised by retrograde slopes, which favoured the
259 potential of Marine Ice Sheet Instability (MISI) (Jamieson et al., 2012; McKay et al., 2016;
260 Colleoni et al., 2018b). Prior to the Late Miocene, climatic conditions were generally warm,
261 the continental shelves were less expanded in most of the Antarctic sectors and did not
262 present strong retrograde slope. Consequently, the ice sheet could retreat relatively easily
263 during warm climate episodes with strong surface melt and oceanic melt (e.g. Levy et al.,
264 2016, Gasson et al 2016). At the end of the Miocene, climate gradually cooled, which favoured
265 terrestrial EAIS stability, but concurrently, the retrograde slope of the bed favoured instabilities
266 and fast AIS grounding line retreat in the marine-based sectors during phases of prolonged or
267 exceptional warmth (Cook et al., 2013, Pollard and DeConto 2009; Naish et al., 2009a;
268 DeConto et al., 2012,; Pollard et al., 2015; DeConto & Pollard, 2016; Golledge et al.
269 2017a, Colleoni et al., 2018b; Levy et al., 2019; Blackburn et al., 2020).

270

271 Fast retreat of the grounding line can, however, be slowed down or stopped by the occurrence
272 of pinning points at the bed that provide a buttressing backstress that resists seaward ice flow
273 (**Mengel and Levermann, 2014**). Pinning points or pinning areas can take different forms. Ice
274 rises for example, form when an ice shelf anchors on a pre-existing bathymetric high,
275 stabilizing the flow (**Matsuoka et al., 2015**) (**Figure 3b**). They can be tectonic structures or
276 volcanic islands. Today, several ice rises are visible from the surface, for example, in the Ross
277 Sea embayment (e.g. Roosevelt Island, Crary Ice Rise, Franklyn Islands and Ross Island) and
278 in the Weddell Sea embayment (Berkner Island). **Halberstadt et al. (2016)** and **Simkins et**
279 **al. (2018)** suggested that the retreat of the grounding line during the last deglaciation was
280 slower in the western Ross Sea than in the eastern Ross Sea, which is characterised by a
281 smoother bed.

282
283 Pinning points can also form temporarily due to the uplift of the bed as a result of glacio-
284 isostatic adjustment (GIA) in ice sheet retreat and unloading of the crust (e.g. Whitehouse et
285 al., 2018; **Figure 3c**). Numerical simulations show that ignoring GIA during ice sheet advance
286 results in smaller, less extended ice sheets, than would occur if GIA was accounted for,
287 because GIA creates pinning opportunities (e.g., **Colleoni et al., 2018b**). **Kingslake et al.**
288 **(2018)** showed that during the early Holocene, the West Antarctic Ice Sheet (WAIS) in both
289 the Weddell Sea and the Ross Sea temporarily retreated beyond its present-day grounding
290 line position. It subsequently re-advanced potentially due to uplift of the bed due to GIA,
291 (**Bradley et al., 2015**) and the occurrence of relief (e.g. Bungenstock Ice Rise, Weddell Sea)
292 on which the ice shelf could pin. Similarly, high-resolution bathymetry acquired from a ridge
293 under the Pine Island Glacier Ice Shelf has revealed geomorphological features that may be
294 consistent with a retreat of Pine Island Glacier inland from its present position earlier during
295 the Holocene and a subsequent re-advance to its early 20th century position (**Graham et al.,**
296 **2013**). These pinning points can be subsequently eroded or can simply “resorb” after glacio-
297 isostatic adjustment of the bed.

298
299 Finally, the ice sheet can build its own pinning points by accumulating sediments in grounding
300 zone wedges (GZW) during deglaciations, which slows its retreat (e.g. Alley et al., 2007;
301 Horgan et al., 2013; **Figure 3d**). An example of this effect was outlined in **Bart et al. (2017,**
302 **2018)**, who analysed a complex of GZWs that formed during the last deglaciation in the
303 Whales Deep basin (Eastern Ross Sea). Proxy analyses and dating of sediment cores
304 revealed that the first four GZWs were built during the first ~5000 years of a gradual 75-km
305 southward ice sheet retreat, between ~17 and ~12.3 ka. They were characterised by low
306 sedimentation rates (i.e., the GZWs are very thin) and sediment compositions indicate that the
307 grounding line was pinned on those GZWs, whilst an extensive ice shelf formed during the
308 retreat. The last three GZWs accumulated, with a clear aggradation sequence, in about 800
309 years between 12.3 ka and 11.5 ka, implying that the grounding line was not retreating during
310 this brief interval. These GZWs were characterised by very high sedimentation rates and were
311 thus relatively thick compared to the older ones. Sediment compositions seaward of those
312 three GZWs indicate that the ice shelf there broke up at the very beginning of this time interval
313 and never reformed, and that the grounding line remained pinned successively on top of those
314 last three GZWs. After building the uppermost GZW, the grounding line stepped back by about
315 100 km within a few decades, resulting in a very brief, massive ice discharge of about 0.1 mm
316 Sea Level Equivalent (SLE, **Bart and Tulaczyk, 2020**). Similar mechanisms and sequences
317 have been inferred from the analysis of Pine Island Bay continental shelf multibeam and
318 marine seismic data from the Amundsen Sea Embayment shelf (**Uenzelmann-Neben et al.,**
319 **2007; Jakobsson et al., 2011; 2012; Klages et al., 2015**). Data show that the ice stream
320 retreat was paused due to the built of GZWs during the last deglaciation. GZWs can also build
321 as a consequence of ice sheet retreat in a narrow trough in which lateral edges serve as a
322 pinning zone that slowdown the retreat. **Livingstone et al. (2013)** and **Jamieson et al. (2012,**
323 **2014)** mapped a series of GZWs in a paleo-ice stream trough in Marguerite Bay (Antarctic
324 Peninsula). Numerical simulations have shown that ice stream retreat rates slowed as the

325 grounding line passed the laterally narrow parts of the trough. If a constant sedimentation rate
326 was assumed, GZWs could form, thus further slowing the retreat.

327

328 The presence or absence of pinning points influences ice sheet dynamics. The estimated rates
329 of sea level change during past periods may have been affected by potential pauses or
330 changes in the rate of AIS (or other ice sheets) advances or retreats, due to ice-bed
331 interactions. These variations may become highly relevant, especially for the interpretation of
332 sea level reconstructions since the LGM, or simulated ice volume changes at the sub-
333 millennial scale (Klages et al., 2017; Bart et al., 2018, Kingslake et al., 2018). However, the
334 erosion of potential paleo-pinning points, during the numerous phases of expansion of the
335 AIS, makes it difficult to know the role of pinning points on past ice sheet variability at sub-
336 millennial time scales in reconstructions older than the LGM. Therefore, pinning points are
337 generally not resolved in paleo-ice sheet simulations, where bed topography cannot be
338 reconstructed with sufficient accuracy or resolution (<5 km). Moreover, shallow ice
339 approximation ice sheet models frequently used for paleo-ice sheet simulations need a
340 smoothing of the bed morphology in order to enable numerical convergence in areas where
341 the morphology is too steep for the applicability of the hydrostatic approximation. For example,
342 the Parallel Ice Sheet Model (PISM, Bueler and Brown, 2009) proposes different levels of
343 smoothing of the bed, and this model is frequently used within the PISM paleo-community
344 (e.g. Golledge et al., 2012, Albrecht et al., 2020). Full-Stokes ice sheet models, in which no
345 hydrostatic approximation is applied, do not require bed smoothing since the physics account
346 for both horizontal and vertical shear of the ice flow. However, full-Stokes models are too
347 computationally demanding and are still not usable for most paleoclimate applications
348 (Colleoni et al., 2018a and references therein). Given that most paleogeographic
349 reconstructions (e.g. Paxman et al., 2019; Hochmuth et al., 2020) are very coarse in spatial
350 resolution and highly uncertain in terms of detail, bed smoothing in ice sheet simulations
351 resulting in the loss of local pinning points is generally of lesser importance than the biased
352 controls on ice sheet dynamics induced by uncertain bed morphologies (e.g. Gasson et al.,
353 2015).

354

355

356 **3. Reconstructions of Southern Ocean sea and air surface** 357 **temperature gradients**

358

359 Equator-to-pole surface temperature gradients influence Earth's latitudinal heat distribution.
360 Reconstructions of meridional temperature gradients since the Late Cretaceous clearly show
361 a gradual steepening during the transition from greenhouse to icehouse conditions as the polar
362 regions cooled and ice sheets developed (e.g. Zhang et al, 2019). Reconstructions also show
363 the emergence of oceanic fronts in the sub-tropics and high latitudes, especially in the
364 Northern Hemisphere (e.g. Zhang et al, 2019). The development of the Southern Ocean
365 frontal system is of importance for reconstructing past AIS. The Antarctic Polar Front (APF) is
366 a region marked by elevated current speeds and strong horizontal gradients in seawater
367 density, temperature, salinity. It is currently located at approximately 50°S in the Atlantic and
368 Indian sectors, and around 60°S in the Pacific sector. During warm periods, proxies imply a
369 substantial southward shift of the Antarctic Polar Front (APF) associated with a significant
370 reduction in sea ice extent (e.g. Taylor-Silva and Riesselman, 2018; Biji et al. 2018;
371 Sangiorgi et al. 2018; Salabarnada et al., 2018; Chadwick et al., 2020; Evangelinos et al.,
372 2020). Conversely, during cold periods, the Antarctic Polar Front shifts northward
373 accompanied by a large expansion of the sea ice cover (Gersonde et al., 2005; Kemp et al.
374 2010; McKay et al., 2012a).

375

376 Fewer sediment cores have been recovered in the Southern Ocean high latitudes than in the
377 North. South of 50°S, sea surface temperature (SST) proxy reconstructions are rare (Figure
378 4). The ACE programme and more recently, the PAIS programme increased the number of

379 SST and Sea Water Temperature (SWT) at 0-200 m depth records from the Southern Ocean's
380 Antarctic margin. SST and SWT records are now available for the MCO from the continental
381 shelf site ANDRILL AND-2A (Western Ross Sea, **Levy et al., 2016**) and from the continental
382 rise at Integrated Ocean Drilling Program (IODP) Site U1356 (Adélie Land margin, **Sangiorgi**
383 **et al., 2018; Hartman et al. 2018**). Mid- to late Pliocene SST records are available from
384 ANDRILL-1B sediment core (Ross Sea shelf, **McKay et al., 2012a**) and from other cores on
385 the continental rise and abyssal plains from the Indian sectors (see **Dowsett et al., 2013** for
386 an SST compilation). MIS 31 SST records are available from continental rise sites such as
387 Ocean Drilling Program (ODP) Site 1101 (Antarctic Peninsula, **Beltran et al., 2020**) and IODP
388 Site U1361 (Adélie Land margin, **Beltran et al., 2020**) and from site ODP Site 1094, (south of
389 APF, South Atlantic sector, **Beltran et al., 2020**). For MIS 11 and MIS 5e, no Antarctic
390 continental margins SST records are available so far. However, recent International Ocean
391 Discovery Program (IODP) Expedition 374 to the Ross Sea (**McKay et al., 2019**), IODP
392 Expedition 379 to the Amundsen Sea (**Gohl et al., 2019**), and expedition INS2017_V01 on
393 the Sabrina Coast (**Armand et al., 2018; O'Brien et al., 2020**) have recovered highly
394 expanded sedimentary sections from the continental rise. This promises upcoming high-
395 resolution SST records for Pleistocene interglacials, for which most of the ice proximal SST
396 information is still missing.

397
398 A comparison between MCO and mPWP global meridional proxy-based SST gradients
399 highlights the difference between the two periods in the Southern Hemisphere and how much
400 the global climate state has evolved between 17 and 3 Ma (**Figure 4a**). During the MCO, the
401 air surface temperature gradient strengthened between 30°S to 40°S, as in the Northern
402 Hemisphere, suggesting that sub-tropical marine frontal system was well developed. The
403 meridional SST and SWT gradients were much weaker than today and a summer warming of
404 16°C to 22°C ($\pm 5^\circ\text{C}$) compared to today, was observed in geochemical proxies at around 60-
405 65°S on the East Antarctic continental rise (**Sangiorgi et al. 2018; Hartman et al., 2018**) and
406 a warming of about 2°C to 12°C ($\pm 5^\circ\text{C}$) compared to today is recorded in the Ross Sea (**Levy**
407 **et al., 2016, Sangiorgi et al., 2018**) indicating a total absence of or rare occurrences of sea
408 ice during this period. The mPWP was characterised by a meridional SST gradient weaker
409 than today (e.g. **Brierley et al., 2009; Haywood et al., 2013**) and with a significant Arctic
410 amplification, while the warming anomaly was more subdued in the high southern latitudes
411 (**Figure 4a**). South of 55°S, East Antarctic continental rise summer SST were warmer than
412 today by about 4°C to 6°C on the East Antarctic continental rise and by up to 7°C on the Ross
413 Sea shelf (**McKay et al., 2012a**), indicative of a highly reduced, if not absent, summer sea ice
414 cover in some sectors.

415
416 During both the MCO and the mPWP, the APF was probably more contracted towards high
417 latitudes in all sectors around Antarctica (**Taylor-Silva and Riesselman, 2018; Sangiorgi et**
418 **al., 2018**). The mPWP presents a meridional SST gradient steeper than during the MCO and
419 it is possible that the APF might not have reached latitudes as poleward as during the MCO.
420 The contrast between the mPWP and MCO meridional SST gradient south of 40°S, suggests
421 that the gradient probably steepened during the Late Miocene (**Herbert et al., 2016**). However,
422 in some sectors of the Antarctic margin, there is strong evidence for warmer conditions during
423 the Early Pliocene compared to the mPWP, i.e. sea-ice reduction and warming west of the
424 Antarctic Peninsula (e.g. **Hillenbrand & Ehrmann 2005; Escutia et al. 2009**) and in Prydz
425 Bay (**Whitehead et al. 2005**). This was accompanied by a poleward shift of the APF (**Bart &**
426 **Iwai 2012; Whitehead & Bohaty 2003; Escutia et al. 2009**).

427
428 During the Pleistocene, MIS 31, MIS 11 and MIS 5e meridional SST gradients highlight the
429 strong impact of precessional astronomical forcing, with SSTs warmer than today especially
430 in the Northern Hemisphere mid-to-high latitudes (**Figure 4b**). All three interglacials present
431 SST gradients quite similar to today in the equatorial to sub-tropical latitudinal bands. The
432 discrepancies between them emerge for latitudes poleward of 50°S. For MIS 31, alkenone
433 and long chain diol analysis on sediment cores revealed an SST warming of 4°C to 12°C on

434 the Adélie Land margins and the Antarctic Peninsula (**Beltran et al., 2020**). Proxies suggest
435 reduced or even absent winter and summer sea ice in the Ross Sea and offshore Adélie Land
436 margin; information is missing for other Antarctic sectors (see references for **Figure 6d**). The
437 abrupt appearance of foraminiferal oozes and bioclastic limestone in the Ross Sea and
438 coccolith-bearing sediments in Prydz Bay during MIS31 (**Bohaty et al., 1998; Scherer et al.,**
439 **2003; Villa et al., 2008, 2012**) indicates a significant southward migration of the APF. In terms
440 of the SST gradient, MIS 31 shows more similarities with the mPWP in the Southern
441 Hemisphere than with the more recent Late Pleistocene interglacials.

442
443 No SST or SWT proxies south of 60°S are available for MIS 11, thus it is difficult to assess the
444 magnitude of a potential warming closer to the Antarctic margins. Interpretation of diatom and
445 geochemical changes could help to estimate SST or SWT from the Wilkes Subglacial Basin
446 and the Ross Sea margins (see **Wilson et al., this volume for references**). North of 40°S,
447 tropical to subtropical MIS 11 SSTs were warmer than modern by about 1-4°C, and between
448 50°S and 60°S, only a 1-2°C warming above modern is recorded (**Kunz-Pirrung et al., 2002**).
449 Apart from just a single exception, no SST reconstructions are available for MIS 5e south of
450 60°S (**Capron et al., 2014, Hoffman et al., 2017; Chadwick et al., 2020**), and the
451 reconstructed SSTs north of 60°S are similar to those of MIS 11 (**Figure 4b**). It is hence difficult
452 to assess the magnitude of surface and ice proximal sub-surface ocean warming during MIS
453 5e. **Capron et al., (2014)** report warmer than present-day conditions that occurred for a longer
454 time interval in southern high latitudes than in northern high latitudes. They also report an
455 earlier MIS5e warming in the Southern Ocean starting from 130 ka compared with the
456 Northern high latitudes and synchronous with Antarctic ice core records. Moreover, **Chadwick**
457 **et al. (2020)** showed that the sea-ice minima and SST maxima were reached at slightly
458 different times in three Southern Ocean sectors. During both MIS 11 and MIS 5e, the few
459 existing records indicate a seasonally sea ice covered ocean (**Kunz-Pirrung et al., 2002;**
460 **Wolff et al., 2006 Escutia et al., 2011; Wilson et al., 2018, Chadwick et al., 2020**). Ice core
461 analyses by **Wolff et al. (2006)** suggested on the basis of sea-ice proxies in the EPICA Dome
462 C ice core that winter sea ice was largely reduced during MIS 5e and MIS 11 in the Indian
463 sector of Antarctica, and that summer sea ice was likely absent. In addition, similar proxy
464 analyses on the EPICA DML ice core from Dronning Maud Land indicate a sea ice reduction
465 in the Atlantic sector during MIS 5e (**Schüpbach et al., 2013**).

466

467 **4. Extent of major Antarctic glaciations**

468

469 This section focuses on glaciations that occurred during the Eocene-Oligocene Transition
470 (EOT, ~34 Ma) (see **Galeotti et al., this volume**), during the Mid-Miocene Climatic Transition
471 (MMCT, 14.5 to 13.5 Ma) (see **Levy et al., this volume**), the M2 glaciation (3.312-3.264 Ma)
472 preceding the mPWP, and the Last Glacial Maximum (LGM, ~21 ka) (see **Siegert et al., this**
473 **volume**).

474

475 **The EOT** was characterised by the development of a continental ice sheet on Antarctica
476 (**Barrett, 1989; Hambrey et al. 1991; Wise et al., 1991; Zachos et al. 1992**) as atmospheric
477 CO₂ level fell (e.g. **DeConto et al., 2003**) and the Southern Ocean cooled (e.g., **Bijl et al.,**
478 **2013**) as a result of the opening of ocean gateways. (e.g. **Kennett et al., 1977**) (**Figure 1**).
479 Across the EOT, deep-sea temperatures cooled by 3° to 5°C (e.g. **Liu et al., 2018**) as a
480 consequence of decreasing CO₂ levels (**Pagani et al., 2005**). Sedimentary cycles from a drill
481 core in the western Ross Sea provided the first direct evidence of orbitally controlled glacial
482 cycles between 34 million and 31 million years ago (**Galeotti et al., 2016**). Initially, under
483 atmospheric CO₂ levels of ≥600 ppm, a smaller AIS, restricted to the terrestrial continent, was
484 highly responsive to local insolation forcing. The establishment of the Antarctic Ice Sheet (AIS)
485 is associated with an approximately +1.5 per mil increase in deep-water marine oxygen
486 isotope values (δ¹⁸O) beginning at ~34 million years ago (Ma) and peaking at ~33.6 Ma
487 (**Coxall et al., 2005; Bohaty et al., 2012**), with two positive δ¹⁸O steps separated by ~200,000

488 years (Figure 1b). The first positive step in the isotope data primarily reflects a temperature
489 decrease (**Lear et al., 2008**) (EOT-1, ~34.46-33.9 Ma); the second one has been interpreted
490 as the onset of a prolonged interval of maximum ice extent at ~33.6 -33.7 Ma (EOT-2) (**Liu et**
491 **al., 2009**). Stratigraphic unconformities identified from the continental margins of Antarctica
492 (**Figure 1b**, e.g. **De Santis et al., 1995; Eitrem et al., 1995; Cooper and O'Brien 2004;**
493 **Escutia et al., 2005; Whitehead et al., 2006; Gohl et al., 2013; Uenzelmann-Neben and**
494 **Gohl; 2014, Gulick et al., 2017**) presumably correspond to one of these $\delta^{18}\text{O}$ excursions.

495
496 **Galeotti et al. (2016)** suggest that a continental-scale AIS with frequent calving at the
497 coastline did not form until ~32.8 million years ago, coincident with the earliest time when
498 atmospheric CO_2 levels fell below ~600 ppm. The atmospheric CO_2 threshold for the onset of
499 large-scale Antarctic glaciations remains, however, uncertain and varies between 900 ppm to
500 560 ppm in numerical climate and ice sheet simulations (**DeConto et al. 2003; Ladant et al.**
501 **2014, Liakka et al., 2014, Gasson et al, 2014**). **Liakka et al., (2014)** showed that when
502 accounting for vegetation-albedo feedbacks, large-scale Antarctic glaciations occurred when
503 atmospheric CO_2 dropped between 1120 ppm and 560 ppm. **Ladant et al. (2014)** simulated
504 a first Antarctic expansion at EOT-1 associated with a first sea level drop of about 10 meters
505 (atmospheric CO_2 set to 900 ppm) and a second one coinciding with early Oligocene glaciation
506 Oi-1 (33.4 to 33.0 Ma, **Miller et al., 1991; Zachos et al., 2005**) of about 63 meters (atmospheric
507 CO_2 set to 700 ppm). Sequence boundary and ice volume proxies suggest that the extent of
508 the AIS gradually increased across the EOT and expanded to either near-modern dimensions
509 (**Miller et al., 2008; 2020a**) or as much as 25% larger than at present day (**Katz et al., 2008;**
510 **Wilson et al., 2013**). Numerical ice sheet modelling studies show a large range of ice volumes
511 across the EOT. Simulated glaciations lead to sea level fall clustered around 10 m SLE and
512 25 m SLE relative to present AIS volume (**DeConto and Pollard 2003; Pollard and DeConto**
513 **2005; Gasson et al., 2014; Ladant et al, 2014; Liakka et al, 2014; Wilson et al., 2013**)
514 (**Figure 1d**), which corresponds to a total simulated AIS volume up to 83 m SLE. This is
515 broadly in agreement with sea level falls up to 70 m estimated from low-latitude shallow-
516 marine sequences (e.g. **Cramer et al., 2011**) (**Figure 1c**). Both **DeConto and Pollard (2003)**
517 and **Ladant et al. (2014)** simulated isolated big ice caps over East Antarctic highlands
518 presumably during EOT-1, that ultimately coalesced during Oi-1 (**Figure 5a**). This is supported
519 by the geological evidence of glacial marine deposits in the Wilkes Land continental shelf and
520 rise since 33.6 Ma (**Escutia et al., 2005, 2011**) and by glacial sediment transport to the
521 continental slope of the Prydz Bay margin since ~35 Ma (**O'Brien et al, 2004**). No ice
522 grounded on the continental shelf at this time (**Figure 5a**, e.g. **Barrett et al., 1989, 2007**), and
523 the continental shelf edge was located farther South than present for most of the Antarctic
524 margins (**Figure 2**).

525
526 **The Mid-Miocene Climatic Transition (MMCT, ~14.8 - 13.5 Ma)** is a period of global cooling
527 following the extreme warmth of the Mid-Miocene Climatic Optimum (MCO). The onset of
528 global climatic cooling at ~14.8 Ma marks the start of the MMCT (**Böhme, 2003; Flower and**
529 **Kennett, 1993; Holbourn et al., 2014; Shevenell et al., 2008**). Disconformities in the
530 ANDRILL AND-2A record (**Levy et al., 2016**) and across the Ross Sea (**De Santis et al.,**
531 **1999**) (**De Santis et al., 1999**), pulsed deposition of ice-rafted debris offshore Prydz Bay and
532 the Adélie Land margin (**Pierce et al., 2017**) together with an increase in sea ice indicators in
533 the Ross Sea and off East Antarctica (**Levy et al., 2016; Sangiorgi et al., 2018**) and major
534 turnover in Southern Ocean diatom species (**Crampton et al., 2016**), suggest marine ice sheet
535 advances across the Ross Sea during glacial intervals for the first time since the onset of the
536 MCO (**Figure 5b**). Ice sheet advance in the Wilkes Land margin is recorded by erosion of
537 older sediments from the shelf (**Escutia et al., 2011**) and an increase in dinocyst assemblages
538 from the seasonal sea ice zone south of the Antarctic Polar Front (**Sangiorgi et al., 2018**).
539 Additionally, less well-dated erosional unconformities in the Weddell Sea (e.g. **Huang et al.,**
540 **2014**), Amundsen Sea (e.g. **Lindeque et al., 2016; Uenzelmann-Neben and Gohl, 2012**),
541 Bellingshausen Sea-Antarctic Peninsula (e.g. **Rebesco et al., 2006; Uenzelmann-Neben,**

542 **2006**), Sabrina Coast (**Gulick et al., 2017**) and in Prydz Bay (e.g. **Whitehead et al., 2006**),
543 are attributed to MMCT marine-based ice expansion, and together imply that both the EAIS
544 and the WAIS expanded onto the continental shelf at this time. An increase in glacial-
545 interglacial amplitude in the far-field $\delta^{18}\text{O}$ data suggests that the AIS expanded further during
546 successively, gradually colder glacial phases. This interval of increased glacial expansion
547 culminated in a major step in the $\delta^{18}\text{O}$ record at 13.9 Ma (**Figure 1b**). During the MMCT,
548 Southern Ocean SSTs cooled by about 6 °C (**Holbourn et al., 2007; Sangiorgi et al., 2008**).
549 Bottom water temperatures generally cooled by 2 to 3 °C (**Cramer et al., 2011; Lear et al.,**
550 **2015; Shevenell et al., 2008**) and global sea level may have dropped by as much as 50 m
551 (**Miller et al., 2020a**), hinting at the possibility of some ice expansion in the Northern
552 Hemisphere (**DeConto et al., 2008**). Summer temperatures in the Trans-Antarctic Mountains
553 declined by >8 °C (**Denton and Sugden, 2005**) and this cooling has been linked with a shift
554 from temperate climate wet-based glaciation with a dynamic ice sheet in a warm to
555 temperature climate to a predominantly dry glaciation style with a more stable terrestrial ice
556 sheet under moder-like Antarctic polar climatic conditions (**Lewis et al., 2008; Lewis and**
557 **Ashworth, 2016; Sugden and Denton, 2004**).

558
559 The largest benthic foraminifera $\delta^{18}\text{O}$ shift during this period is of about 1.3 ‰ (e.g. **Holbourn**
560 **et al., 2013**), partly corresponding to an estimated a sea level drop of 35–40 m from interglacial
561 to glacial. Interestingly, numerical ice sheet models can only simulate such a large interglacial-
562 to-glacial amplitude in ice volume (**Gasson et al., 2016, Colleoni et al., 2018a**), when using
563 a reconstructed Mid-Miocene paleogeography (e.g. **Paxman et al., 2019**). Backstripped sea
564 level data (**Miller et al., 2005, Kominz et al., 2008**) and calibrated benthic $\delta^{18}\text{O}$ sea level
565 changes (**Miller et al., 2020a**) revealed potential sea level falls up to 10 to 20 meters below
566 the present-day mean sea level during the MMCT (**Figure 1c**), implying a greatly expanded
567 AIS, perhaps up to 30% larger than today. The compilation of simulated Antarctic ice volume
568 contributions to global mean sea level for this cold period ranges between +10 to -20 m SLE
569 relative to present (**Gasson et al., 2016, Colleoni et al., 2018a**) (**Figure 1d**, cyan squares).

570
571 **The Mid-Pliocene M2 glaciation (~3.312-3.264 Ma)** corresponds to a large transient increase
572 in the deep-sea benthic $\delta^{18}\text{O}$ records (**Figure 1b**) with a cooling of at least 3.5°C preceding
573 the peak of M2 (**Karas et al., 2020**) and an atmospheric CO₂ level drop of about 320-343 ppm
574 (**de la Vega et al., 2020**). A compilation of climate proxy data suggests that during this
575 glaciation, Greenland mountain glaciers expanded (**Thiede et al., 2011; Jensen et al., 2000**)
576 and that other ice caps also grew in the Northern Hemisphere (**De Schepper et al., 2013; Tan**
577 **et al., 2017**). In fact, this glaciation marks the end of global warmth of the early Pliocene (5.5
578 to 3.3 Ma) and the beginning of a step-wise transition towards bipolar cooling that culminated
579 in continental-scale Northern Hemisphere glaciations ~2.7 Ma. Numerous sedimentary
580 hiatuses, including the M2 glaciation, are observed in the AND-1B sediment record (western
581 Ross Sea, **Naish et al., 2009a**) during the Mid to Late Pliocene. Continental margin
582 morphology appears to have allowed the AIS to advance to the shelf edge during the M2
583 glaciation in the Ross Sea (e.g. **Kim et al, 2018, McKay et al., 2012a; McKay et al. 2019**),
584 Prydz Bay (**O'Brien et al., 2007**), Sabrina Coast (**Gulick et al., 2017**), Wilkes Land (**Eitrem**
585 **et al., 1995; Escutia et al., 1997; De Santis et al., 2003**), and the Antarctic Peninsula and
586 Amundsen Sea (**Rebesco et al., 2006, Gohl et al., 2013**). The glacio-eustatic sea level drop
587 of this period is represented by a major erosional sequence boundary on the New Jersey shelf
588 (**Miller et al., 2005**) and global sea level fall of about 30 m at the M2 glaciation (**Naish and**
589 **Wilson, 2009; Miller et al., 2012; Grant et al., 2019; Miller et al., 2020a**) (**Figure 1c**). Based
590 on the review of circum-Antarctic evidence of grounding events and sequence stratigraphy,
591 **Bart (2001)** suggested indeed, an Antarctic ice volume larger than today and almost as large
592 as during the LGM, implying the existence of relatively small Northern Hemisphere ice sheets.
593 In contrast, the compilation of simulated Antarctic ice volume, however, likely underestimates
594 the ice sheet expansion during this glaciation (**Figure 1d**) and, instead, yields a global mean
595 sea level rise up to 5 m above present-day mean sea level (**Pollard and DeConto, 2009; Tan**
596 **et al., 2017; De Boer et al., 2017a**).

597
598 **The Last Glacial Maximum (LGM, ~19-23 ka)** is the most recent glaciation that occurred
599 before present, and as such, is the best documented glaciation. Ice core records have shown
600 that the atmospheric CO₂ levels dropped to about 185 ppm (Lüthi et al., 2008). Global climatic
601 reconstructions revealed that the global mean temperature dropped by about 4-7 °C (e.g.
602 Schneider von Deimling et al., 2006; Tierney et al., 2020) compared to present. Marine
603 benthic and planktic foraminifera recorded a clear $\delta^{18}\text{O}$ increase (Imbrie et al., 1984, Lisiecki
604 and Raymo, 2005), actually, observable concomitantly to all past cold glacial periods (Imbrie
605 et al., 1984, SPECMAP stack; Lisiecki and Raymo 2005, LR04 stack; Westerhold et al.,
606 2020, CENOGRID; Zachos et al., 2008, Figure 1b). Calibrated conversions of the $\delta^{18}\text{O}$
607 record or dated paleo coral reefs suggest a global mean sea level drop ranging between 80
608 m to 130 m relative to present (Figure 1c) (e.g. Waelbroeck et al., 2009; Bard et al., 1990;
609 Shackleton, 2000), with a cluster between 110 m and 130 m below present-day mean sea
610 level. Diatoms and radiolarians show that the sea ice cover was larger than today. Winter sea
611 ice cover shifted northward by about 5 to 10° (e.g. Gersonde et al., 2005; Benz et al., 2016)
612 and summer sea ice edge, although more uncertain, might have been located around 60.5°S
613 (Green et al., 2020 and references therein). Compilation of climate proxies suggest a potential
614 strengthening and equatorward shift of the Southern Hemisphere westerlies (e.g. Kohfield et
615 al., 2014; Lamy et al., 2014; Struve et al., 2020), which remains debated (e.g. Kim et al.,
616 2017; Sime et al., 2016; Lamy et al., 2019).

617
618 There is persuasive evidence from the geological record to indicate that the AIS was larger
619 than present around the time of the global sea level lowstand at ~20 ka, although the extent
620 of this expansion is well constrained at only a few sites around the continental margin
621 (Whitehouse, 2018). Both marine and terrestrial geological data indicate that at the LGM, the
622 AIS almost extended to the continental-shelf break in most sectors (Eitrem et al., 1995;
623 Anderson et al., 2002, 2014; Hillenbrand et al., 2012, 2014; The RAISED Consortium,
624 2014; Mackintosh et al., 2014; Arndt et al., 2017; Bart et al., 2018) (Figure 5c), as during
625 many previous Pleistocene glaciations (e.g. Escutia et al., 2003). However, the AIS did not
626 advanced up to the continental shelf edge in Prydz Bay (O'Brien et al., 2007; Mackintosh et
627 al., 2014; Wu et al., 2021, in the Western Ross Sea (Halberstadt et al., 2016; Prothro et al.,
628 2018) and in parts of the Amundsen Sea (e.g. Larer et al., 2014; Klages et al., 2017).
629 Furthermore, the scenario for ice advance in the Weddell Sea embayment remains uncertain
630 (The RAISED consortium, 2014; Whitehouse et al., 2017; Nichols et al. 2019). Ice sheet
631 expansion during the LGM led to a thickening of the AIS of several hundreds of meters almost
632 in all sectors, especially around West Antarctica as supported by exposure data (see Siegert
633 et al., this volume). On the Antarctic plateau, ice core $\delta^{18}\text{O}$ isotopes records suggest that
634 elevation increased of 270 to 660 meters between the LGM and present-day (Werner et al.,
635 2018). Over West Antarctica, the increase in elevation during the LGM is up to 850 to 1800
636 meters (Werner et al., 2018).

637
638 The relatively small number of proximal geological records on AIS extent and thickness during
639 the LGM prevents an accurate constraint on LGM ice volume. Distal, deep ocean benthic
640 foraminifera $\delta^{18}\text{O}$ records may provide overall ice volume estimates, but do not allow
641 disentangling contributions from individual contribution of each ice sheets at the LGM (Simms
642 et al., 2019, and references therein; Clark and Tarasov, 2014). Ice sheet modeling is one of
643 the possible approaches to simulate the volume of the AIS at the LGM. Such modeling has
644 yielded an increase in ice volume of 5.9 to 19.2 m of sea level equivalent (SLE) (Bentley,
645 1999; Huybrechts, 2002) in the late 1990 and early 2000s. With the improvement of ice sheet
646 models and climate forcing, the range of AIS contributions to sea level change at LGM has
647 narrowed to about -5 to -12 m SLE (e.g. Huybrechts, 2002; Golledge et al., 2012; Gomez
648 et al., 2013; Maris et al., 2014; Briggs et al., 2014; Quiquet et al., 2018, Sutter et al., 2019),
649 with a cluster around -7 to -8 m SLE (Figure 1d and references therein). Another approach is
650 to inverse AIS by means of glacial-hydro isostatic adjustment (GIA) models, which describe
651 the viscous response of the solid Earth to past changes in surface loading by ice and water

652 (Whitehouse et al., 2018). This approach has also been used in combination with direct ice
653 sheet modeling (e.g. Whitehouse et al., 2012b) and/or by making use of constraints on ice
654 thickness from reconstructions based on exposure age dating, as well as satellite observations
655 of current uplift (Whitehouse et al., 2012b; Ivins et al., 2013; Argus et al., 2014). Estimates
656 from GIA modelling for the AIS contribution to global mean sea level amount to -5 to -30 m
657 SLE with most of the contributions smaller than -13 m SLE (Figure 1d). Older studies had
658 estimated large sea level contributions generally above 15 m (e.g. Nakada et al., 2000;
659 Huybrechts, 2002; Peltier and Fairbanks, 2006; Philippon et al., 2006; Bassett et al.,
660 2007), but more recent modeling studies and reconstructions have refined these estimates to
661 below 13.5 m (Mackintosh et al., 2011; Whitehouse et al., 2012a; Gomez et al., 2013;
662 Argus et al., 2014; Briggs et al., 2014) with an average contribution of about -10 m SLE (e.g.
663 Simms et al., 2019 and references therein).

664
665 Despite those improvements, AIS contributions to sea level changes at the LGM remains
666 poorly constrained (Simms et al., 2019, and references therein, Clark and Tarasov, 2014)
667 and this has global consequences on the assessment of past, present and future sea level
668 changes. Land ice retreat in both hemispheres during the last deglaciation have produced a
669 residual GIA signal that still affects present-day sea level changes measurements (Martín-
670 Español et al., 2016). This residual signal is estimated from modelled reconstructions of
671 global land ice thickness changes, and spatio-temporal deglaciation history (e.g. ICE-5G to
672 ICE 7G, GLAC-1, ANU; Peltier et al., 2004; Peltier et al., 2015; Roy and Peltier, 2018;
673 Tarasov and Peltier, 2002, 2003; Lambeck and Chappell, 2001; Lambeck et al., 2002). To
674 date, there is no consensus on AIS volumes at the LGM and through the last deglaciation, A
675 compilation of cosmogenic exposure ages from low-elevation sites shows that the AIS
676 substantially thinned throughout the Holocene, but mainly after the MWP-1A (Small et al.,
677 2019). The RAISED consortium (2014) provided partial pan-Antarctic grounding line position
678 at ~15 ka, 10ka and 5ka. In the ice sheets deglaciation scenarios ICE-6G and ICE-7G (Peltier
679 et al., 2015; Roy and Peltier, 2018), the AIS extent at LGM has been set up to its present-
680 day extent, but with grounded ice filling the embayments currently occupied by the Ross Ice
681 Shelf, by the Ronne-Filchner Ice Shelf and by the Amery ice shelf. This surely affects the
682 calculation of GIA and its residual signal and, as such, the assessment of post-glacial and
683 present-day land ice contribution to on-going sea level changes (Martín-Español et al., 2016).

684
685 At regional scale, the inclusion of realistic, spatially variable relative sea-level forcing through
686 coupled simulations of 3-D ice-sheet and GIA-modulated sea-level change results in a
687 stabilising effect on marine-grounded ice sheet dynamics (Gomez et al., 2010). The grounding
688 line, in fact, advances or retreats in response to the regional ice fluctuation. The latter triggers
689 viscoelastic solid Earth rebound as well as a change of the local geoid height in response to
690 the variation of the gravitational pull (e.g. Stocchi et al. 2013). In particular, the predicted
691 increase in the volume of the WAIS during the last glacial cycle is smaller in the coupled
692 simulations due to negative feedbacks associated with an increase in near-field water depth.
693 The latter stems for the combination of ice-driven solid Earth subsidence and counterintuitive
694 local sea-level rise caused the gravitational attraction of the growing ice sheet's mass (Gomez
695 et al., 2013; De Boer et al., 2014b, 2017b; Konrad et al., 2014). At global scale, Gomez et
696 al. (2020) showed that the retreat of Northern Hemisphere ice sheets during the last
697 deglaciation and associated sea level rise directly impacts on the dynamical behaviour of the
698 AIS and conditions its own retreat. Modelled AIS sensitivity on different paleobathymetries
699 since the Mid-Miocene shows that the position of the AIS advance on the continental shelf
700 depends on glacio-isostatic adjustment (generating pinning points, see Section 2) and on the
701 magnitude of global mean sea level changes (Colleoni et al., 2018b; Paxman et al., 2020).
702 A similar relationship between the AIS stability and global mean sea level changes has
703 recently been inferred from a North Atlantic deep-ocean benthic $\delta^{18}\text{O}$ record of the Plio-
704 Pleistocene Transition and the early Pleistocene (Jakob et al., 2020). Based on a range of
705 Mg/Ca paleothermometer calibrations, the sea level record suggests that the gradual
706 expansion of the Northern Hemisphere ice sheets, and the consequent substantial lowering

707 of global mean sea level, led to an increasing stability of the terrestrial EAIS (Jakob et al.,
708 2020). Other studies also highlight the sensitivity of the marine-based sectors of the AIS to
709 rapid sea level rise at millennial to sub-millennial time-scales, such as the impact of rapid sea
710 level rise during the various meltwater pulses episodes of past deglaciations (e.g. Golledge
711 et al., 2014; Petrini et al., 2018; Turney et al., 2020).

712
713
714

715 5. Antarctic Ice Sheet response to past climate warmings

716

717 Assessing the AIS behaviour during past periods warmer than today can inform on the
718 magnitude and timing of past and future sea level changes, as well as on various mechanisms
719 triggering ice sheet retreats that can vary through time (i.e. atmospheric and/or oceanic
720 warming). At millennial to sub-millennial scales, the crossing of tipping points caused by
721 Earth's climate system feedbacks can cause rapid ice sheet retreats. One example is ocean
722 warming triggering MISI. Because the global climatic state has been constantly evolving, the
723 conditions necessary to cross these tipping points have also evolved as well. To highlight this
724 aspect, several policy-relevant warm periods in the geologic past have been analysed, based
725 on a few climatic and glaciological indicators synthesized in Figure 6. Note that except for the
726 sea ice (Figure 6d), all the other variables are expressed as anomaly relative to their present-
727 day value (20th century for MAT and SST).

728

729 The compilation of global mean sea level changes and simulated Antarctic contributions is
730 exhaustive and illustrates a key focus of the paleo polar community has been producing over
731 recent decades. We do not discard computed estimates of AIS contribution to global mean
732 sea level change that could appear out of the range of data. Instead, we consider such values
733 as part of the uncertainties associated with uncertain models physics and boundary conditions.
734 References for all compiled data and simulated ice volumes are provided in the caption of
735 Figure 1.

736

737 **The Mid-Miocene Climatic Optimum** (MCO, 17-14.8 Ma). The MCO presents an interesting
738 analogue for assessment of climate projected for the next decades to centuries
739 (Steinthorsdottir et al., 2020). At that time, Antarctica hosted the only existing continental-
740 size ice sheet. Geological proxy data indicate atmospheric CO₂ concentrations generally
741 varied between 300 ppm and 600 ppm on glacial-interglacial (orbital) time scales during much
742 of the MCO (Foster et al., 2012; Greenop et al., 2014), but it may have reached values as
743 high as 840 ppm (Retallack, 2009) (Figure 1a). The limited existing geological proxies of
744 terrestrial Antarctic temperature, from the Ross Sea (Warny et al., 2009) and off Adélie Land
745 (Sangiorgi et al., 2018), indicate a surface air temperature warming of approximately 14°C to
746 25°C relative to today. Comparison with the global Mean Annual Temperature (MAT) clearly
747 emphasises strong polar amplification occurred during the MCO (Goldner et al., 2014). Sub-
748 Water Temperature (SWT) and SST reconstructions from the Ross Sea (ANDRILL-2A, Levy
749 et al., 2016) and from the Adélie Land margins (Sangiorgi et al., 2018, Hartman et al., 2018)
750 also support this polar amplification (Figure 6c). On the continental rise (paleo latitude 53°S,
751 Sangiorgi et al., 2018), a 5-10°C SWT warming (likely summer) was recorded, but on the
752 continental shelf (~77°S) this estimated warming was even larger, reaching 10-20°C through
753 the MCO.

754 Together, far-field data and modelling experiments suggest a highly dynamic ice sheet during
755 the MCO. The AIS was mostly responsive to eccentricity-modulated precession affecting local
756 insolation and leading to widespread inland retreat of the land-terminating ice sheet on glacial-
757 interglacial timescales (e.g. Holbourn et al., 2013). Levy et al. (2019) suggested glacial to
758 interglacial ice volume fluctuations were of about 30 to 46 m SLE for a $\delta^{18}\text{O}$ shift of about
759 0.88‰, which was successfully simulated by Gasson et al., (2016) and Colleoni et al.,

760 **(2018a)** using idealised (but representative) mid-Miocene boundary conditions. Geological
761 records recovered adjacent to the EAIS suggest it advanced and retreated many times through
762 the TAM during the MCO (**Hauptvogel and Passchier, 2012**), but did not advance far beyond
763 the coastline during glacial intervals (**Levy et al., 2016**). The cored interval spanning ~17 to
764 15 Ma at Integrated Ocean Discovery Program (IODP) Site U1521 (**McKay et al., 2019**)
765 consists of diatom-rich mudstone and diatomite, which also indicates ice distal environments
766 in the Ross Sea through the MCO. Sediments collected at IODP Site U1356, off the coast of
767 the Adélie Land margin (East Antarctica), suggest open-water conditions at the site
768 throughout the MCO (**Sangiorgi et al., 2018**). Modelling studies suggest the Wilkes Subglacial
769 Basin remained free of grounded ice during warm interglacial episodes through the early to
770 mid-Miocene (**Gasson et al., 2016; Colleoni et al., 2018a; Paxman et al., 2020**) but it is
771 unclear whether grounded ice advanced across the region during glacial intervals prior to the
772 MMCT (**Pierce et al., 2017**). Mg/Ca calibrated sea level and sequence boundary estimates
773 suggest Global Mean Sea Level (GMSL) rise ranging from +20 meters to +30 meters above
774 present (**Miller et al., 2005; Kominz et al., 2008**) (**Figure 6e**). The compilation of simulated
775 AIS contributions to GMSL vary between +15 m SLE to +35 m SLE (**Langebroek et al 2009;**
776 **Gasson et al. 2016; Colleoni et al., 2018b; Stap et al. 2019**) (**Figure 6e**). Such a large range
777 mostly results from the use of different ice sheet models, different bed topographies and
778 bathymetries, and different climate forcing in the mid-Miocene experiments. The range of
779 potential Antarctic ice sheet GMSL contribution was significantly to +16 to +17 meters by
780 **Gasson et al. (2016)**, and **Colleoni et al. (2018b)** using an idealised Mid-Miocene
781 paleotopography similar to that of **Paxman et al. (2019)**, a prescribed atmospheric CO₂ of 500
782 ppm.

783 **The mid-Pliocene Warm Period (mPWP, 3.3 - 3 Ma)** is considered as one of the most
784 geologically accessible and relevant examples of climate change driven by atmospheric CO₂
785 levels equivalent to present-day one (**Naish & Zwartz, 2012; Masson-Delmotte, 2013;**
786 **Haywood et al., 2016**). Atmospheric CO₂ levels ranged between 300 ppm and 450 ppm and
787 global mean temperature was about 2-3°C warmer than present during the warmest
788 interglacials (**Masson-Delmotte, 2013**) (**Figure 6a & 6b**). One of the striking characteristics
789 of the mPWP is that the SST proxy compilations reveal a meridional temperature gradient
790 weaker than today (**Figure 4**), characterised by expansion of tropical to sub-tropical bands,
791 no boreal and reduced austral summer sea-ice and thus a strong northern and southern polar
792 amplification (e.g. **Lunt et al., 2012; Haywood et al., 2020**). Modelling showed that such SST
793 patterns reflected a weaker Hadley circulation than today (**Brierley et al., 2009; Haywood et**
794 **al., 2020**). In the Southern high-latitudes, the coastal Antarctic region was up to 6°C warmer
795 than today (e.g. **McKay et al., 2012a; compilation in Dowsett et al., 2012**) (**Figure 6b**) mostly
796 due to the fact that summer sea-ice and the ice sheet had retreated and the APF had
797 contracted to more southern latitudes (**Taylor-Silva and Riesselman, 2018**). Evidence
798 documents episodic sea ice in the Ross Sea, and offshore Adélie Land and in Prydz Bay (e.g.
799 **McKay et al., 2012a; compilation in Dowsett et al., 2012**) (**Figure 6d**). Seasonal sea ice was
800 likely present in the Weddell Sea (**Burckle et al. 1990**). Reconstructed SSTs show a pan-
801 Antarctic warming of up to 5°C on the continental slope and rise (**Whitehead and Bohaty,**
802 **2003; Escutia et al., 2009**). SSTs also show a warming up to 6°C in the Ross Sea (**McKay**
803 **et al., 2012**) (**Figure 6c**), which was likely caused by the sea-ice albedo feedback, and
804 decreasing local albedo due to the retreat of coastal land ice.

805
806
807 Global mean sea level reconstructions (paleo-shorelines and sequence stratigraphy) indicate
808 a sea level rise between about +15 m to +28 m (**Wardlay and Quinn, 1991; Dwyer and**
809 **Chandler, 2009; Kulpecz et al 2009; Naish and Wilson, 2009; Sosdian and Rosenthal,**
810 **2009; Miller et al., 2012; Winnick and Caves, 2015 ; Dimitru et al 2019; Miller et al., 2020a**),
811 whereas Mg/Ca paleothermometry calibration of benthic δ¹⁸O records suggest a GMSL up to
812 +40 m above present (**Figure 6e**). GMSL changes based solely on benthic δ¹⁸O records,
813 however, yield large uncertainties (±15m) (e.g. **Raymo, 2018**). GMSL change amplitudes

814 larger than +30 m above present can only be explained by melting the terrestrial sectors of
815 the AIS, but retreat of the the EAIS in the Ross Sea since 8 Ma appears not likely because a
816 recent study that found extremely low concentrations of cosmogenic ^{10}Be and ^{26}Al isotopes in
817 the ANDRILL AND-1B marine sediment core (**Shakun et al., 2018**). In addition, many of these
818 peak GMSL estimates (e.g. **Miller et al., 2012; Hearty et al., 2020**) have not been corrected
819 for regional deviations due to tectonics, glacio-isostatic adjustment, and dynamic topography
820 (**Raymo et al., 2011; Rovere et al., 2015; Dumitru et al., 2019**). A reassessment of **Grant et**
821 **al. (2019)** based on far-field data implies GMSL during the warmest mid-Pliocene interglacial
822 was no higher than +21 m (**Grant & Naish, 2021**). This new estimate is very close to the
823 average of +20 m above present provided by sea level reconstructions based on sequence
824 stratigraphy and paleo-shore lines.

825
826 The compilation of simulated Antarctic ice sheet contributions to GMSL ranges from $\sim +3$ m
827 SLE to +15 m SLE (**de Boer et al., 2017; Pollard and DeConto 2009; Pollard & DeConto,**
828 **2012; de Boer et al., 2015; Austerman et al., 2015; Gasson et al., 2015, Yan et al., 2016;**
829 **DeConto & Pollard, 2016; Dolan et al., 2018**) (**Figure 6e**). Although there is no observational
830 evidence of a potential melting from the Greenland Ice Sheet so far, recent transient numerical
831 simulations suggest that the Greenland ice sheet melting could have contributed up to about
832 6 m SLE to GMSL rise (**De Boer et al., 2017**). Based on this estimate, the lower bound GMSL
833 rise (+15 m) implies a contribution of the AIS no larger than 9 m SLE. Considering the upper
834 bound of GMSL rise of about +20 m to + 28 m above present, the maximum contribution of
835 the AIS thus ranges between +15 to +22 m SLE, implying melting of the WAIS and all marine-
836 based sectors of the EAIS (e.g. **DeConto and Pollard, 2016; Golledge et al., 2017**). Site
837 ANDRILL AND-1B in the Ross Sea recorded numerous occurrences of open-marine
838 conditions suggesting frequent retreats of the Ross Ice Shelf during the mPWP (**Naish et al.,**
839 **2009**). Provenance of fine-grained detritus offshore the Wilkes Subglacial Basin and ice-rafted
840 debris offshore the Aurora Subglacial Basin and Prydz Bay was attributed to the retreat of
841 marine-based sectors of the East Antarctic ice sheet (**Whitehead et al. 2006; Cook et al.,**
842 **2013, 2014; Bertram et al., 2018; Blackburn et al., 2020**). Similar circum-Antarctic retreat
843 of the marine-based sectors was simulated for one of the Early Pliocene interglacials
844 (**Golledge et al., 2017**), supported by sedimentological and geological evidence of a circum-
845 Antarctic warming events during that period (e.g. **Whitehead and Bohaty, 2003; Escutia et**
846 **al 2009; McKay et al., 2012a**).

847
848 **Marine Isotope Stage 31** (MIS 31, 1.081-1.062 Ma) is a prominent mid-Pleistocene
849 interglacial categorised as “super interglacial” based on the expanded lacustrine sediment
850 record from Lake El'gygytgyn in Siberia (**Melles et al., 2012**). It corresponded to an
851 exceptionally high eccentricity and obliquity inducing particularly intense high-latitude
852 summers. The level of atmospheric CO_2 is not well known for this interval but ranges from 300
853 to 420 ppm (**Honisch et al., 2009**) (**Figure 6a**). A circum-Antarctic warming has been inferred
854 from sediment core analysis in the Ross Sea (**Scherer et al., 2008; Naish et al., 2009**), in
855 Prydz Bay (**Villa et al., 2008**), on the Adélie Land margin and in the Antarctic Peninsula
856 (**Beltran et al., 2020**). In particular, the presence of diatoms in the Cape Roberts sediment
857 record (**Scherer et al. 2008**) suggested a 3-5 °C warming of upper ocean temperatures
858 compared to today, with seasonally open-ocean (no summer sea ice) (**Figure 6d**). For the
859 Adélie Land margin and the Antarctic Peninsula, **Beltran et al. (2020)** reconstructed summer
860 SSTs that were on average were 3°C to 6°C warmer than today (**Figure 6c**). Similar warm
861 conditions are recorded in the Ross Sea at site ANDRILL AND-1B as indicated by seasonal
862 open-ocean conditions (**Figure 6d**) and suggesting a retreat of the Ross Ice Shelf (**Naish et**
863 **al., 2009; McKay et al., 2012b**). Global mean sea level rise during MIS 31 is relatively poorly
864 constrained from far-field records. Sea-level indicators preserved in coastal cliffs of the
865 Northern Cape Province of South Africa and from Cape Range, Western Australia, suggest
866 highstands not more higher than +15 – 16.5 m above present mean sea level (**Hearty et al.,**
867 **2020; Sandstrom et al., 2020**). Note that those estimates are not corrected from GIA,
868 dynamic topography and local tectonic. Far-field evidences of four consecutive Middle

869 Pleistocene Transition sea-level highstands between MIS 31 and MIS 35 were identified in a
870 speleothem record from a western Sicily cave (Mediterranean Sea) (**Stocchi et al., 2017**).
871 The peculiarity of this marine cave is that it has been last flooded between MIS 35 and MIS
872 31, and has been tectonically uplifted to higher elevations afterward. Among several GIA-
873 modulated relative sea level scenarios, only those accounting for a significant AIS retreat up
874 to about 25 m SLE at MIS 31 and 35, are capable to flood the marine Sicilian cave. The
875 compilation of simulated AIS melting contribution to GMSL ranges from 2 to 10 m SLE
876 (**DeConto et al., 2012; de Boer et al. 2013; Beltran et al 2020**) (**Figure 6e**). The upper bound
877 of this range is in agreement with far-field, though uncorrected, sea level changes and indicate
878 a large WAIS retreat, with a modest contribution from East Antarctic marine-based sectors. In
879 fact, mineralogical provenance from IBRD from ODP Site U1090 (South Atlantic) and ODP
880 Site U1165 (Prydz Bay) revealed that the EAIS retreated significantly over MIS 31 and
881 particularly in the Prydz Bay region. However, other sectors of the EAIS were still
882 characterized by active marine margins (**Teitler et al., 2015**). **Beltran et al. (2020)** suggested
883 that the AIS retreat was caused by a stronger advection of Circumpolar Deep Water (CDW)
884 resulting from the changes of the westerlies (subpolar jet). Such process was also inferred
885 from changes in the geochemical composition of Holocene foraminifera shells from the
886 Amundsen Sea and the aeolian dust from a West Antarctic ice core record. Both geological.
887 evidence support the notion of enhanced advection of CDW onto the continental shelf due to
888 a strengthening / poleward shift of the westerlies can drive WAIS retreat (**Hillenbrand et al.,**
889 **2017**).
890

891 **Marine Isotope Stage 11** (MIS 11, 425-375 ka) occurred close to the Mid-Bruhnes Event
892 (**Figure 1**). It is the Late Pleistocene warm stage considered as one of the closest analogues
893 to our future because astronomical forcing of a few time slices within MIS 11 are very similar
894 to today (**Loutre and Berger, 2003**). MIS 11 is also the oldest middle Pleistocene interglacial
895 categorised as a “super interglacial” based on lacustrine sediment records from the Lake
896 El'gygytgyn in Siberia (**Melles et al, 2012**). Global mean air temperature was 1.5-3°C higher
897 compared to modern temperatures (**Figure 6b**) although atmospheric CO₂ levels were around
898 280 ppm (**Figure 6a**). On the Antarctic plateau, the surface air temperature increased by 2°C
899 to 3°C (**Jouzel et al., 2007; Uemura et al., 2018**). A polar amplification occurred during that
900 period but was reduced compared to MIS 31 or older warm periods. MIS 11 is not really an
901 intense but brief interglacial such as MIS 5e (130-116 ka, see below); its major characteristic
902 is its longer duration of ~ 50,000 years (**Tzedakis et al., 2012**), which may have been key to
903 ice sheet melting (**Irvali et al., 2020**). Reconstructed SSTs were not much warmer than
904 modern temperatures (e.g. **Hodell et al., 2000; King and Howard, 2000; Becquey and**
905 **Gersonde, 2002, 2003a, 2003b**). In fact, geological evidence supports the idea that a modest
906 but sustain warming was at the origin of ice sheet retreat in the Wilkes Subglacial basin during
907 MIS 11 (**Wilson et al., 2018; Blackburn et al., 2020**). Recent modelling studies, indeed,
908 showed that the WAIS and part of the EAIS retreat could occur with a limited warming of
909 +0.4°C if applied for a duration of 4 000 years (**Mas e Braga et al., 2021**). As with other past
910 intervals, the absence of ice proximal oceanic temperature reconstructions is thus one of the
911 critical gaps to constrain ice sheet simulations of this interval. Reconstructed GMSL from data
912 suggest a rise of about +13 m above present sea level (**Raymo and Mitrovica, 2012; Roberts**
913 **et al. 2012**) and up to +20 m during MIS 11 (**Kindler and Hearty, 2000; Hearty et al., 1999;**
914 **Brigham-Grette, 1999**). Such a range of sea level rise implies the complete melting of both
915 the Greenland Ice Sheet and the WAIS, which would account for about 12 m SLE, leaving
916 about 8 m SLE from the EAIS melting (e.g. **Lythe et al., 2001; Warrick et al., 1996. Mas e**
917 **Braga et al. (2021)** recently simulated a contribution from the WAIS around 4.3 - 4.5 m SLE
918 and a contribution from the EAIS ranging from 2.3 to 3.7 m SLE. Sedimentological analyses
919 from Erik Drift, Southeast Greenland reveal that most of South Greenland deglaciated during
920 MIS 11 (**Reyes et al., 2014**). The compilation of simulated AIS contributions to GMSL ranges
921 from ~ -3 m SLE to + 13 m SLE (**Tigchelaar et al. 2018; Sutter et al. 2019; Mas e Braga et**

922 al., 2021) (Figure 6e) and in absence of further geological constraints, it is difficult to refine
923 this range.

924 **Marine Isotope Stage 5e or Last Interglacial (LIG, 130-116 ka)** was the most recent
925 interglacial with temperatures warmer than today. It has long been considered as an analogue
926 for the future climatic changes (Jansen et al., 2007). However, at the peak of the LIG, the
927 astronomical forcing differed too much from the present-day to be a true analogue
928 (Ganopolsky and Robinson, 2011). Nevertheless, the LIG presents a very useful time period
929 for understanding the Earth System response (e.g. internal feedbacks in the climate system)
930 to the Paris Agreement temperature targets (e.g. IPCC 1.5C Special Report). Atmospheric
931 CO₂ concentration were low (Figure 6a), and reconstructed global mean temperature is
932 estimated to have been about 0.5-2°C higher than today (Masson-Delmotte et al., 2013;
933 Hoffman et al., 2017) (Figure 6b). The East Antarctic plateau recorded a warming up to 5.5°C
934 at ~128.66 ka followed by a plateau around 2°C (Petit et al., 1999; Watanabe et al., 2003;
935 Jouzel et al., 2007). A polar amplification thus occurred during this period (Capron et al.,
936 2017), and was broadly of the same magnitude than during MIS 11. Antarctic continental
937 margin sediment records imply seasonal sea ice in most of the sensitive marine-based sectors
938 (e.g. Konfirst et al. 2012; Presti et al. 2011) (Figure 6d). Global mean sea level rise is
939 estimated to about +5.9 m to +9.3 m above present level from paleo-shorelines (Dutton et al.,
940 2015 and ref. therein) and up to almost +20 m based on calibration of benthic and planktonic
941 $\delta^{18}\text{O}$ records (Waelbroeck et al., 2009; Rohling et al., 2009) (Figure 6d), also involving some
942 Greenland Ice Sheet melting. However, ice core constraints and modelling studies suggest
943 that the contribution from Greenland was likely about +2-3m (Dahl-Jensen et al, 2013),
944 implying a significant meltwater contribution from Antarctica, although also a Greenland Ice
945 Sheet contribution of up to +5.1 m SLE has been suggested (Yau et al., 2016). The
946 compilation of simulated AIS melting contributions to GMSL range from about -2 m SLE to +
947 8 m SLE (Figure 6e) (e.g. Huybrechts et al. 2002; Pollard and DeConto 2012; de Boer et
948 al. 2015; Goelzer et al. 2016; Sutter et al. 2016; DeConto and Pollard 2016; Tigchelaar et
949 al. 2018; Quiquet et al. 2018; Colleoni et al. 2018b; Sutter et al. 2019; compilation in De
950 Boer et al., 2019). Antarctic ice core records of $\delta^{18}\text{O}$, considered as a proxy for ice volume
951 changes, have been analysed in an attempt to better constrain the individual contribution of
952 Antarctica to GMSL. Based on these analyses, numerical climate and ice sheet simulations
953 suggest that part of the $\delta^{18}\text{O}$ signal could be explained by sea ice reduction rather than ice
954 sheet retreat (e.g. Holloway et al., 2016). In absence of ice proximal ocean temperature
955 reconstructions, as for other Late Pleistocene interglacials, it is very difficult to constrain the
956 magnitude and timing of the Antarctic ice sheet retreat during this interval. The magnitude of
957 oceanic warming required to trigger a large retreat of the marine-based sectors at that time
958 varies between models from +2°C to +3°C relative to pre-industrial temperature (e.g. Sutter
959 et al., 2016, DeConto and Pollard, 2016, Turney et al., 2020). However, Turney et al. (2020)
960 also showed that with a modest ocean warming of +0.4°C, the major ice shelves disintegrated
961 within 600 years. While continental margin sediments offshore from the Wilkes Subglacial
962 Basin suggested a reduction of this marine-based sector of the EAIS during MIS 5e (Wilson
963 et al. 2018), geological evidence from the WAIS are contradictory and suggests either that no
964 major ice sheet retreat occurred (e.g. Hillenbrand et al. 2002,2009; Spector et al., 2018;
965 Clark et al., 2020) or that considerable retreat took place (e.g. Turney et al. 2020).

966

967 **6. Antarctica and global teleconnections: the bipolar seesaw**

968

969 Inter-hemispheric heat transport, the so-called bipolar see-saw (Stocker and Johnsen,
970 2003), is another key process affecting AIS evolution. It regulates oceanic and atmospheric
971 temperatures at sub-millennial to millennial time scales. The bipolar see-saw mechanism was
972 hypothesized by Stoker et al. (1998) on the basis of observed asynchronous changes in ice
973 core records between Greenland and Antarctica for some of the Dansgaard/Oeschger events

974 that occurred during the last glacial cycle (**Blunier et al., 1998**). **Stocker and Johnsen, (2003)**
975 hypothesized that icebergs melting and meltwater discharges close to the North Atlantic
976 convection sites caused a substantial weakening of the Atlantic Meridional Oceanic Circulation
977 (AMOC). Such a slowdown of the AMOC could have induced a gradual heat transfer to the
978 South, with a lag of a few centuries to millenia, thus explaining the asynchronous temperature
979 changes between Greenland and Antarctic ice core records during the last glacial period
980 (**EPICA Community Members, 2006, Pedro et al., 2018**). Recent findings confirm that for
981 example, the cooling of the Antarctic Cold Reversal is synchronous with the Bølling–Allerød
982 warming in the Northern Hemisphere 14,600 years ago (**Stenni et al., 2011**). The Bølling–
983 Allerød is coincident with the occurrence of meltwater pulse 1A (MWP-1A) that caused a rapid
984 sea level rise of about 9 to 20 m (e.g. **Deschamps et al., 2012; Lambeck et al., 2014; Peltier**
985 **et al., 2015; Liu et al., 2016**) at a rate of 4 meters/100 yr (e.g. **Peltier and Fairbanks, 2006;**
986 **Deschamps et al., 2012; Carlson et al., 2012**). Although some studies have considered the
987 AIS as a potential contributor to MWP-1A (e.g. **Clark et al., 1996; Bassett et al., 2007;**
988 **Weaver et al., 2003; Golledge et al., 2014**), most geological and glaciological studies argue
989 against a large Antarctic contribution from either sector (e.g. **Licht et al. 2004; Bentley et al.,**
990 **2010, The RAISED Consortium, 2014; Spector et al., 2017**). However, IBRD records from
991 “Iceberg Alley” in the Scotia Sea showed recorded the occurrence of eight events between 20
992 ka and 9 ka, including the MWP-1A (e.g. **Weber et al., 2014**). **Etourneau et al., (2019)** showed
993 that a +0.3–1.5 °C increase in subsurface ocean temperature (50–400 m) in the northeastern
994 Antarctic Peninsula drove a major collapse and recession of the regional ice shelf during both
995 the instrumental period and the last 9000 years. Modeling studies support the idea of a
996 responsive marine-based sectors of the AIS at millennial time scales, driven by oceanic
997 melting rather than by atmospheric forcing triggering fast ice sheet instabilities (e.g. **DeConto**
998 **and Pollard (2009); Golledge et al., 2014; Blasco et al., 2019; Lowry et al., 2019**).

1000 Meltwater sources of such millennial oscillations are poorly constrained (e.g. **Clark et al.,**
1001 **2002, Peltier et al., 2005; Liu et al., 2016**). This limits our understanding of the causes of the
1002 events, i.e. warm water advection to the grounding line (e.g. **Golledge et al., 2014**) or bipolar
1003 seesaw caused by melting Northern Hemisphere ice sheets (e.g. **Menviel et al., 2011**), abrupt
1004 global mean sea level rise (e.g. **Clark et al., 2002; Golledge et al., 2014; Gomez et al., 2020**),
1005 atmospheric forcing (e.g. **WAIS Divide Project members, 2015**), or feedbacks within the
1006 climate system. Past, present and future meltwater-climate feedbacks have been widely
1007 studied and there is an extensive literature on modelling the global climate response to
1008 freshwater discharge from ice sheets (e.g. **Stammer et al., 2008; Roche et al., 2014; Boning**
1009 **et al., 2016; Bronselaer et al., 2018, Golledge et al., 2019; Sadai et al., 2020**). Results from
1010 these studies highlight the role of altered inter-hemispheric heat transport on the global climate
1011 both in the past and in the future. Different mechanisms respond to the freshwater at different
1012 timescales but the overall feedbacks loop spans the millennial scale (**Turney et al., 2020**).
1013 The sequence of those feedbacks loops is illustrated in **Figure 7** and is based on two recent
1014 contributions, i.e., **Turney et al. (2020)** for the LIG (130-116 ka), and **Golledge et al. (2019)**
1015 for projected climate changes until 2100 CE following RCP 8.5 emission scenario.

1016
1017 **Turney et al (2020)** reported evidence of substantial ice discharge across the Weddell Sea
1018 sector during the LIG based on a blue-ice core record. Substantiated by with climate and ice
1019 sheet simulations, they suggest that the ice discharge (and subsequent multi-meter global
1020 mean sea level rise) was caused by a millennial-scale oceanic warming following freshwater
1021 discharge in the Northern high latitudes (Heinrich event 11 at ~ 135-130 ka) and a weakening
1022 of the AMOC (**Böhm et al., 2015**). This mechanism corresponds to the bipolar see-saw.
1023 **Turney et al., (2020)** identified a loop of positive ice-sheet-climate feedbacks that further
1024 amplified the warming close to the Antarctic margin. **Grant et al. (2014)** identified two main
1025 meltwater pulses, one at 139 ka pre-dating Heinrich event 11 (135 ± 1 and 130 ± 2 ka) and
1026 one occurring at about 133 ka during this Heinrich event. **Marino et al. (2015)** found that
1027 Heinrich event 11 coincided with a rapid sea-level rise mostly explained by Northern
1028 hemisphere ice sheets deglaciation. The occurrence of this meltwater pulse supports the

1029 positive feedbacks described in **Turney et al. (2020)** and potentially explains the delayed
1030 timing of AIS contribution to the GMSL highstand at the LIG. A delay of a few thousands of
1031 years is supported by the idealised modelling study by **Blasco et al. (2019)**, suggesting that
1032 the bipolar seesaw accumulated heat in the Southern Hemisphere, enhancing ocean warming
1033 on a millennial time scale during the last deglaciation. Similarly, **Clark et al. (2020)** suggested
1034 that the rate of global mean sea level changes during the LIG as well as spatial sea level
1035 variations could be explained by the responses of the Antarctic and Greenland ice sheets to
1036 Heinrich event 11 and associated climate feedbacks. The sequence of feedbacks in **Turney**
1037 **et al. (2020)** can be applied to other interglacials and is as follows (**Figure 7**, top):
1038

- 1039 (1) Northern high-latitude freshwater was released during the Heinrich 11 event (~135 and
1040 130 ka);
- 1041 (2) Subsequently, a weakening of North Atlantic Deep Water (NADW) flow was observed,
1042 and heat was transferred gradually southward.
- 1043 (3) An increased in meridional inter-hemispheric thermal gradient due to Northern high
1044 latitudes cooling induced a southward shift of the Inter-Tropical Convergence Zone
1045 (ITCZ) and of the Southern Hemisphere westerly winds (e.g. **Shevenell et al., 2011**).
- 1046 (4) The southward shift and strengthening of the westerlies (e.g. **Hillenbrand et al., 2017**,
1047 **Etourneau et al., 2019**; **Lamy et al., 2019**, **Dickens et al., 2019**) drove an enhanced
1048 northward Ekman transport and a stronger southward advection of CDW on the
1049 continental shelf (e.g. **Hillenbrand et al., 2017**, **Minzoni et al., 2017**).
- 1050 (5) Enhanced advection of CDW amplified the melting of the AIS and of the sea ice,
1051 triggering the AIS retreat. Northward transport of cool surface waters caused sea ice
1052 expansion and local atmospheric cooling.
- 1053 (6) Large freshwater discharge caused a reduction in Antarctic Bottom Water (AABW)
1054 formation and a subsequent increase in NADW formation. Increase NADW formation
1055 led to heat transfer towards northern high latitudes, and thus a bipolar see-saw swing
1056 towards the north.

1057 **Golledge et al. (2019)** simulated a similar ice-sheet-climate sequence of feedbacks by
1058 considering on-going and projected meltwater discharge from the Greenland and Antarctic ice
1059 sheets until 2100 CE at the same time. Results show that a slow-down of the AMOC occurs
1060 in response to Greenland Ice Sheet melting, and that projected meltwater discharge from
1061 Antarctica can trap heat of CDW at intermediate depths on the continental shelf (**Silvano et**
1062 **al., 2018**, **Bronselear et al., 2018**; **Sadai et al., 2020**), establishing a positive feedback
1063 establishes that further enhances AIS melting (**Figure 7**, bottom):
1064

- 1065 (1) Projected freshwater release at Northern and Southern high-latitudes;
- 1066 (2) A weakening of NADW formation is observed, and heat is transferred gradually
1067 southward; In the South, freshwater stratifies the continental shelf waters.
- 1068 (3) Increased in meridional inter-hemispheric thermal gradient induces a weak southward
1069 shift of the ITCZ and of the Southern Hemisphere Westerly winds.
- 1070 (4) Southward shift of the westerly winds drives an enhanced northward Ekman transport
1071 compensated by a stronger southward advection of CDW on the continental shelves,
1072 which amplifies the melting of Antarctic ice shelves and sea ice.
- 1073 (5) Continental shelf water stratification fosters a northward Ekman transport of cool
1074 surface waters associated with sea ice expansion and local atmospheric cooling. This
1075 mechanism further amplifies the advection of CDW to the AIS grounding line and
1076 initiates its retreat.
- 1077 (6) Larger freshwater release further causes a reduction in AABW formation.

1078 Compared to **Turney et al. (2020)**, the sequence of processes and feedbacks in 2100 remains
1079 incomplete and stops before all the heat from the North is transferred to South. This suggests
1080 that additional decades to centuries are needed for the effects of the bipolar see-saw on
1081 southern high latitudes to be felt.
1082
1083

1084
1085
1086
1087
1088
1089
1090
1091
1092
1093
1094
1095
1096
1097
1098
1099
1100
1101
1102
1103
1104
1105
1106
1107
1108
1109
1110
1111
1112
1113
1114
1115
1116
1117
1118
1119
1120
1121
1122
1123
1124
1125
1126
1127
1128
1129
1130
1131
1132
1133
1134
1135

7. The PAIS legacy: bridging the past and the future

7.1 The PAIS legacy

The PAIS legacy is clearly one of successful delivery on addressing high-level scientific priorities. Beyond this, it is also the story of a long-lasting network of collaborations, among different nations and researchers and striving to share scientific infrastructure and capability to investigate remote and challenging Antarctic regions and to address high-level scientific priorities. The multidisciplinary concept of the PAIS programme represented the key to its success. Eight years after the start of the programme, PAIS achievements are many, both in terms of field campaigns and in terms of scientific advances concerning Antarctic ice sheet dynamics. Several projects fostered by the PAIS programme fostered, which contributed to major scientific advances in constraining AIS contribution to past sea level changes, fostered by the PAIS programme, are briefly summarized below. This list is far from being exhaustive and the interested readers can refer to the **other chapters of this book** for more detailed descriptions of PAIS research outcomes and other time periods not discussed here.

Antarctic Ice Sheet sensitivity during past high-CO₂ worlds and its contribution to global sea-level change

Geological proxies from the Antarctic continental margin have improved reconstructions of ocean and land temperatures, sea-ice extent, ice sheet extent, subglacial hydrology, carbon cycle feedbacks and paleogeography for past warm climate states. This has provided improved boundary conditions for testing and developing ice sheet and climate models skills and performance, as well as evaluating model sensitivity. Significant outcomes include:

- Reconciling southern high-latitude meridional temperature gradients and polar amplification between model simulations and data during Greenhouse climates (e.g. **Pross et al., 2012; DeConto et al., 2012**) and new knowledge of Antarctic margins SSTs and SWTs during the MCO, the mPWP and MIS 31 (**McKay et al., 2012, Levy et al., 2016, Sangiorgi et al., 2018; Hartman et al., 2018; Beltran et al, 2020**). Polar amplification is much larger during the MCO, mPWP and MIS 31 than during the Pleistocene interglacials. Those findings allow an estimate of Earth's climate sensitivity to high atmospheric CO₂ concentrations.
- Constraining equilibrium and transient ice volumes (e.g. **de Boer et al., 2015; DeConto et al., 2012; Pollard et al., 2015; DeConto & Pollard, 2016; Goelzer et al., 2016; Gasson et al., 2016; Golledge et al., 2017; Dolan et al., 2018; Clark et al., 2019, Stap et al., 2019**), and the contribution to global sea-level under past "warmer-than-present" climates (e.g. **Miller et al., 2012; Dutton et al., 2015; Miller et al., 2020a, 2020b**).
- Recognition of the importance of bedrock topography and paleobathymetry on past Antarctic ice volume reconstructions (e.g. **Gasson et al., 2016** building on **Wilson & Luyendyke, 2009; Hochmuth and Gohl, 2019; Paxman et al., 2019; Hochmuth et al., 2020, Paxman et al., 2020**) and sensitivity to ocean warming (e.g. **Colleoni et al., 2018a; Paxman et al., 2020**).
- Recognition of the sensitivity of marine-based sectors of the EAIS from models and data (e.g. **Cook et al., 2013, 2014; Reinardy et al., 2015; Bertram et al., 2018; Pierce et al., 2017; Scherer et al., 2016; Levy et al., 2016; Gasson et al., 2016; Aitken et al., 2016; Gulick et al., 2017; Simkins et al., 2017; Golledge et al., 2017b; Wilson et al., 2018; Blackburn et al., 2020**).

- 1136 ▪ Insights into the influence of mean climate state (CO₂) on the response of the AIS to
1137 orbital forcing (e.g. **Dolan et al., 2011; Patterson et al., 2014; Levy et al., 2019**
1138 building on concepts in **Naish et al., 2009; Stap et al., 2019, 2020, Sutter et al., 2019**).

1139
1140 ***Geological evidence of ocean forcing and marine ice sheet instability:***

1141
1142 The potential for abrupt and non-linear “runaway” retreat of the marine-based sectors of the
1143 AIS due to marine ice sheet instability (MISI) and potentially also marine ice cliff instability
1144 (MICI) up until recently had only been mathematically simulated in ice sheet models.

- 1145
1146 ▪ Geological observations of the last deglaciation and recent observations coupled with
1147 models have now identified MISI during the Holocene after atmospheric forcing had
1148 weakened in the Ross Sea (e.g. **Jones et al., 2015; McKay et al., 2016; Spector et**
1149 **al., 2017; Bart and Tulaczyk, 2020**), and potentially MICI in the Amundsen Sea sector
1150 (**Wise et al., 2017**) and Antarctic Peninsula (**Rebesco et al., 2014**)
1151 ▪ There are geological and modern oceanographic observations of oceanic warm waters
1152 reaching the grounding line of marine-based ice sheets (e.g. **Joughin et al., 2011;**
1153 **Schmidko et al., 2014; Hillenbrand et al., 2017; Rintoul et al., 2016; Smith et al.,**
1154 **2017; Hansen and Passier, 2017**)

1155
1156 ***Improved temporal and spatial patterns of AIS retreat and its contribution to global***
1157 ***Melt-Water Pulse 1A:***

1158
1159 Improved geological and bathymetric constraints combined with ice sheet models have shown:

- 1160 ▪ An improved understanding of the extent and dynamics of the Last Glacial Maximum
1161 ice sheet and deglaciation into the Holocene (e.g. **Hillenbrand et al., 2014; Larer et**
1162 **al., 2014; O’Cofaigh et al., 2014; Hodgson et al., 2014; Golledge et al., 2013;**
1163 **Mackintosh et al., 2014; The RAISED Consortium, 2014; Anderson et al., 2014;**
1164 **Johnson et al., 2014; Lee et al 2017; McKay et al., 2016**).
1165 ▪ the AIS contributed to melt-water pulse 1A (e.g. **Golledge et al., 2014; Weber et al.,**
1166 **2014**), though not from all sectors (e.g. **Spector et al., 2017**) and to other millennial
1167 scale fluctuations with estimated contributions to global mean sea level up to 6 m SLE
1168 (**Blasco et al., 2019, Golledge et al., 2014**), at a rate of about 1 meter/century in the
1169 case of MWP-1A (e.g. **Golledge et al., 2014**).

1170
1171 ***A better understanding of ice-sheet-ocean interactions***

- 1172
1173 ▪ During the last deglaciation, proxy data and model simulations consistently find that
1174 ocean warming drove the ice sheet retreat in different sectors of Antarctica (e.g.
1175 **Hillenbrand et al., 2017; Crosta et al., 2018, Wilson et al., 2018**).
1176 ▪ Ocean warming is also thought to have accelerated the last deglaciation in the Ross
1177 Sea during MWP-1A (e.g. **Golledge et al., 2014**), although this finding is challenged
1178 by geological evidence from the Tran-Antarctic Mountains (e.g. **Spector et al., 2017**).
1179 Based on regional ice sheet simulations, atmospheric forcing can enhance, diminish
1180 or compensate for oceanic warming during the first half of the deglaciation, while during
1181 the second half, ocean warming clearly drove the end of the ice sheet retreat (**Buizert**
1182 **et al., 2015; Blasco et al., 2109; Lowry et al. 2019**).
1183 ▪ Strengthening of the subpolar jet during deglaciation (e.g. **Lamy et al., 2020**)
1184 enhanced advection of CDW towards the continental margins. (**Hillenbrand et al.,**
1185 **2017; Minzoni et al., 2017; Salabarnada et al., 2018; Evangelinos et al., 2020**).
1186 ▪ Improved understanding of sedimentological facies indicative of sub-ice shelf
1187 environment opens new perspectives on quantifying the influence of the ocean on the
1188 AIS evolution through time (e.g. **Yokoyama et al., 2016; Smith et al., 2019**).
1189 ▪ Freshwater release from the Northern high latitudes can induce a bipolar seesaw,
1190 transferring heat to the Southern Hemisphere and fostering AIS retreat a few

1191 thousands of years later (**Buizert et al., 2015; Blasco et al., 2019; Turney et al.,**
1192 **2020; Clark et al., 2020**). Likewise, freshwater release from Antarctica can stratify the
1193 ocean, reduces vertical mixing and the release of heat and gas to the surface, increase
1194 heat transport at the grounding lines of marine-based ice sheets (e.g. **Golledge et al.,**
1195 **2019; Silvano et al., 2019**)

1196
1197

Antarctic ice-Earth interactions and their influence on regional sea-level variability and Antarctic Ice Sheet dynamics

1199

1200
1201 The importance of departures in regional sea-level changes from eustatic sea-level due to
1202 rotational, visco-elastic and gravitational changes as water mass is transferred between the
1203 ice sheets and the ocean has been identified in the far and near-fields of the AIS from paleo-
1204 reconstructions (e.g. **Clark et al., 2002; Milne et al. 2008, Raymo et al. 2011, Raymo and**
1205 **Mitrovica, 2012; Stocchi et al., 2013; Rovere et al., 2014**). This has been established
1206 through 1D and 3D glacio-isostatic adjustment models that couple (runtime or asynchronously)
1207 ice sheets and solid Earth processes constrained by both near-field and far-field geological
1208 reconstructions of sea-level changes. Important outcomes include:

1209

- 1210 ▪ Role of Earth deformation processes (GIA and dynamic topography) on near-field sea-
1211 level changes and ice sheet dynamics (e.g. **Gomez et al., 2018; Stocchi et al., 2013;**
1212 **Austermann et al., 2015; Gomez et al., 2015; Whitehouse et al., 2017, 2019;**
1213 **Gomez et al., 2018; Pollard et al., 2017; Kingslake et al., 2018**).
- 1214 ▪ Impact of global gravitationally consistent sea level changes induced by Northern
1215 Hemisphere ice sheets fluctuations on the retreat of the AIS (e.g. Gomez et al., 2020).
- 1216 ▪ Impact of long-term global mean sea level changes on the stability of EAIS (e.g.
1217 **Shakun et al., 2018; Jakob et al., 2020**).

1218

Improved interpretation of subglacial processes from mapping seabed

1219

- 1220 ▪ Multibeam campaigns in different sectors of Antarctica have mapped the
1221 geomorphological footprints of paleo ice streams and their associated paleo-drainage
1222 networks (e.g. **Nitsche et al., 2013, The RAISED consortium, 2014; Simkins et al.,**
1223 **2017, Larter et al., 2019, Kirkham et al., 2019**) as well as other subglacial features
1224 (**Kuhn et al., 2017; Bart et al., 2018; Stokes et al., 2018; Dowdeswell et al. 2020**).
- 1225 ▪ Analysis of the characteristics of those geomorphological features inform the long-term
1226 mean and potential maximum rates of grounding line retreat (e.g. 1 to 10 km/yr, **Bart**
1227 **et al., 2018, Dowdeswell et al. 2020**), but also show that meltwater can enhance ice
1228 flow and cause ice surges and meltwater outbursts (e.g. **Simkins et al., 2017; Kuhn**
1229 **et al., 2017**). These reconstructions provide constraints on the ice flow regime during
1230 both advances and retreats and on the mechanics and dynamics of ice stream (**Stokes**
1231 **et al., 2018**).

1232

Paleo-data calibrated ice sheets models provide revised global sea-level predictions for IPCC scenarios

1233

1234 A new generation of continental scale ice sheet models that simulate MISI and in one case
1235 MICI have been developed and tested by reconstructing past AIS volume and extent
1236 constrained by paleoclimate and paleo-ice extent data. These models have been used to
1237 simulate future Antarctic meltwater contribution to global mean sea-level changes based on
1238 the Representative Concentration Pathways. Implications include:

1239

- 1240 ▪ That Antarctic contribution to global sea-level rise for the year 2100 CE and beyond
1241 may have been under-estimated in IPCC AR5 projections especially for high emission

1242
1243
1244

- 1245 scenarios (e.g. **Golledge et al., 2015; DeConto & Pollard, 2016; Edwards et al.,**
1246 **2019; Golledge et al., 2020**).
- 1247 ▪ These paleo-calibrated AIS models show that a threshold for marine ice sheet stability
1248 may exist at ~1.5-2°C global warming above pre-industrial (e.g. around RCP 2.6, the
1249 target of the Paris Agreement) (e.g. **Golledge et al., 2015; Clarke et al., 2015; Pollard**
1250 **& DeConto, 2016**).
 - 1251 ▪ Recent paleo-studies have stressed that a moderate local oceanic warming, lower than
1252 the upper bound of +1.5°C-2°C for pan-Antarctic ocean warming can also trigger fast
1253 ice sheet retreat if applied for a few centuries: **Beltran et al. (2020); Turney et al.,**
1254 **(2020); Golledge et al., (2017a); Bakker et al., (2017); Feldmann and Levermann,**
1255 **(2015)**. This highlights the importance of polar amplification for the fast response of
1256 polar areas under past and future global warming conditions.

1260 7.2 Challenges for the next programmes

1261
1262 Gaps illustrated above highlight the necessity to assess whether or not the WAIS only partially
1263 retreated or totally disintegrated during past warm periods. Records of such massive ice sheet
1264 retreats are possibly located below the ice sheet. Locating subglacial drilling sites that could
1265 have recorded such extensive retreat represents a high priority challenge worthy of future field
1266 campaigns (e.g. **Bradley et al., 2012; Spector et al., 2018**). Similarly, it is urgent to assess
1267 the EAIS marine-based sectors sensitivity to oceanic and atmospheric warming during past
1268 warm periods (e.g. **Cook et al., 2013, 2014; Reinardy et al, 2015; Aitken et al., 2016; Gulick**
1269 **et al., 2017; Pierce et al., 2017; Wilson et al., 2018; Blackburn et al., 2020**) and their
1270 potential contribution to global mean sea level change (e.g. **DeConto and Pollard 2016;**
1271 **Paxman et al., 2020; Mas e Braga et al., 2021**) to refine their future contribution to on-ongoing
1272 sea level rise (e.g. **Golledge et al., 2017b; Rignot et al., 2019**).

1273
1274 Paradoxically, even though the Pleistocene interglacials are more recent and well documented
1275 in many places around the world, AIS fluctuations through time have destroyed most of the
1276 ice proximal geological evidence of these interglacials on the continental shelf, making direct
1277 records of the ice sheet's behaviour difficult to find. Only a few precious SST records are
1278 currently available from the Antarctic continental slope and rise and those records are indirect
1279 and cannot fill the gap of ice proximal ocean temperature records. This data gap directly
1280 impedes the validation of numerical paleo-climate and paleo-ice sheet numerical simulations.
1281 The interpretation of sedimentary facies and geomorphological features on the seafloor,
1282 however, does allow to infer the type of sub-glacial environments and thus the ice flow during
1283 past deglaciations to be reconstructed (e.g. **Smith et al., 2019; Simkins et al., 2017; Bart et**
1284 **al., 2018; Prothro et al., 2020**).

1285
1286 Another observational challenge is to recover records with sub-millennial temporal resolution
1287 for the different past warm periods. Such high-resolution archives can be recovered from the
1288 continental slope and rise, by drilling levee deposits and contourite systems, or from the on
1289 the continental shelf in overdeepened basins and fjords (e.g. ODP leg 178 The Palmer Deep
1290 **Domack et al., 2001; IODP Exp 318, Ashley et al., 2020; IODP Expedition 374 Ross Sea,**
1291 **McKay et al., 2019; IODP Expedition 379 Amundsen Sea, Gohl et al., 2019; approved IODP**
1292 **proposal 732 Antarctic Peninsula, Channell et al.**). High-resolution data represent the bridge
1293 between the past and the future, in particular for centennial to millennial-scale climate
1294 oscillations (e.g. **Weber et al. 2014; Bakker et al., 2017; Bracegirdle et al., 2019; Noble et**
1295 **al., 2020; Golledge et al., 2020**). High-resolution sedimentary data are also important for
1296 correlating marine sediment records with ice core records of the past 800,000 years. The on-
1297 going Beyond EPICA: Oldest Ice project (e.g. **Fischer et al. 2013; Parrenin et al., 2017;**
1298 <https://www.beyondepica.eu/>) will allow correlation with expanded sediment records from the
1299 Ross Sea (IODP Exp. 374) (**McKay et al., 2019**) including the MIS-31 super-interglacial event

1300 and the Amundsen Sea (IODP Exp. 379) (Gohl et al., 2019) across the Mid-Pleistocene
1301 Transition and from future expeditions, for example the IODP proposal 732-Full2.
1302

1303 To maintain pace with advances of the observational ice sheet community, the paleoclimate
1304 modelling community will need to expand efforts more in regional atmospheric and oceanic
1305 modelling for different past periods representing both glacial and interglacial contexts.
1306 Regional modelling is computationally expensive and also requires highly resolved boundary
1307 conditions at high frequency to capture the local variability of processes. Improved large-scale
1308 global climate simulations will also be required to support regional modelling. Many on-going
1309 data-model comparison initiatives already exist, and some of them focus on the periods
1310 described in this chapter, as for example the Paleoclimate Model Intercomparison Project
1311 (PMIP, now in phase 4) (Kageyama et al., 2018), the Pliocene Model Intercomparison Project
1312 (PLIOMIP, now in phase 2) (Haywood et al., 2020), the recently started Miocene Model
1313 Intercomparison Project (MIOMIP) (Steinthorsdottir et al., 2020 and related special issue)
1314 and the Deep-Time Model Intercomparison Project (DEEPMIP) (Lunt et al. 2017). PMIP
1315 focuses on the Late Pleistocene and now also includes transient simulations of entire
1316 interglacials using coupled atmosphere-ocean models. DEEPMIP focuses mainly on the EOT
1317 and the Eocene warmth. More refined global mean sea level records are also necessary to
1318 better assess Antarctic ice volume fluctuations over the past 34 Myrs. Both MCO and mPWP
1319 periods are of high interest to assess Earth climate sensitivity to high CO₂ concentrations
1320 (similar to the projected ones) and global mean sea level rise (e.g. Haywood et al., 2016;
1321 Steinthorsdottir et al., 2020). Sequence stratigraphy of the continental margins is a powerful
1322 approach and the key to fill this gap. However, improvements are needed, especially to correct
1323 those records from glacio-hydro-isostasy (e.g. Grant et al., 2019,2021). Thus, coupled ice-
1324 sheet-GIA-sediment erosion and transport models are needed (e.g. Pollard & DeConto,
1325 2003, 2019, Whitehouse et al., 2019).
1326

1327 Finally, while the climate and paleoclimate communities are currently putting efforts in the
1328 development of fully coupled Earth System Models, such models are too computationally
1329 demanding to allow for long-term transient simulations. With upcoming progress in scientific
1330 computing, and progress in the computing facilities themselves, using fully coupled Earth
1331 System Models now seems an achievable objective for paleo studies.
1332

1333 7.3 Long-term projections and the role of PAIS and future programs 1334

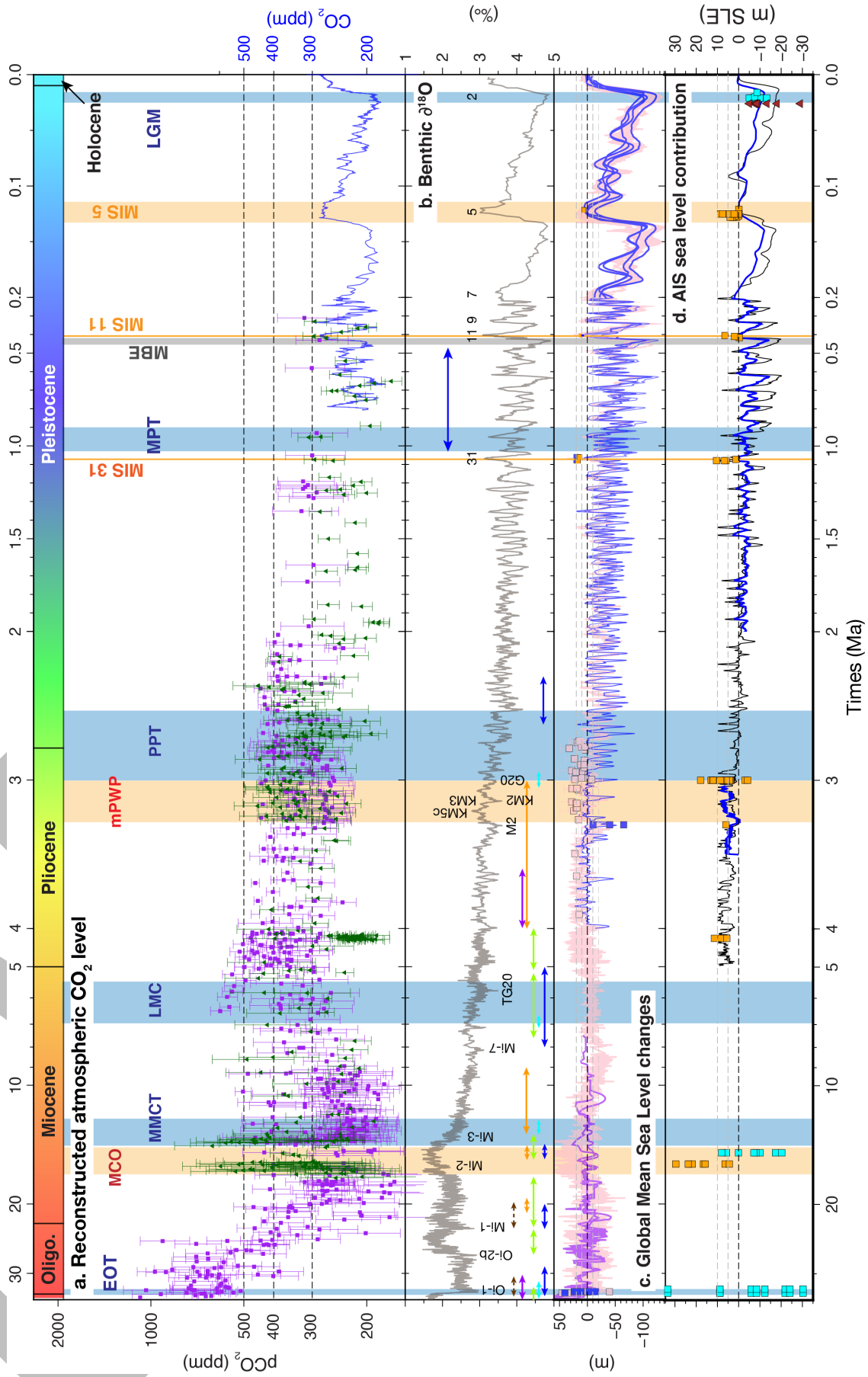
1335 Future projections of AIS evolution have shown large improvements over the past few years
1336 (e.g. DeConto and Pollard, 2016; Pattyn et al., 2018; Edwards et al., 2019). However,
1337 related uncertainties remain large, indicating that fundamental knowledge gaps still persist
1338 about ice sheet dynamics, and interactions with the atmosphere, ocean and the solid earth
1339 (Whitehouse et al., 2019). Morlighem et al. (2020) released an updated subglacial
1340 topography map revealing the high-resolution bed morphology of some of the glacial troughs
1341 and their potential in causing AIS instability in case of fast retreat of the grounding line. Many
1342 of them are still unexplored, despite their clear importance in reconstructing the AIS past,
1343 present and future dynamics. The release of the IPCC Special Report “The Ocean and the
1344 Cryosphere in a Changing Climate” (SROCC) in September 2019 (IPCC, 2019) showed that
1345 our understanding of the various contributions to GMSL change has improved since the last
1346 IPCC Assessment Report 5 (AR5) in 2013. After the release of AR5, further satellites
1347 observations revealed that Antarctic ice shelves were thinning faster than previously thought
1348 (Paolo et al., 2015), caused by observed warming in the surrounding ocean (Pritchard et al.,
1349 2012). Recent re-assessments of 20th century observations confirmed the AIS has been
1350 losing mass since the publication the publication of IPCC AR5 and that this mass loss strongly
1351 accelerated at the end of the 20th century (e.g. Shepherd et al., 2018, Rignot et al., 2019).
1352

1353 To precisely assess the AIS contributions to GMSL changes, the polar community has
1354 increased the monitoring and modelling of AIS evolution. Attention has been focused on ice

1355 shelf buttressing and on large partly marine-based drainage basins of the West and East
1356 Antarctic ice sheet (**Fürst et al., 2016**) (e.g. Pine Island Glacier, Thwaites glacier, Totten
1357 glacier, Recovery ice stream, Foundation ice stream) and ice-ocean interactions around
1358 Antarctica. The particularity of most of the marine-based sectors of the Antarctic ice sheet is
1359 that they are grounded on a bed with retrograde slope (**Joughin and Alley, 2011**;
1360 **Morlinghem et al., 2020**) or that their buttressing ice shelves are pinned on a sill with
1361 retrograde slope bed and are thus vulnerable to future MISI. New estimates of future GMSL
1362 rise from the **IPCC SROCC (2019)** amount to 0.43 m (0.29–0.59 likely range, RCP 2.6
1363 scenario) and 0.84 m (0.61–1.10, likely range, RCP 8.5) in 2100 CE , with the possibility of
1364 multi-meter sea level rise by 2300 CE (**Golledge et al., 2015**; **Clark et al., 2016**) but with
1365 “deep uncertainty (**IPCC SROCC, 2019**). Ice shelf loss is a key prerequisite for the onset of
1366 marine ice shelf instabilities. The large uncertainties in the most recent estimates of sea level
1367 rise from Antarctica mostly result from our inability to assess the potentially unstable behaviour
1368 of the marine-based sectors of the AIS, and in particular: the sensitivity of ice shelves to sub-
1369 ice shelf melting from below and surface warming above. These gaps inevitably lead to model-
1370 dependent results, particularly for processes that are parameterized (**Asay-Davis and**
1371 **Jourdain, 2017**). This is where the past can close those knowledge gaps, and provide
1372 necessary observational constraints to model the past and the future evolution of the Antarctic
1373 ice sheet (e.g. **Gasson and Keisling, 2020**).

1374
1375 The Earth’s past provides a natural laboratory for testing realistic cases of ice-sheet-climate-
1376 solid earth interactions at different timescales (**Bracegirdle et al., 2019**). The research
1377 produced within the PAIS programme has shown that the AIS potentially crossed its tipping
1378 point for major ice loss many times since the onset of large-scale glaciation (~34 Ma) under
1379 climatic conditions warmer than today. Past periods have the potential to identify thresholds
1380 for instability (e.g. **Naish et al. 2009**; **Cook et al., 2013**; **Weber et al., 2014**; **Wilson et al.**
1381 **2018**) or large retreat/re-advance events (e.g. **Scherer et al., 2016**; **Golledge et al., 2017**;
1382 **Kingslake et al., 2018**; **Wilson et al. 2018**) and thus to provide credibility to future scenarios.
1383 Paleo-records also have the potential to reveal new mechanisms as for example the marine-
1384 ice cliff instability (MICI, **Pollard et al., 2015**; ; **DeConto & Pollard 2016**). MICI involves the
1385 fast disintegration of ice shelves by surface-melt induced hydro-fracturing that can trigger
1386 MISI, and rapid calving at thick, marine-terminating ice margins. This mechanism has been
1387 implied to explain rapid major mass loss from the WAIS and EAIS during MIS 5e and the
1388 mPWP (**Pollard et al. 2015**; **DeConto & Pollard 2016**) but many open questions about MICI
1389 and its possible role in past and future sea level rise remain (e.g., **Edwards et al. 2019**; **Pattyn**
1390 **et al., 2018**). Geological and glaciological evidence can also highlight feedbacks in the ice
1391 sheet-climate system (**Turney et al., 2020**) or processes that might not appear policy-relevant,
1392 but are indeed determinant in understanding the future sensitivity of the AIS and sea level rise
1393 to ongoing and projected climate changes (**Haywood et al., 2019**).

1394
1395
1396

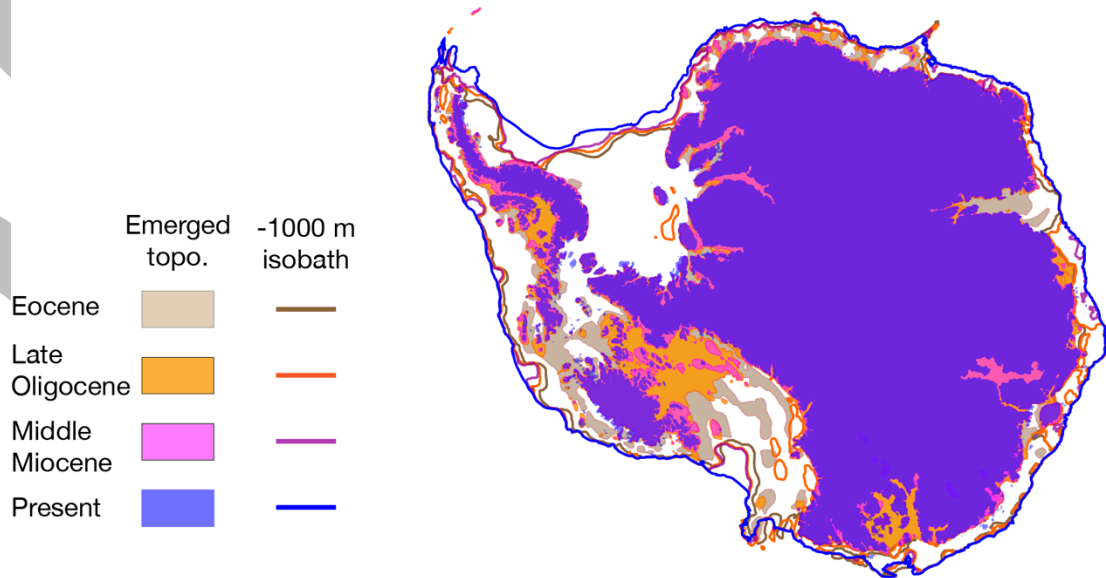
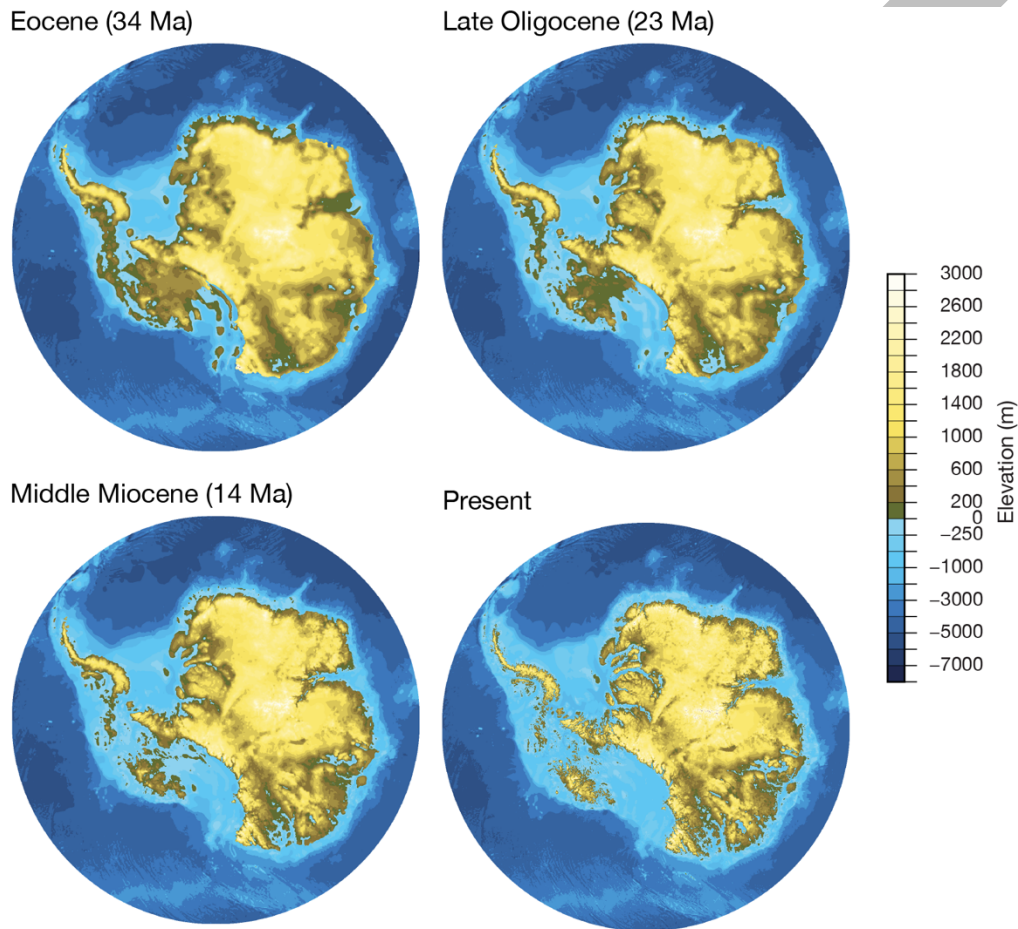


1399
1400
1401
1402
1403
1404
1405
1406
1407
1408
1409
1410
1411
1412
1413
1414
1415
1416
1417
1418
1419
1420
1421
1422
1423
1424
1425
1426
1427
1428
1429
1430
1431
1432
1433
1434
1435
1436
1437
1438
1439
1440
1441
1442
1443
1444
1445
1446
1447
1448
1449
1450
1451
1452
1453
1454
1455
1456
1457

Figure 1: Proxies and simulations synthesis over the past 34 million years. Note that the time scale is logarithmic **a.** Reconstructed atmospheric $p[CO_2]$ levels are based on alkenone (Pagani et al. 2005, 2010, 2011; Seki et al., 2010; Badger et al. 2013a, 2013b; Zhang et al., 2013; Super et al. 2018) and on boron (Honisch et al., 2009; Bartoli et al., 2011; Foster et al., 2012; Greenop et al., 2014; Martinez-Boti, 2015). Late Pleistocene atmospheric CO_2 levels are based on the Antarctic ice core composite record from Bereiter et al., (2015); **b.** Deep sea benthic $\delta^{18}O$ record from Zachos et al. (2001a, 2008). Marine isotope stages (glacials and interglacials) discussed or named in the chapter are indicated and based on Miller et al., (1991) for the Oligocene and Miocene, on Haywood et al. (2016) for the Pliocene and on Lisiecki and Raymo (2005) for the Pleistocene. Note that marine isotope stages EOT-1 (~34.46-33.9 Ma) and EOT-2 (33.7 Ma) are not indicated. Seismic stratigraphic unconformities from different Antarctic sectors are reported with arrows, based on Hochmuth et al., 2020 and references therein (Ross Sea: dark blue; Wilkes Land: green; Weddell Sea: cyan; Amundsen Sea: orange; Cosmonaut Sea: brown; Prydz Bay: purple); **c.** Reconstructed (pink, purple) and simulated (blue) global mean sea level changes (GMSL). Proxy-based reconstructions: benthic $\delta^{18}O$ (Miller et al., 2020a) from EOT to present, backstripped sequence stratigraphy from New Jersey from EOT until the Late Miocene (Miller et al., 2005, Kominz et al., 2008). For the EOT (pink solid squares): Pekar et al., (2002); Pekar and Christie-Blick, (2008); Lear et al. (2008), Katz et al., (2008), Miller et al., (2009); Bohaty et al. 2(012); Houben et al., (2012); Stocchi et al. (2013). For the Pliocene: converted benthic $\delta^{18}O$ record from Dimitru et al., (2019) until the PPT. Pink squares correspond to reconstructed Pliocene highstands (Wardlay and Quinn, 1991; Dwyer and Chandler, 2009; Kulpecz et al 2009; Naish and Wilson, 2009; Sosdian and Rosenthal, 2009; Miller et al., 2012; Winnick and Caves, 2015; Dimitru et al 2019) and to M2 glaciation (Miller et al., 2005; Naish and Wilson, 2009; Dwyer and Chandler, 2009). For Pleistocene: sea level reconstructions are taken from Hearty et al., (2020); Sandstrom et al., (2020) for MIS 31 (uncorrected from GIA and dynamic topography) and from Raymo and Mitrovica (2012) and Roberts et al. (2012) for MIS 11. For the last 400 kyrs, reconstructed curves of sea level changes are from Waelbroeck et al. (2002) and from Rohling et al. (2009). For MIS5, paleoshorelines data are from the compilation in Dutton et al. (2015) and references therein. Simulated GMSL changes are from: Bintanja et al., (2005), de Boer et al., (2015) and (Stap et al., 2017) and from Raymo et al (2006) for MIS 31 (blue squares); **d.** Simulated Antarctic ice sheet melting contributions (meter Sea Level Equivalent, m SLE) to GMSL changes are from ice sheet simulations (squares and curves) and from Glacio-isostatic-Adjustment simulations (dark red triangles). Note that some of the reported simulated ice volumes do not refer to volumes above floatation. For the EOT: DeConto and Pollard (2003), Pollard and DeConto (2005), Gasson et al (2014), Ladant et al (2014), Liakka et al (2014), Wilson et al (2013). For the Miocene: Langebroek et al (2009), Gasson et al. (2016), Colleoni et al. (2018b), Stap et al. (2019). For Early Pliocene: Pollard and DeConto (2009, transient and black line), Golledge et al. (2017, orange squares). For mPWP to Late Pliocene: de Boer et al. (2017, transient blue line), Pollard and DeConto (2009, transient black line). Orange squares come from Tan et al. (2017) for M2 glaciation and remaining symbols are for the mPWP considering Pollard and DeConto, (2012), de Boer et al., (2015), Austerman et al. (2015), Gasson et al. (2015), Yan et al., (2016), De Conto and Pollard (2016), Dolan et al. (2018). When simulations were run with averaged mPWP climatic conditions, orange squares are indicatively plotted at 3 Ma. For the entire Pleistocene: blue line - de Boer et al (2014) and black line - Pollard and De Conto (2009). For MIS 31: De Conto et al. (2012), de Boer et al. (2013), Beltran et al (2020). For MIS 11: Tigchelaar et al. (2018), Sutter et al. 2019, Mas e Braga et al. (2020). For MIS 5: Huybrechts et al. (2002), Pollard and DeConto (2012), de Boer et al. (2015), Goelzer et al. (2016), Sutter et al. (2016), DeConto and Pollard (2016), Tigchelaar et al. (2018), Quiquet et al. (2018), Colleoni et al. (2018b), Sutter et al. (2019). For LGM based on ice sheet simulations: Philippon et al. (2006), Mackintosh et al (2011), Golledge et al. (2012), Brigg et al (2013), de Boer et al (2013), Golledge et al. (2014), Pollard et al. (2016), Quiquet et al. (2018), Colleoni et al (2018b), Sutter et al (2019). For LGM based on glacio-isostatic adjustment simulations: Peltier et al. (2004), Ivins and James (2005), Lambeck et al. (2014), Whitehouse et al. (2012), Ivins et al. (2013), Gomez et al. (2013), Argus et al. (2014). Cold periods of interest in this chapter are indicated with blue bars: EOT - Eocene-Oligocene Transition; MMCT - Mid-Miocene Climatic Transition; LMC - Late Miocene Cooling; PPT - Plio-Pleistocene Transition; MPT - Mid-Pleistocene Transition; MBE - mid-Brunhes Event; LGM - Last Glacial Maximum. Warm periods of mentioned in this chapter are indicated with orange bars: MCO - Mid-Miocene Climatic Optimum; mPWP - mid-Pliocene Warm Period, MIS 31, MIS 11, MIS 5.

1458
1459

Figure 2



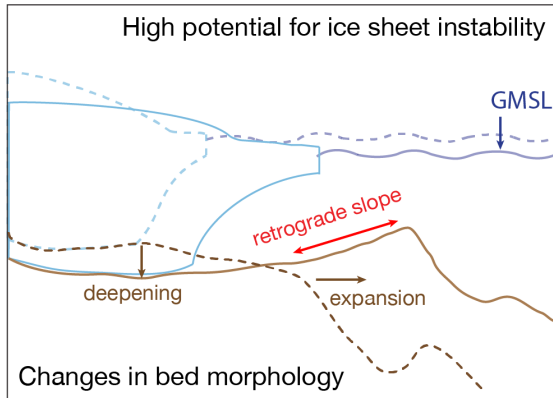
1460
1461
1462
1463
1464
1465
1466

Figure 2 Top: Pan-Antarctic isostatically-relaxed paleogeographic reconstructions from **Paxman et al. (2019)** for the Eocene (34 Ma), the Late Oligocene (23 Ma), the Middle Miocene (14 Ma) and BEDMAP2 for modern pan-Antarctic geography (**Fretwell et al., 2013**). Bottom: superimposed Eocene (brown), Late Oligocene (orange), Middle Miocene (pink) and modern (blue) emerged topography. Isobath at -1000 meters for each time slices is also indicated.

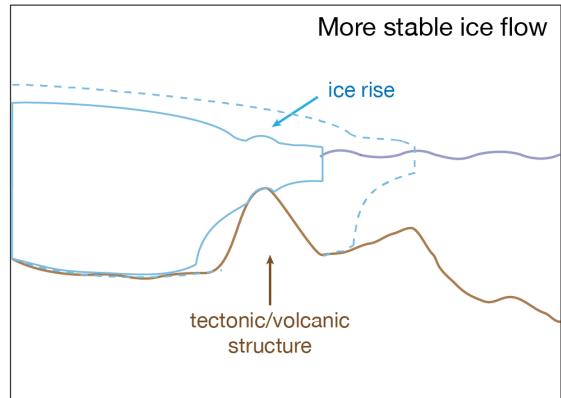
1467
1468

Figure 3

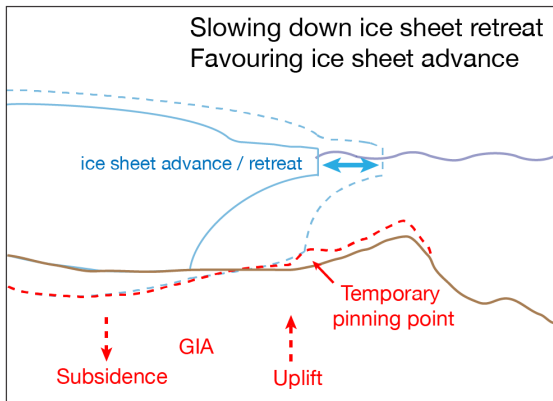
a. Long-term margin evolution



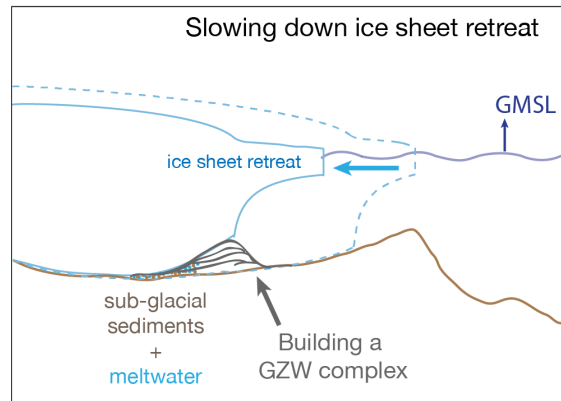
b. Bathymetric highs



c. Glacio-isostatic adjustment

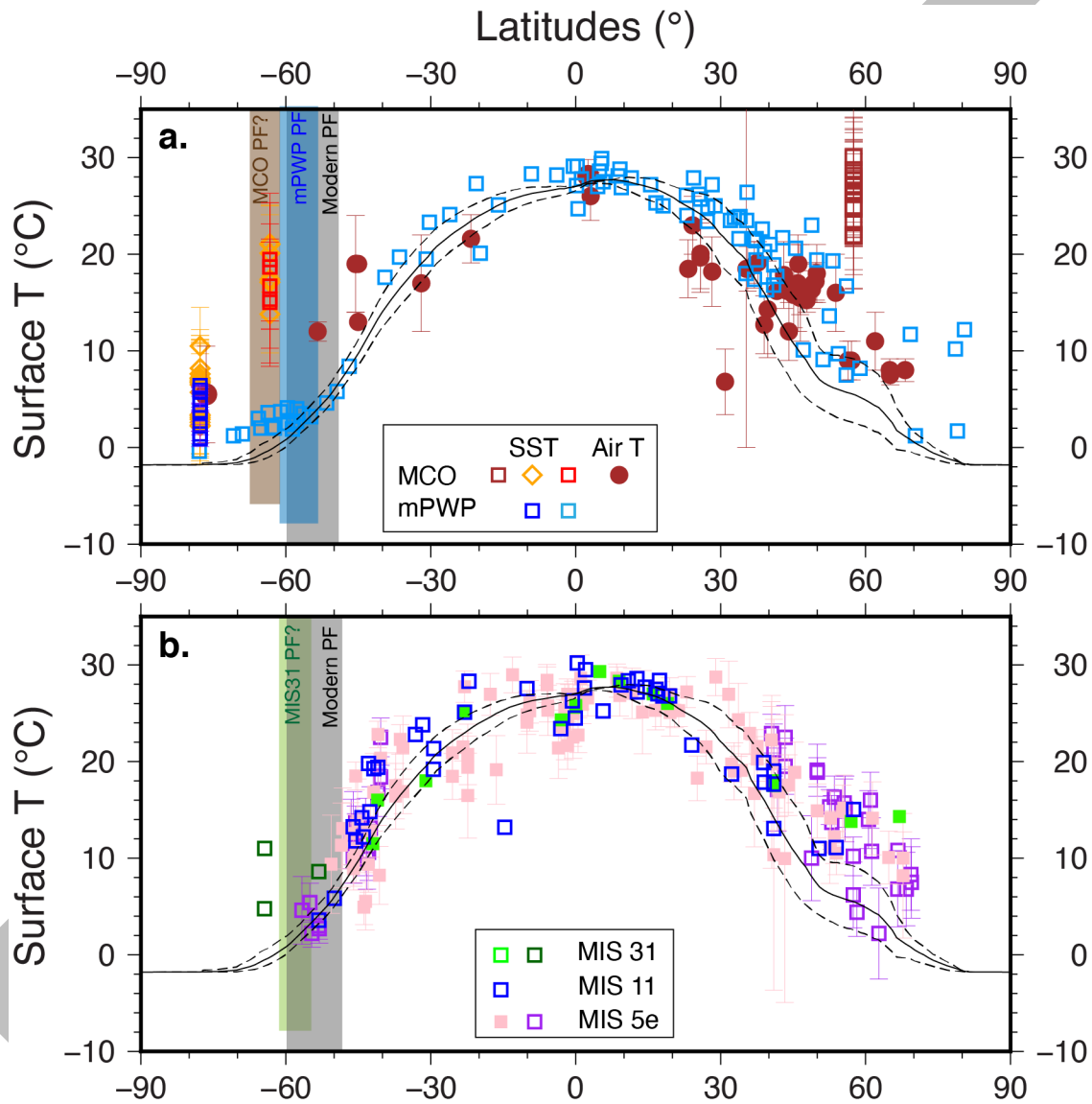


d. Grounding Zone Wedges



1469
1470
1471
1472
1473
1474
1475

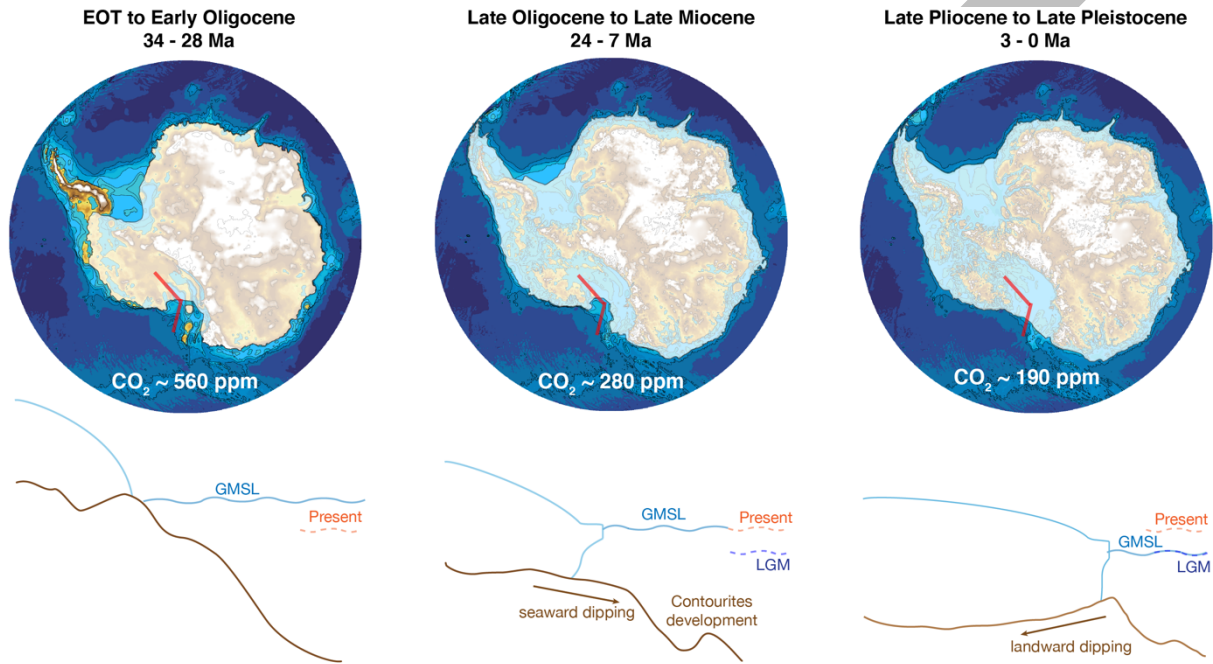
Figure 3 Schematics of the different ways by which an ice sheet can anchor on the bed. GMSL: global mean sea level; GZW: grounding zone wedge; GIA: glacio-isostatic adjustment.



1478 **Figure 4:** Proxies compilation of reconstructed meridional sea surface temperature (SST) for the MCO
 1479 and the mPWP (a.), MIS 31, MIS 11 and MIS 5 (b.). Note that vertical colour bars correspond to our
 1480 interpretation of approximated location of the zonal-averaged circum-Antarctic Polar Front. Mean Air
 1481 Temperature (MAT) and SST proxies for the MCO are from **Golder et al. (2014)** for global compilation.
 1482 Due to the paucity of data, we also include terrestrial proxies (MAT, dots). We also include from **Super**
 1483 **et al. (2020)** BAYSPAR calibration of TEX₈₆ for North Atlantic ODP Site 982 (brown open squares), from
 1484 **Levy et al., (2016)** TEX₈₆ Ross Sea SWT 0-200 m depth and Adélie Land margin (**Sangiori et al.,**
 1485 **2018**; orange open diamonds) and **Hartman et al. (2018)** for TEX₈₆ BAYSPAR calibrated Adélie Land
 1486 margin SST records (red open squares). MAT and SST proxies for the mPWP are from **Dowsett et al.**
 1487 **(2012)** global compilation (light blue open squares) and **McKay et al. (2012)** for TEX₈₆ Ross Sea SST
 1488 record (dark blue open squares). SST proxies for MIS 31 are from **Justino et al. (2017)** for global
 1489 compilation and **Beltran et al. (2020)** for Antarctic Peninsula, Weddell Sea and Adélie Land margin
 1490 SST records (dark green open squares). SST proxies for MIS 11 are from **Justino et al. (2017)**. SST
 1491 proxies for MIS 5 are from **Capron et al. (2014)** (solid pink squares) and **Hoffman et al. (2017)** (open
 1492 purple squares), both at 125 ka. Black continuous (mean annual) and dashed lines (boreal and austral
 1493 summers) correspond to pre-industrial HadISST reconstruction from **Rayner et al. (2003)**. Note that
 1494 many of the SST proxies plotted here from the various compilations tend to be more representative of
 1495 boreal or austral summer conditions rather than of mean annual conditions.
 1496
 1497
 1498

1499
1500

Figure 5

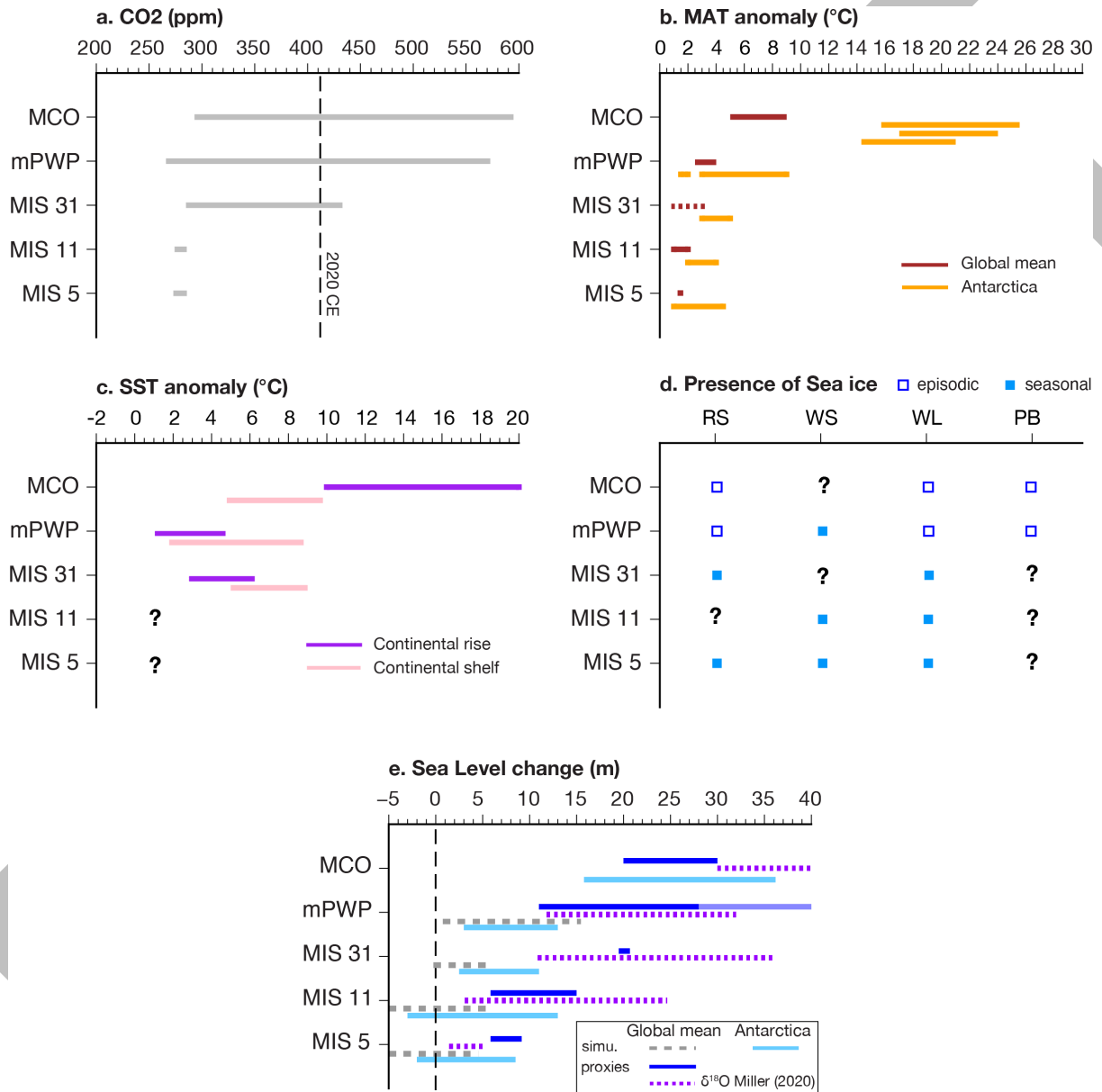


1501
1502
1503
1504
1505
1506
1507
1508
1509
1510
1511
1512
1513
1514
1515
1516

Figure 5: Simulated Antarctic ice sheet extent during past glaciations of different intervals. EOT to Early Oligocene (34 - 28 Ma): extent adapted from simulations by **Ladant et al. (2014)** with prescribed atmospheric CO₂ of 700 to 560 ppm. Late Oligocene to Late Miocene (24 - 7 Ma): extent adapted from simulations by **Gasson et al. (2016)** and **Colleoni et al. (2018b)** prescribing an atmospheric CO₂ of 280 ppm. Late Pliocene to Late Pleistocene (3 Ma to 0): extent adapted from **Colleoni et al. (2018b)** with prescribed atmospheric CO₂ of 190 ppm. Paleotopographies and bathymetries are from **Paxman et al. (2019)**. Note that ice shelves are not represented on the different panels. Schematics below each circum-Antarctic view corresponds to an idealised transect along the red lines indicated on the Antarctic maps above. Those schematics illustrate the evolution of the continental margin through time, with corresponding global mean sea level variations (GMSL, see **Figure 1c**) referred to present sea level (dashed orange line) and Last Glacial Maximum sea level (LGM, 21 ka, dashed blue line).

1517
1518

Figure 6



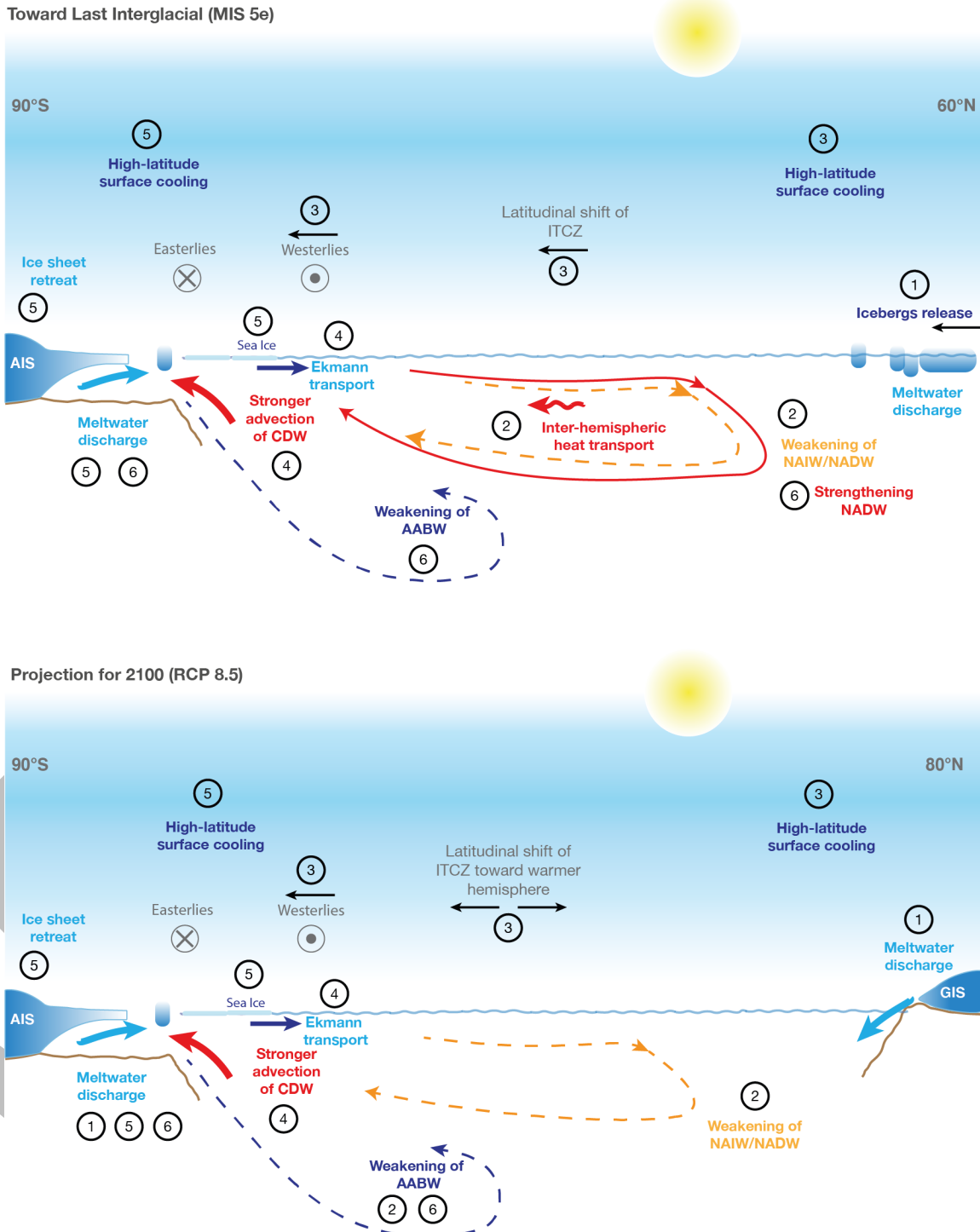
1519
1520
1521
1522
1523
1524
1525
1526
1527
1528
1529
1530
1531
1532
1533
1534
1535
1536
1537

Figure 6: Main climatic indicators of each warm periods considered in the chapter (a. to d.) and associated simulated range of Antarctic contributions to global mean sea level changes (e.). Each panel shows ranges of climatic proxies or simulated quantities at global scale and for Antarctica relative to their present-day value. Note that for each range (global or Antarctic), minimum and maximum account for the minimum and maximum uncertainties of the represented proxies when found. **a.** atmospheric CO₂ levels, see **Figure 1a** for references. **b.** Global mean annual temperature (MAT, °C) anomaly relative to 20th century average: **MCO** - **Goldner et al. (2014)**; **mPWP** - **Salzmann et al. (2013)** terrestrial proxies (see their Table S3b) and **Dowsett et al. (2012)** for SST compilation; **MIS 31** - **Justino et al (2019)** averaged SST compilation also accounting for **Beltran et al. (2020)** Antarctic margin proxy-based SST. However, there is no northern high-latitude MAT or SST reconstructions. Proxies in the northern high latitudes suggest sea ice free conditions (**Detlef et al., 2018**) as during the mPWP. Given the high similarities with mPWP SST gradient (**Figure 4**), MIS 31 global MAT is tentatively extended to mean mPWP MAT (dashed line); **MIS 11** - **Lang and Wolff (2011)** and **MIS 5** - **Turney and Jones (2010)**; MAT (°C) for Antarctic region (including ice core records) anomaly are relative to 1990 at the closest weather station to the sediment cores location: **MCO** - **Warny et al. (2009)**, **mPWP** - **Passchier et al. (2011)**, **Haywood et al. (2020)**, **MIS 31** - **Scherer et al. (2008)**, **MIS 11** - **Jouzel et al. (2007)**, **MIS 5** - **Jouzel et al. (2007)**, **Lang & Wolff (2011)**. **c.** Sea surface temperatures (SST, °C) anomaly

1538 relative to present value at each core location: continental shelf values (pink) are from Cape Roberts or
1539 ANDRILL sites: MCO - **Sangiorgi et al. (2018)** are sea water temperature (0-200 m depth), mPWP -
1540 **McKay et al. (2012)**, MIS 31 - **Scherer et al. (2008)**. SST records from continental slope and rise
1541 (purple) are from: MCO - **Sangiorgi et al (2018)** are sea water temperature (0-200 m depth), **Hartman**
1542 **et al. (2018)**, mPWP - **Dowsett et al. (2012)** compilation of proxies below 60°S, MIS 31 - **Beltran et al.**
1543 **(2020)**. Note that many of the SST proxies could be representative of boreal or austral summer
1544 conditions rather than annual mean. **d.** Proxies for presence/absence of sea ice are shown for different
1545 Antarctic sectors, RS (Ross Sea), WS (Weddell Sea), WL (Wilkes Land margin), PB (Prydz Bay). Open
1546 blue squares indicate intermittent sea ice cover during the period, solid blue squares indicate seasonal
1547 sea ice (mostly no sea ice during austral summer) and question mark correspond to absence of
1548 information for the sector. For MCO - **Sangiorgi et al. (2018)**, **Levy et al. (2016)**, **Hannah (2006)**; for
1549 mPWP - **Burckle et al. (1990)**, **Whitehead et al. (2005)**, **McKay et al (2012a)**, **Taylor-Silva and**
1550 **Riesselman (2018)**; for MIS 31 - **Bohaty et al. (1998)**, **Scherer et al (2008)**, **Villa et al. (2008)**, **Beltran**
1551 **et al. (2020)**; for MIS 11 - **Kunz-Pirrung et al. (2002)**, **Wolff et al. (2006)**, **Wilson et al. (2018)**, **Escutia**
1552 **et al. (2011)**; for MIS 5 - **Kunz-Pirrung et al. (2002)**, **Wolff et al. (2006)**, **Konfirst et al. (2012)**, **Presti**
1553 **et al. (2011)**, **Hartman et al. (2016)**, **Wilson et al. (2018)**. **e.** Ranges for global mean sea level changes
1554 (GMSL, dark blue) relative to today from data and models (dotted grey). For mPWP, the proxies
1555 indicate a sea level rise up to + 40 m above present that is indicated by the transparent blue line on the
1556 plot. For MIS 31, GMSL data are uncorrected from GIA and dynamical topography. Simulated ranges
1557 of Antarctic Ice Sheet melting contributions are shown in light blue. Range from recent GMSL
1558 reconstruction based on benthic $\delta^{18}\text{O}$ records from **Miller et al. (2020a)** is shown with dotted purple
1559 line. See **Figure 1c and 1d** and the main text for references.
1560
1561

1562
1563

Figure 7



1564
1565
1566
1567
1568
1569
1570
1571
1572
1573
1574

Figure 7: Cartoons for the impact of freshwater release and associated feedbacks loop at global scale and on Antarctica. Top cartoon is based on **Turney et al. (2020)** and describes the evolution of those feedback as a consequence of Heinrich event 11 (~135 ka) and subsequent evolution until MIS 5e (time frame of few millennia). Numbers indicate the order of the sequence. Bottom cartoon shows similar feedback but as projected until 2100 for the RCP 8.5 high-emission scenario (time frame of few decades) based on **Golledge et al. (2019)**. AABW: Antarctic Bottom Water; CDW: Circumpolar Deep Water; ITCZ: Inter-Tropical Convergence Zone; NAIW: North Atlantic Intermediate Water; NADW: North Atlantic Deep Water.

1575 **List of Co-authors for the PAIS community:**

- 1576
1577 **Denise K. Kulhanek**, Texas A&M University, College Station, TX, United States
1578 **David Pollard**, Pennsylvania State University, University Park, Pennsylvania, USA
1579 **Carolina Acosta Hospitaleche**, CONICET, División Paleontología Vertebrados, Museo de La Plata (Facultad de
1580 Ciencias Naturales y Museo, UNLP) La Plata, Argentina
1581 **Robert M. McKay**, Antarctic Research Centre, Victoria University of Wellington, Wellington, New Zealand
1582 **Riccardo Geletti**, National Institute of Oceanography and Applied Geophysics - OGS, Trieste, Italy
1583 **Robert B Dunbar**, Stanford University, Stanford, California, USA
1584 **Amy Leventer**, Colgate University, Hamilton, NY, USA
1585 **Marcelo A. Reguero**, Instituto Antártico Argentino, B1650HMK, San Martín, Buenos Aires, Argentina
1586 **Karsten Gohl**, Alfred Wegener Institute Helmholtz-Centre for Polar and Marine Research, Bremerhaven, Germany
1587 **Guy J. G., Paxman**, Lamont-Doherty Earth Observatory, Columbia University, New York, USA
1588 **Julia S. Wellner**, University of Houston, Houston, USA
1589 **Francesca Battaglia**, University of Venice Cá Foscari, Italy
1590 **Marco Taviani**, Institute of Marine Sciences (ISMAR), National Research Council (CNR), 40129, Bologna, Italy
1591 and Biology Department, Woods Hole Oceanographic Institution, 02543, Woods Hole, USA
1592 **Aisling M Dolan**, University of Leeds, Leeds, UK
1593 **Nigel, Wardell**, OGS, Trieste, Italy
1594 **Martin J. Siegert**, Imperial College London, London, UK
1595 **Isabel Sauermilch**, University of Tasmania, Institute for Marine and Antarctic Studies, Australia
1596 **Laura, Crispini**, University of Genova (DISTAV, Genova, Italy)
1597 **Dominic A Hodgson**, British Antarctic Survey, Cambridge, UK
1598 **Renata G., Lucchi**, National Institute of Oceanography and Applied Geophysics (OGS), Sgonico-Trieste, Italy
1599 **Ursula Röhl**, MARUM, University of Bremen, Bremen, Germany
1600 **Suzanne OConnell**, Wesleyan University, Middletown, CT, USA
1601 **Richard C.A. Hindmarsh**, British Antarctic Survey & Durham University, Cambridge & Durham, United Kingdom
1602 **Paolo Montagna**, Institute of Polar Sciences, National Research Council, Bologna, Italy
1603 **Gerhard Kuhn**, Alfred-Wegener-Institut Helmholtz-Zentrum für Polar- und Meeresforschung, Bremerhaven,
1604 Germany
1605 **Edward G.W., Gasson**, University of Bristol, UK
1606 **Sidney R Hemming**, Columbia University, New York, USA
1607 **Sandra Passchier**, Montclair State University, Montclair, U.S.A.
1608 **Jan Sverre Laberg**, Department of Geosciences, UiT The Arctic University of Norway, NO-9037 Tromsø, Norway
1609 **Reed P. Scherer** Northern Illinois University, DeKalb, IL, USA
1610 **Yasmina M. Martos** NASA Goddard Space Flight Center, Greenbelt, MD, USA & University of Maryland College
1611 Park, MD, USA
1612 **Phillip J. Bart**, Louisiana State University, Baton Rouge USA
1613 **David J. Wilson**, Department of Earth Sciences, University College London, London, UK
1614 **Frank O., Nitsche**, Lamont-Doherty Earth Observatory of Columbia University, Palisades, USA
1615 **Raffaella Tolotti**, University of Genoa, Genoa, Italy
1616 **Sean P S Gulick**, University of Texas at Austin, Austin, Texas
1617 **Stefanie Brachfeld**, Montclair State University, New Jersey, USA
1618 **David, Harwood**, University of Nebraska-Lincoln, Lincoln, Nebraska, USA
1619 **Johann P, Klages**, Alfred Wegener Institute Helmholtz Center for Polar and Marine Research, Bremerhaven,
1620 Germany
1621 **Fausto Ferraccioli**, NERC/British Antarctic Survey, Cambridge, UK
1622 **Trevor Williams**, International Ocean Discovery Program, Texas A&M University, College Station, USA
1623 **Alan K. Cooper**, U.S. Geological Survey Emeritus, Menlo Park, USA
1624 **Mathieu, Casado**, Alfred Wegener Institute Helmholtz Centre for Polar and Marine Research, Potsdam, Germany
1625 **Marvin A. Speece**, Montana Technological University, Butte, USA
1626 **Christopher C. Sorlien**, Earth Research Institute, University of California, Santa Barbara, Santa Barbara,
1627 California, USA
1628 **Marcelo A. Reguero**, Instituto Antártico Argentino, Buenos Aires, Argentina
1629 **Richard H Levy**, GNS Science and Victoria University of Wellington, Lower Hutt and Wellington, New Zealand
1630 **Carolina Acosta Hospitaleche** CONICET- División Paleontología Vertebrados, Museo de La Plata, Facultad de
1631 Ciencias Naturales y Museo, UNLP; La Plata, Argentina
1632 **Javier N. Gelfo** CONICET - UNLP, División Paleontología Vertebrados, Museo de La Plata, Argentina
1633 **Georgia R, Grant**, GNS Science Wellington, New Zealand
1634 **Jamey Stutz**, Antarctic Research Centre at Victoria University of Wellington, New Zealand
1635 **Ian D. Goodwin**, Climate Change Research Centre, University of New South Wales, Sydney, Australia
1636 **Mike Weber**, University of Bonn, Institute for Geosciences, Department of Geochemistry and Petrology, 53115
1637 Bonn, Germany
1638 **Leanne K. Armand**, Australian National University, Canberra, Australia.
1639 **Philip E O'Brien**, Macquarie University, Sydney, Australia
1640 **Nicholas R, Golledge**, Antarctic Research Centre Victoria University of Wellington, Wellington 6140, New Zealand

- 1641 **Andrea, Bergamasco**, C.N.R. (National Research Council) ISMAR, Venice, Italy
1642 **Michele Rebesco**, OGS, Trieste, Italy
1643 **Alessandra Venuti**, Istituto Nazionale di Geofisica e Vulcanologia, Rome, Italy
1644 **Christine S Siddoway**, Colorado College, Colorado Springs, USA
1645 **Peter J Barrett**, Antarctic Research Centre, Victoria University of Wellington, Wellington, NEW ZEALAND.
1646 **R Selwyn Jones**, Monash University (Melbourne, Australia)
1647 **Minoru Ikehara** Kochi University, Japan
1648 **Robert D Larter**, British Antarctic Survey, Cambridge, UK
1649 **Fernando Bohoyo**, Instituto Geológico y Minero de España, Madrid, Spain
1650 **Peter K., Bijl**, Utrecht University, Utrecht, The Netherlands
1651 **Catalina, Gebhardt**, Alfred Wegener Institute Helmholtz Centre of Polar and Marine Research, Bremerhaven,
1652 Germany
1653

1654
1655
1656
1657
1658
1659
1660
1661
1662
1663
1664
1665
1666
1667
1668
1669
1670
1671
1672
1673
1674
1675
1676
1677
1678
1679
1680
1681
1682
1683
1684
1685
1686
1687
1688
1689
1690
1691
1692
1693
1694
1695
1696
1697
1698
1699
1700
1701
1702
1703
1704
1705
1706
1707
1708
1709
1710
1711
1712
1713
1714
1715
1716
1717

1718
1719

References

- Aitken, A. R. A., Roberts, J. L., Van Ommen, T. D., Young, D. A., Golledge, N. R., Greenbaum, J. S., ... & Siegert, M. J. (2016). Repeated large-scale retreat and advance of Totten Glacier indicated by inland bed erosion. *Nature*, 533(7603), 385-389.
- Albrecht T., Winkelmann R., Levermann A. (2020). Glacial-cycle simulations of the Antarctic Ice Sheet with the Parallel Ice Sheet Model (PISM) – Part 1: Boundary conditions and climatic forcing. *The Cryosphere*, 14:599–632, <https://doi.org/10.5194/tc-14-599-2020>.
- Alley, R. B., Anandakrishnan, S., Dupont, T. K., Parizek, B. R., & Pollard, D. (2007). Effect of sedimentation on ice-sheet grounding-line stability. *Science*, 315(5820), 1838-1841.
- Anderson, J. B., Shipp, S. S., Lowe, A. L., Wellner, J. S., & Mosola, A. B. (2002). The Antarctic Ice Sheet during the Last Glacial Maximum and its subsequent retreat history: a review. *Quaternary Science Reviews*, 21(1-3), 49-70.
- Anderson, J. B., Conway, H., Bart, P. J., Witus, A. E., Greenwood, S. L., McKay, R. M., ... & Stone, J. O. (2014). Ross Sea paleo-ice sheet drainage and deglacial history during and since the LGM. *Quaternary Science Reviews*, 100, 31-54.
- Argus, D. F., Peltier, W. R., Drummond, R., & Moore, A. W. (2014). The Antarctica component of postglacial rebound model ICE-6G_C (VM5a) based on GPS positioning, exposure age dating of ice thicknesses, and relative sea level histories. *Geophysical Journal International*, 198(1), 537-563.
- Armand, L., O'Brien, P., Ambrecht, L., Barker, H., Caburlotto, A., Connell, T., ... & Fazey, J. (2018). Interactions of the Totten Glacier with the Southern Ocean through multiple glacial cycles (IN2017-V01): Post-survey report. *Australian Antarctic Science Grant Program (AAS# 4333)*. The grant title is "Interactions of the Totten Glacier with the Southern Ocean through multiple glacial cycles" and the PI's are: Armand, LK O'Brien, P., Post, A., Goodwin, I., Opdyke, B., Leventer, A., Domack, E., Escuita-Dotti, C. & DeSantis, L.
- Arndt, J. E., Hillenbrand, C. D., Grobe, H., Kuhn, G., & Wacker, L. (2017). Evidence for a dynamic grounding line in outer Filchner Trough, Antarctica, until the early Holocene. *Geology*, 45(11), 1035-1038.
- Asay-Davis, X. S., Jourdain, N. C. & Nakayama, Y. Developments in simulating and parameterizing interactions between the Southern Ocean and the Antarctic Ice sheet. *Curr. Clim. Change Rep.* 3, 316–329 (2017). <https://doi.org/10.1007/s40641-017-0071-0>.
- Ashley, K. E., McKay, R., Etourneau, J., Jimenez-Espejo, F. J., Condron, A., Albot, A., ... & Bendle, J. A. (2021). Mid-Holocene Antarctic sea-ice increase driven by marine ice sheet retreat. *Climate of the Past*, 17(1), 1-19.
- Austermann, J., Pollard, D., Mitrovica, J. X., Moucha, R., Forte, A. M., DeConto, R. M., ... & Raymo, M. E. (2015). The impact of dynamic topography change on Antarctic ice sheet stability during the mid-Pliocene warm period. *Geology*, 43(10), 927-930. <https://doi.org/10.1130/G36988.1>.
- Badger MPS, Lear CH, Pancost RD, Foster GL, Bailey T, et al. (2013a). CO2 drawdown following the middle Miocene expansion of the Antarctic Ice Sheet. *Paleoceanography* 28: 42-53. <https://doi.org/10.1002/palo.20015>.
- Badger MPS, Schmidt DN, Mackensen A, Pancost RD. (2013b). High resolution alkenone palaeobarometry indicates relatively stable pCO2 during the Pliocene (3.3 to 2.8 Ma). *Philosophical Transaction of the Royal Society A* 347: 20130094. <https://doi.org/10.1098/rsta.2013.0094>.
- Bakker, P., Clark, P. U., Golledge, N. R., Schmittner, A., & Weber, M. E. (2017). Centennial-scale Holocene climate variations amplified by Antarctic Ice Sheet discharge. *Nature*, 541(7635), 72-76.
- Bamber, J. L., Oppenheimer, M., Kopp, R. E., Aspinall, W. P., & Cooke, R. M. (2019). Ice sheet contributions to future sea-level rise from structured expert judgment. *Proceedings of the National Academy of Sciences*, 116(23), 11195-11200.
- Bard, E., Hamelin, B., & Fairbanks, R. G. (1990). U-Th ages obtained by mass spectrometry in corals from Barbados: sea level during the past 130,000 years. *Nature*, 346(6283), 456-458.
- Barrett, P. 1989. Antarctic Cenozoic history from the CIROS-1 drillhole, McMurdo Sound, Antarctica. *NZ DSIR Bulletin*, 245, 254.
- Barrett, P.J. 2007. Cenozoic climate and sea level history from glaciomarine strata off the Victoria Land coast, Cape Roberts Project, Antarctica. Pp. 259–288 in *Glacial Sedimentary Processes and Products*. M.J. Hambrey, P.

- 1720 Bart, P. J. (2001). Did the Antarctic ice sheets expand during the early Pliocene?. *Geology*, 29(1), 67-70.
1721 [https://doi.org/10.1130/0091-7613\(2001\)029%3C0067:DTAISE%3E2.0.CO;2](https://doi.org/10.1130/0091-7613(2001)029%3C0067:DTAISE%3E2.0.CO;2).
- 1722 Bart, P. J. (2003). Were West Antarctic ice sheet grounding events in the Ross Sea a consequence of East Antarctic
1723 ice sheet expansion during the middle Miocene?. *Earth and Planetary Science Letters*, 216(1-2), 93-107.
1724 [https://doi.org/10.1016/S0012-821X\(03\)00509-0](https://doi.org/10.1016/S0012-821X(03)00509-0).
- 1725 Bart, P. J., DeCesare, M., Rosenheim, B. E., Majewski, W., & McGlannan, A. (2018). A centuries-long delay
1726 between a paleo-ice-shelf collapse and grounding-line retreat in the Whales Deep Basin, eastern Ross Sea,
1727 Antarctica. *Scientific reports*, 8(1), 1-9. <https://doi.org/10.1038/s41598-018-29911-8>.
- 1728 Bart, P. J., & De Santis, L. (2012). Glacial intensification during the Neogene: A review of seismic stratigraphic
1729 evidence from the Ross Sea, Antarctica, continental shelf. *Oceanography*, 25(3), 166-183.
- 1730 Bart, P. J., & Iwai, M. (2012). The overdeepening hypothesis: how erosional modification of the marine-scape
1731 during the early Pliocene altered glacial dynamics on the Antarctic Peninsula's Pacific margin. *Palaeogeography,*
1732 *Palaeoclimatology, Palaeoecology*, 335, 42-51.
- 1733 Bart, P. J., Krogmeier, B. J., Bart, M. P., & Tulaczyk, S. (2017). The paradox of a long grounding during West
1734 Antarctic Ice Sheet retreat in Ross Sea. *Scientific reports*, 7(1), 1-8. <https://doi.org/10.1038/s41598-017-01329-8>.
- 1735 Bart, P. J., & Tulaczyk, S. (2020). A significant acceleration of ice volume discharge preceded a major retreat of a
1736 West Antarctic paleo-ice stream. *Geology*, 48(4), 313-317. <https://doi.org/10.1130/G46916.1>.
- 1737 Bartoli, G., Hönisch, B., & Zeebe, R. E. (2011). Atmospheric CO2 decline during the Pliocene intensification of
1738 Northern Hemisphere glaciations. *Paleoceanography*, 26(4). <https://doi.org/10.1029/2010PA002055>.
- 1739 Bassett, S. E., Milne, G. A., Bentley, M. J., & Huybrechts, P. (2007). Modelling Antarctic sea-level data to explore
1740 the possibility of a dominant Antarctic contribution to meltwater pulse IA. *Quaternary Science Reviews*, 26(17-18),
1741 2113-2127.
- 1742 Becquey, S., & Gersonde, R. (2002). Past hydrographic and climatic changes in the Subantarctic Zone of the South
1743 Atlantic—The Pleistocene record from ODP Site 1090. *Palaeogeography, Palaeoclimatology, Palaeoecology*,
1744 182(3-4), 221-239.
- 1745 Becquey, S., & Gersonde, R. (2003). A 0.55-Ma paleotemperature record from the Subantarctic zone: Implications
1746 for Antarctic Circumpolar Current development. *Paleoceanography*, 18(1).
- 1747 Becquey, S., & Gersonde, R. (2003). 14. Data Report: Early and Mid-Pleistocene (MIS 65-11) Summer Sea-
1748 Surface Temperature, Foraminiferal Fragmentation, and Ice-Rafted Debris Records from the Subantarctic (ODP
1749 Leg 177 Site 1090). *Proc. Ocean Drill. Program Sci. Results*, 177, 1 –23.
- 1750 Beltran, C., Golledge, N. R., Ohneiser, C., Kowalewski, D. E., Sicre, M. A., Hageman, K. J., ... & Mainié, F. (2020).
1751 Southern Ocean temperature records and ice-sheet models demonstrate rapid Antarctic ice sheet retreat under
1752 low atmospheric CO2 during Marine Isotope Stage 31. *Quaternary Science Reviews*, 228, 106069.
1753 <https://doi.org/10.1016/j.quascirev.2019.106069>.
- 1754 Bentley, M.J., 1999. Volume of Antarctic ice at the Last Glacial Maximum, and its impact on global sea level change.
1755 *Quaternary Science Reviews* 18, 1569–1595.
- 1756 Bentley, M. J., Fogwill, C. J., Le Brocq, A. M., Hubbard, A. L., Sugden, D. E., Dunai, T. J., & Freeman, S. P. (2010).
1757 Deglacial history of the West Antarctic Ice Sheet in the Weddell Sea embayment: Constraints on past ice volume
1758 change. *Geology*, 38(5), 411-414.
- 1759 Bereiter, B., Eggleston, S., Schmitt, J., Nehrbass-Ahles, C., Stocker, T. F., Fischer, H., ... & Chappellaz, J. (2015).
1760 Revision of the EPICA Dome C CO2 record from 800 to 600 kyr before present. *Geophysical Research Letters*,
1761 42(2), 542-549. <https://doi.org/10.1002/2014GL061957>.
- 1762 Bertram, R. A., Wilson, D. J., van de Flierdt, T., McKay, R. M., Patterson, M. O., Jimenez-Espejo, F. J., ... &
1763 Riesselman, C. R. (2018). Pliocene deglacial event timelines and the biogeochemical response offshore Wilkes
1764 Subglacial Basin, East Antarctica. *Earth and Planetary Science Letters*, 494, 109-116.
1765 <https://doi.org/10.1016/j.epsl.2018.04.054>.
- 1766 Benz, V., Esper, O., Gersonde, R., Lamy, F., & Tiedemann, R. (2016). Last Glacial Maximum sea surface
1767 temperature and sea-ice extent in the Pacific sector of the Southern Ocean. *Quaternary Science Reviews*, 146,
1768 216-237.
- 1769
1770
1771
1772
1773
1774
1775
1776
1777
1778
1779
1780
1781
1782
1783
1784
1785

- 1786 Bintanja, R., Van De Wal, R. S., & Oerlemans, J. (2005). Modelled atmospheric temperatures and global sea levels
1787 over the past million years. *Nature*, 437(7055), 125-128. <https://doi.org/10.1038/nature03975>.
1788
- 1789 Bijl, P. K., Bendle, J. A., Bohaty, S. M., Pross, J., Schouten, S., Tauxe, L., ... & Brinkhuis, H. (2013). Eocene cooling
1790 linked to early flow across the Tasmanian Gateway. *Proceedings of the National Academy of Sciences*, 110(24),
1791 9645-9650.
- 1792 Bijl, P.K., A.J.P. Houben, J.D. Hartman, J. Pross, A. Salabarnada, C. Escutia, and F. Sangiorgi. (2018)
1793 Paleoceanography and ice sheet variability off-shore Wilkes Land, Antarctica – Part 2: Insights from Oligocene–
1794 Miocene dinoflagellate cyst assemblages. *Climate of the Past* 14:1,015–1,033, [https://doi.org/10.5194/cp-14-1015-
1795 2018](https://doi.org/10.5194/cp-14-1015-2018).
- 1796 Blackburn, T., Edwards, G. H., Tulaczyk, S., Scudder, M., Piccione, G., Hallet, B., ... & Babbe, J. T. (2020). Ice
1797 retreat in Wilkes Basin of East Antarctica during a warm interglacial. *Nature*, 583(7817), 554-559.
1798 <https://doi.org/10.1038/s41586-020-2484-5>.
- 1799 Blasco, J., Tabone, I., Alvarez-Solas, J., Robinson, A., & Montoya, M. (2019). The Antarctic Ice Sheet response to
1800 glacial millennial-scale variability. *Climate of the Past*, 15(1), 121-133.
- 1801 Blunier, T., Chappellaz, J., Schwander, J., Dällenbach, A., Stauffer, B., Stocker, T. F., ... & Johnsen, S. (1998).
1802 Asynchrony of Antarctic and Greenland climate change during the last glacial period. *Nature*, 394(6695), 739-
1803 743.
- 1804 Bohaty, S., Scherer, R., & Harwood, D. M. (1998). Quaternary diatom biostratigraphy and palaeoenvironments of
1805 the CRP-1 drillcore, Ross Sea, Antarctica. *Terra Antarctica*, 5(3), 431-453.
- 1806 Bohaty, S. M., Zachos, J. C., & Delaney, M. L. (2012). Foraminiferal Mg/Ca evidence for southern ocean cooling
1807 across the eocene–oligocene transition. *Earth and Planetary Science Letters*, 317, 251-261.
1808 <https://doi.org/10.1016/j.epsl.2011.11.037>.
- 1809 Böhm, E., Lippold, J., Gutjahr, M., Frank, M., Blaser, P., Antz, B., ... & Deininger, M. (2015). Strong and deep
1810 Atlantic meridional overturning circulation during the last glacial cycle. *Nature*, 517(7532), 73-76.
1811 <https://doi.org/10.1038/nature14059>.
- 1812 Böhme, M. (2003). The Miocene climatic optimum: evidence from ectothermic vertebrates of Central Europe.
1813 *Palaeogeography, Palaeoclimatology, Palaeoecology*, 195(3-4), 389-401.
- 1814 Böning, C. W., Behrens, E., Biastoch, A., Getzlaff, K., & Bamber, J. L. (2016). Emerging impact of Greenland
1815 meltwater on deepwater formation in the North Atlantic Ocean. *Nature Geoscience*, 9(7), 523-527.
1816 <https://doi.org/10.1038/ngeo2740>.
- 1817 Bracegirdle, T. J., Colleoni, F., Abram, N. J., Bertler, N. A., Dixon, D. A., England, M., ... & Goosse, H. (2019). Back
1818 to the future: Using long-term observational and paleo-proxy reconstructions to improve model projections of
1819 Antarctic climate. *Geosciences*, 9(6), 255.
- 1820 Bradley, S. L., Siddall, M., Milne, G. A., Masson-Delmotte, V., & Wolff, E. (2012). Where might we find evidence of
1821 a Last Interglacial West Antarctic Ice Sheet collapse in Antarctic ice core records?. *Global and Planetary Change*,
1822 88, 64-75. <https://doi.org/10.1016/j.gloplacha.2012.03.004>.
- 1823 Bradley, S. L., Hindmarsh, R. C., Whitehouse, P. L., Bentley, M. J., & King, M. A. (2015). Low post-glacial rebound
1824 rates in the Weddell Sea due to Late Holocene ice-sheet readvance. *Earth and Planetary Science Letters*, 413, 79-
1825 89.
- 1826 Brancolini, G., Cooper, A.K., Coren, F., (1995a). Seismic facies and glacial history in the Western Ross Sea
1827 Antarctica.. In: Cooper, A.K., Barker, P.F., Brancolini, G. Eds., *Geology and seismic stratigraphy of the Antarctic*
1828 *margin*. Antarctic Research Series 68 AGU, Washington, DC, pp. 209–233.
- 1829 Brancolini, G., Busetto, M., Marchetti, A., De Santis, L., Zanolla, C., Cooper, A.K., Cochrane, G.R., Zayatz, I.,
1830 Belyaev, V., Knyazev, M., Vinnikovskaya, O., Davey, F.J., Hinz, K., (1995b). Descriptive text for the Seismic
1831 Stratigraphic Atlas of the Ross Sea. In: Cooper, A.K., Barker, P.F., Brancolini, G. Eds., *Geology and Seismic*
1832 *Stratigraphy of the Antarctic Margin*. Antarctic Research Series 68 AGU, Washington, DC, pp. A268–A271.
- 1833 Brierley, C. M., Fedorov, A. V., Liu, Z., Herbert, T. D., Lawrence, K. T., & LaRiviere, J. P. (2009). Greatly expanded
1834 tropical warm pool and weakened Hadley circulation in the early Pliocene. *Science*, 323(5922), 1714-1718.
1835 <https://doi.org/10.1126/science.1167625>.

- 1836 Brigham-Grette, J. (1999), Marine isotope stage 11 high sea level record from northwest Alaska, in Marine Oxygen
 1837 Isotope Stage 11 and Associated Terrestrial Records, edited by R.Z. Poore et al., U.S. Geol. Surv., Open File
 1838 Rep., 99-312, 19–20.
- 1839 Briggs, R. D., & Tarasov, L. (2013). How to evaluate model-derived deglaciation chronologies: a case study using
 1840 Antarctica. *Quaternary Science Reviews*, 63, 109-127. <https://doi.org/10.1016/j.quascirev.2012.11.021>.
- 1841 Briggs, R. D., Pollard, D., & Tarasov, L. (2014). A data-constrained large ensemble analysis of Antarctic evolution
 1842 since the Eemian. *Quaternary science reviews*, 103, 91-115.
- 1843 Bronselaer, B., Winton, M., Griffies, S. M., Hurlin, W. J., Rodgers, K. B., Sergienko, O. V., ... & Russell, J. L. (2018).
 1844 Change in future climate due to Antarctic meltwater. *Nature*, 564(7734), 53-58. <https://doi.org/10.1038/s41586-018-0712-z>.
 1845
- 1846 Bueler, E., & Brown, J. (2009). Shallow shelf approximation as a “sliding law” in a thermomechanically coupled ice
 1847 sheet model. *Journal of Geophysical Research: Earth Surface*, 114(F3). <https://doi.org/10.1029/2008JF001179>.
 1848
- 1849 Buono, M. R., Fordyce, R. E., Marx, F. G., Fernández, M. S., & Reguero, M. (2019). Eocene Antarctica: a window
 1850 into the earliest history of modern whales. *Advances in Polar Science*, 30(3), 293-302.
- 1851 Burckle, L. H., Gersonde, R. and Abrams, N. (1990). Late Pliocene-Pleistocene paleoclimate in the Jane Basin
 1852 Region ODP site 697, [Series].
- 1853 Carlson, A. E., & Clark, P. U. (2012). Ice sheet sources of sea level rise and freshwater discharge during the last
 1854 deglaciation. *Reviews of Geophysics*, 50(4).
- 1855 Capron, E., Govin, A., Stone, E. J., Masson-Delmotte, V., Mulitza, S., Otto-Bliesner, B., ... & Wolff, E. W. (2014).
 1856 Temporal and spatial structure of multi-millennial temperature changes at high latitudes during the Last Interglacial.
 1857 *Quaternary Science Reviews*, 103, 116-133. <https://doi.org/10.1016/j.quascirev.2014.08.018>.
- 1858 Capron, E., Govin, A., Feng, R., Otto-Bliesner, B. L., & Wolff, E. W. (2017). Critical evaluation of climate syntheses
 1859 to benchmark CMIP6/PMIP4 127 ka Last Interglacial simulations in the high-latitude regions. *Quaternary Science
 1860 Reviews*, 168, 137-150. <https://doi.org/10.1016/j.quascirev.2017.04.019>.
- 1861 Chadwick, M., Allen, C. S., Sime, L. C., & Hillenbrand, C. D. (2020). Analysing the timing of peak warming and
 1862 minimum winter sea-ice extent in the Southern Ocean during MIS 5e. *Quaternary Science Reviews*, 229, 106134.
 1863
- 1864 Clark, P. U., Alley, R. B., Keigwin, L. D., Licciardi, J. M., Johnsen, S. J., & Wang, H. (1996). Origin of the first global
 1865 meltwater pulse following the last glacial maximum. *Paleoceanography*, 11(5), 563-577.
 1866
- 1867 Clark, P. U., Mitrovica, J. X., Milne, G. A., & Tamisiea, M. E. (2002). Sea-level fingerprinting as a direct test for the
 1868 source of global meltwater pulse 1A. *Science*, 295(5564), 2438-2441.
 1869
- 1870 Clark, P. U., & Tarasov, L. (2014). Closing the sea level budget at the Last Glacial Maximum. *Proceedings of the
 1871 National Academy of Sciences*, 111(45), 15861-15862.
- 1872 Clark, P. U., Shakun, J. D., Marcott, S. A., Mix, A. C., Eby, M., Kulp, S., ... & Schrag, D. P. (2016). Consequences
 1873 of twenty-first-century policy for multi-millennial climate and sea-level change. *Nature climate change*, 6(4), 360-
 1874 369. <https://doi.org/10.1038/nclimate2923>.
- 1875 Clark, P. U., He, F., Golledge, N. R., Mitrovica, J. X., Dutton, A., Hoffman, J. S., & Dendy, S. (2020). Oceanic
 1876 forcing of penultimate deglacial and last interglacial sea-level rise. *Nature*, 577(7792), 660-664.
 1877 <https://doi.org/10.1038/s41586-020-1931-7>.
- 1878 Colleoni, F., L. De Santis, C.S. Siddoway, A. Bergamasco, N.R. Golledge, G. Lohmann, S. Passchier, and M.J.
 1879 Siegert. (2018a). Spatio-temporal variability of processes across Antarctic ice-bed-ocean interfaces. *Nature
 1880 Communications* 9:2289, <https://doi.org/10.1038/s41467-018-04583-0>.
- 1881 Colleoni, F., De Santis, L., Montoli, E., Olivo, E., Sorlien, C. C., Bart, P. J., Gasson, E.G. W., Bergamasco, A.,
 1882 Sauli, C., Wardell, N. & Prato, S. (2018b). Past continental shelf evolution increased Antarctic ice sheet sensitivity
 1883 to climatic conditions. *Scientific reports*, 8(1), 1-12. <https://doi.org/10.1038/s41598-018-29718-7>.

- 1884 Cook, C. P., Van De Flierdt, T., Williams, T., Hemming, S. R., Iwai, M., Kobayashi, M., ... & McKay, R. M. (2013).
 1885 Dynamic behaviour of the East Antarctic ice sheet during Pliocene warmth. *Nature Geoscience*, 6(9), 765-769.
 1886 <https://doi.org/10.1038/ngeo1889>.
- 1887 Cook, C. P., Hill, D. J., van de Flierdt, T., Williams, T., Hemming, S. R., Dolan, A. M., ... & Gonzales, J. J. (2014).
 1888 Sea surface temperature control on the distribution of far-traveled Southern Ocean ice-rafted detritus during the
 1889 Pliocene. *Paleoceanography*, 29(6), 533-548. <https://doi.org/10.1002/2014PA002625>.
- 1890 Cooper, A. K., Barrett, P. J., Hinz, K., Traube, V., Letichenkov, G., & Stagg, H. M. (1991). Cenozoic prograding
 1891 sequences of the Antarctic continental margin: a record of glacio-eustatic and tectonic events. *Marine Geology*,
 1892 102(1-4), 175-213.
- 1893
 1894 Cooper, A.K., P.E. O'Brien, and C. Richter, eds. (2004). *Proceedings of the Ocean Drilling Program, Scientific*
 1895 *Results, Volume 188*, College Station, TX, <https://doi.org/10.2973/odp.proc.sr.188.2004>.
- 1896
 1897 Cooper, A., Barker, P., Barrett, P., Behrendt, J., Brancolini, G., Childs, ., Escutia, C., Jokat, W., Kristoffersen, Y.,
 1898 Leitchenkov, G., others (2011). The ANTOSTRAT legacy: science collaboration and international transparency in
 1899 potential marine mineral resource exploitation of Antarctica. *Science Diplomacy: Antarctica, Science, and the*
 1900 *Governance of International Spaces*.
- 1901
 1902 Coxall, H. K., Wilson, P. A., Pälike, H., Lear, C. H., & Backman, J. (2005). Rapid stepwise onset of Antarctic
 1903 glaciation and deeper calcite compensation in the Pacific Ocean. *Nature*, 433(7021), 53-57.
- 1904
 1905 Cramer, B. S., Miller, K. G., Barrett, P. J., & Wright, J. D. (2011). Late Cretaceous–Neogene trends in deep ocean
 1906 temperature and continental ice volume: Reconciling records of benthic foraminiferal geochemistry ($\delta^{18}\text{O}$ and
 1907 Mg/Ca) with sea level history. *Journal of Geophysical Research: Oceans*, 116(C12).
- 1908
 1909 Crampton, J. S., Cody, R. D., Levy, R., Harwood, D., McKay, R., & Naish, T. R. (2016). Southern Ocean
 1910 phytoplankton turnover in response to stepwise Antarctic cooling over the past 15 million years. *Proceedings of the*
 1911 *National Academy of Sciences*, 113(25), 6868-6873.
- 1912
 1913 Crosta, X., Crespin, J., Swingedouw, D., Marti, O., Masson-Delmotte, V., Etourneau, J., ... & Shemesh, A. (2018).
 1914 Ocean as the main driver of Antarctic ice sheet retreat during the Holocene. *Global and Planetary Change*, 166,
 62-74. <https://doi.org/10.1016/j.gloplacha.2018.04.007>.
- 1915
 1916 Dahl-Jensen, D., Albert, M. R., Aldahan, A., Azuma, N., Balslev-Clausen, D., Baumgartner, M., ... & Zheng, J.
 1917 (2013). Eemian interglacial reconstructed from a Greenland folded ice core. *Nature*, 493(7433), 489.
- 1918
 1919 de Boer, B., Van de Wal, R. S. W., Lourens, L. J., Bintanja, R., & Reerink, T. J. (2013). A continuous simulation of
 1920 global ice volume over the past 1 million years with 3-D ice-sheet models. *Climate Dynamics*, 41(5-6), 1365-1384.
 1921 <https://doi.org/10.1007/s00382-012-1562-2>.
- 1922
 1923 de Boer, B., Lourens, L. J., & Van De Wal, R. S. (2014). Persistent 400,000-year variability of Antarctic ice volume
 1924 and the carbon cycle is revealed throughout the Plio-Pleistocene. *Nature Communications*, 5, 2999.
 1925 <https://doi.org/10.1038/ncomms3999>.
- 1926
 1927 de Boer, B., Stocchi, P., and van de Wal, R.W.S. (2014b). A fully coupled 3-D ice- sheet – sea-level model:
 1928 algorithm and applications, *Geosci. Model Dev. Discuss.*, 7, 2141-2156,
 1929 DOI:10.5194/gmd-7-2141-2014.
- 1930
 1931 de Boer, B., Dolan, A. M., Bernales, J., Gasson, E., Golledge, N. R., Sutter, J., ... & Saito, F. (2015). Simulating
 1932 the Antarctic ice sheet in the late-Pliocene warm period: PLISMIP-ANT, an ice-sheet model intercomparison
 1933 project. *The Cryosphere*, 9, 881-903. <https://doi.org/10.5194/tc-9-881-2015>.
- 1934
 1935 de Boer, B., Haywood, A. M., Dolan, A. M., Hunter, S. J., & Prescott, C. L. (2017a). The transient response of ice
 1936 volume to orbital forcing during the warm late Pliocene. *Geophysical Research Letters*, 44(20), 10-486.
 1937 <https://doi.org/10.1002/2017GL073535>.
- 1938
 1939 de Boer, B., Stocchi, P., Whitehouse, P., and Van de Wal, R.S.W. (2017b), Current state and future perspectives
 1940 on coupled ice-sheet – sea-level modelling, *Quaternary Science Reviews*, 169:13-28, doi
 1941 10.1016/j.quascirev.2017.05.013.
- 1942
 1943 de Boer, B., Colleoni, F., Golledge, N. R., & DeConto, R. M. (2019). Paleo ice-sheet modeling to constrain past
 1944 sea level. *PAGES Magazine*, 27(1), 20.

- 1945 DeConto, R. M., & Pollard, D. (2003). Rapid Cenozoic glaciation of Antarctica induced by declining atmospheric
 1946 CO₂. *Nature*, 421(6920), 245-249. <https://doi.org/10.1038/nature01290>.
 1947
 1948 DeConto, R.M., Pollard, D., Harwood, D., 2007. Sea ice feedback and Cenozoic evolution of Antarctic climate and
 1949 ice sheets. *Paleoceanography* 22, PA3214, <https://doi.org/10.1029/2006PA001350>.
 1950
 1951 DeConto, R.M., Pollard, D., Wilson, P.A., Pälike, H., Lear, C., Pagani, M., 2008. Thresholds for Cenozoic bipolar
 1952 glaciation. *Nature* 455, 653-656.
 1953
 1954 Pollard, D., & DeConto, R. M. (2009). Modelling West Antarctic ice sheet growth and collapse through the past five
 1955 million years. *Nature*, 458(7236), 329-332.
 1956
 1957 DeConto, R. M., Pollard, D., & Kowalewski, D. (2012). Reprint of: Modeling Antarctic ice sheet and climate
 1958 variations during Marine Isotope Stage 31. *Global and Planetary Change*, 96, 181-188.
 1959 <https://doi.org/10.1016/j.gloplacha.2012.05.018>.
 1960
 1961 DeConto, R.M., and D. Pollard. 2016. Contribution of Antarctica to past and future sea level rise. *Nature* 531:591–
 1962 597, <https://doi.org/10.1038/nature17145>.
 1963
 1964 Denton, G. H., & Sugden, D. E. (2005). Meltwater features that suggest Miocene ice-sheet overriding of the
 1965 Transantarctic Mountains in Victoria Land, Antarctica. *Geografiska Annaler: Series A, Physical Geography*, 87(1),
 1966 67-85.
 1967
 1968 de La Vega, E., Chalk, T. B., Wilson, P. A., Bysani, R. P., & Foster, G. L. (2020). Atmospheric CO₂ during the Mid-
 1969 Piacenzian Warm Period and the M2 glaciation. *Scientific reports*, 10(1), 1-8.
 1970
 1971 Deschamps, P., Durand, N., Bard, E., Hamelin, B., Camoin, G., Thomas, A. L., ... & Yokoyama, Y. (2012). Ice-
 1972 sheet collapse and sea-level rise at the Bølling warming 14,600 years ago. *Nature*, 483(7391), 559-564.
 1973
 1974 Detlef, H., Belt, S. T., Sosdian, S. M., Smik, L., Lear, C. H., Hall, I. R., ... & Kender, S. (2018). Sea ice dynamics
 1975 across the Mid-Pleistocene transition in the Bering Sea. *Nature communications*, 9(1), 1-11.
 1976
 1977 De Schepper, S., Gibbard, P. L., Salzmann, U., & Ehlers, J. (2014). A global synthesis of the marine and terrestrial
 1978 evidence for glaciation during the Pliocene Epoch. *Earth-Science Reviews*, 135, 83-102.
 1979 <https://doi.org/10.1016/j.earscirev.2014.04.003>.
 1980
 1981 De Santis, L., Anderson, J. B., Brancolini, G. & Zayatz, I. In Antarctic Research Series Vol. 71 (eds Cooper, A. K.
 1982 et al.) 235–260 (Springer International, 1995).
 1983
 1984 De Santis, L., Prato, S., Brancolini, G., Lovo, M., & Torelli, L. (1999). The Eastern Ross Sea continental shelf during
 1985 the Cenozoic: implications for the West Antarctic ice sheet development. *Global and Planetary Change*, 23(1-4),
 1986 173-196. [https://doi.org/10.1016/S0921-8181\(99\)00056-9](https://doi.org/10.1016/S0921-8181(99)00056-9).
 1987
 1988 De Santis, L., Brancolini, G., & Donda, F. (2003). Seismo-stratigraphic analysis of the Wilkes Land continental
 1989 margin (East Antarctica): influence of glacially driven processes on the Cenozoic deposition. *Deep Sea Research*
 1990 *Part II: Topical Studies in Oceanography*, 50(8-9), 1563-1594. [https://doi.org/10.1016/S0967-0645\(03\)00079-1](https://doi.org/10.1016/S0967-0645(03)00079-1).
 1991
 1992 De Vleeschouwer, D., M. Vahlenkamp, M. Crucifix, H. Pälike (2017). Alternating Southern and Northern
 1993 Hemisphere climate response to astronomical forcing during the past 35 m.y.. *Geology*, 45 (4): 375–378. doi:
 1994 <https://doi.org/10.1130/G38663.1>
 1995
 1996 Dickens, W. A., Kuhn, G., Leng, M. J., Graham, A. G. C., Dowdeswell, J. A., Meredith, M. P., ... & Smith, J. A.
 1997 (2019). Enhanced glacial discharge from the eastern Antarctic Peninsula since the 1700s associated with a positive
 1998 Southern Annular Mode. *Scientific reports*, 9(1), 1-11.
 1999
 2000 Dumitru, O. A., Austermann, J., Polyak, V. J., Fornós, J. J., Asmerom, Y., Ginés, J., ... & Onac, B. P. (2019).
 2001 Constraints on global mean sea level during Pliocene warmth. *Nature*, 574(7777), 233-236.
 2002 <https://doi.org/10.1038/s41586-019-1543-2>.
 2003
 2004 Dolan, A. M., De Boer, B., Bernales, J., Hill, D. J., & Haywood, A. M. (2018). High climate model dependency of
 2005 Pliocene Antarctic ice-sheet predictions. *Nature communications*, 9(1), 1-12. <https://doi.org/10.1038/s41467-018-05179-4>.
 2006
 2007
 2008 Domack, E., Leventer, A., Dunbar, R., Taylor, F., Brachfeld, S., & Sjunneskog, C. (2001). Chronology of the
 2009 Palmer Deep site, Antarctic Peninsula: a Holocene palaeoenvironmental reference for the circum-Antarctic. *The*
 2010 *Holocene*, 11(1), 1-9.
 2011

- 2012 Donda F., Brancolini G., O'Brien P. E., De Santis L., Escutia C., 2007. Sedimentary processes in the Wilkes Land
2013 margin: a record of the Cenozoic East Antarctic Ice Sheet evolution. *Journal of the Geological Society of London*,
2014 Vol. 164, , pp. 243–256.
- 2015
2016 Dowdeswell, J. A., Batchelor, C. L., Montelli, A., Ottesen, D., Christie, F. D. W., Dowdeswell, E. K., & Evans, J.
2017 (2020). Delicate seafloor landforms reveal past Antarctic grounding-line retreat of kilometers per year. *Science*,
2018 368(6494), 1020-1024. <https://doi.org/10.1126/science.aaz3059>.
- 2019
2020 Dowsett, H. J., Robinson, M. M., Haywood, A. M., Hill, D. J., Dolan, A. M., Stoll, D. K., ... & Riesselman, C. R.
2021 (2012). Assessing confidence in Pliocene sea surface temperatures to evaluate predictive models. *Nature Climate*
2022 *Change*, 2(5), 365-371.
- 2023
2024 Dowsett, H. J., Foley, K. M., Stoll, D. K., Chandler, M. A., Sohl, L. E., Bentsen, M., ... & Dolan, A. M. (2013). Sea
2025 surface temperature of the mid-Piacenzian ocean: a data-model comparison. *Scientific reports*, 3.
2026 <https://doi.org/10.1038/srep02013>.
- 2027
2028 Dowsett, H., Dolan, A., Rowley, D., Moucha, R., Forte, A. M., Mitrovica, J. X., ... & Foley, K. (2016). The PRISM4
2029 (mid-Piacenzian) paleoenvironmental reconstruction. *Climate of the Past*, 12(7), 1519-1538.
- 2030 Dutton, A., A.E. Carlson, A.J. Long, G.A. Milne, P. Clark, R. DeConto, B.P. Horton, S. Rahmstorf, and M.E. Raymo.
2031 (2015). Sea-level rise due to polar ice-sheet mass loss during past warm periods. *Science* 349:1:6244,
2032 <https://doi.org/10.1126/science.aaa4019>.
- 2033 Dwyer, G. S., & Chandler, M. A. (2009). Mid-Pliocene sea level and continental ice volume based on coupled
2034 benthic Mg/Ca palaeotemperatures and oxygen isotopes. *Philosophical Transactions of the Royal Society A:*
2035 *Mathematical, Physical and Engineering Sciences*, 367(1886), 157-168. <https://doi.org/10.1098/rsta.2008.0222>.
- 2036 Edwards, T. L., Brandon, M. A., Durand, G., Edwards, N. R., Golledge, N. R., Holden, P. B., ... & Wernecke, A.
2037 (2019). Revisiting Antarctic ice loss due to marine ice-cliff instability. *Nature*, 566(7742), 58-64.
2038 <https://doi.org/10.1038/s41586-019-0901-4>.
- 2039
2040 Eldrett, J.S., Harding, I.C., Wilson, P.A., Butler, E., and Roberts, A.P., 2007, Continental ice in Greenland during
2041 the Eocene and Oligocene: *Nature*, v. 446, no. 7132, p. 176, <https://doi.org/10.1038/nature05591>.
- 2042 EPICA Community Members. One-to-one coupling of glacial climate variability in Greenland and Antarctica. *Nature*
2043 **444**, 195–198 (2006). <https://doi.org/10.1038/nature05301>.
- 2044 Escutia C., Eitrem S.L., Cooper A.K.(1997). Cenozoic glaciomarine sequences on the Wilkes Land continental
2045 rise, Antarctica. *Proceedings Volume-VII International Symposium on Antarctic Earth Sciences*, pp. 791-795.
- 2046
2047 Escutia, C., Warnke, D., Acton, G. D., Barcena, A., Burckle, L., Canals, M., & Frazee, C. S. (2003). Sediment
2048 distribution and sedimentary processes across the Antarctic Wilkes Land margin during the Quaternary. *Deep Sea*
2049 *Research Part II: Topical Studies in Oceanography*, 50(8–9), 1481–1508. [https://doi.org/10.1016/S0967-](https://doi.org/10.1016/S0967-0645(03)00073-0)
2050 0645(03)00073-0.
- 2051 Escutia, C., De Santis, L., Donda, F., Dunbar, R. B., Cooper, A. K., Brancolini, G., & Eitrem, S. L. (2005). Cenozoic
2052 ice sheet history from East Antarctic Wilkes Land continental margin sediments. *Global and Planetary Change*,
2053 45(1-3), 51-81. <https://doi.org/10.1016/j.gloplacha.2004.09.010>.
- 2054 Escutia, C., M.A. Barcena, R.G. Lucchi, O. Romero, M. Ballegeer, J.J. Gonzalez, and D. Harwood (2009). Circum-
2055 Antarctic warming events between 4 and 3.5 Ma recorded in sediments from the Prydz Bay (ODP Leg 188) and
2056 the Antarctic Peninsula (ODP Leg 178) margins. *Global and Planetary Change* 69:170–184,
2057 <https://doi.org/10.1016/j.gloplacha.2009.09.003>.
- 2058 Escutia, C., H. Brinkhuis, A. Klaus, and the Expedition 318 Scientists. (2011). Wilkes Land Glacial History:
2059 Cenozoic East Antarctic Ice Sheet evolution from Wilkes Land margin sediments. *Proceedings of the Integrated*
2060 *Ocean Drilling Program, Volume 318*. Integrated Ocean Drilling Program Management International Inc., Tokyo,
2061 <https://doi.org/10.2204/iodp.proc.318.2011>.
- 2062
2063 Escutia, C., DeConto, R. M., Dunbar, R., Santis, L. D., Shevenell, A., & Naish, T. (2019). Keeping an eye on
2064 Antarctic Ice Sheet stability. *Oceanography*, 32(1), 32-46.
- 2065
2066 Etourneau, J., G. Sgubin, L. Crosta, D. Swingedouw, V. Willmott, L. Barbara, M.-N. Houssais, S. Schouten, J.
2067 Sinninghe Damst., H. Goose, and others. (2019). Ocean temperature impact on ice shelf extent in the eastern
2068 Antarctic Peninsula. *Nature Communications* 10:304, <https://doi.org/10.1038/s41467-018-08195-6>.
- 2069

- 2070 Eitrem, S. L., Cooper, A. K., & Wannesson, J. (1995). Seismic stratigraphic evidence of ice sheet advances on
 2071 the Wilkes Land margin of Antarctica. *Sedimentary Geology*, 96(1–2), 131–156. [https://doi.org/10.1016/0037-](https://doi.org/10.1016/0037-0738(94)00130-M)
 2072 [0738\(94\)00130-M](https://doi.org/10.1016/0037-0738(94)00130-M).
 2073
 2074 Evangelinos, D., Escutia, C., Etourneau, J., Hoem, F., Bijl, P., Boterblom, W., van de Fliedert, T., Valero, L., Flores,
 2075 J.-A., Rodriguez-Tovar, F. J., Jimenez-Espejo, F. J., Salabarnada, A., & López-Quirós, A. (2020). Late Oligocene-
 2076 Miocene proto-Antarctic Circumpolar Current dynamics off the Wilkes Land margin, East Antarctica. *Global and*
 2077 *Planetary Change*, 191, 103221. <https://doi.org/10.1016/j.gloplacha.2020.103221>.
 2078
 2079 Fischer, H., Severinghaus, J., Brook, E., Wolff, E., Albert, M., Alemany, O., ... & Wilhelms, F. (2013). Where to find
 2080 1.5 million yr old ice for the IPICS" Oldest-Ice" ice core. *Climate of the Past*, 9(6), 2489-2505.
 2081
 2082 Flower, B. P., & Kennett, J. P. (1993). Middle Miocene ocean-climate transition: High-resolution oxygen and carbon
 2083 isotopic records from Deep Sea Drilling Project Site 588A, southwest Pacific. *Paleoceanography*, 8(6), 811-843.
 2084
 2085 Foster GL, Lear CH, Rae JWB. 2012. The evolution of pCO₂, ice volume and climate during the middle Miocene.
 2086 *Earth and Planetary Science Letters* 341-344: 243-54. <https://doi.org/10.1016/j.epsl.2012.06.007>.
 2087
 2088 Fretwell, P., Pritchard, H. D., Vaughan, D. G., Bamber, J. L., Barrand, N. E., Bell, R., ... & Catania, G. (2013).
 2089 Bedmap2: improved ice bed, surface and thickness datasets for Antarctica. *The Cryosphere*, 7(1), 375-393.
<https://doi.org/10.5194/tc-7-375-2013>.
 2090
 2091 Fürst, J. J., Durand, G., Gillet-Chaulet, F., Tavard, L., Rankl, M., Braun, M., & Gagliardini, O. (2016). The safety
 2092 band of Antarctic ice shelves. *Nature Climate Change*, 6(5), 479-482. <https://doi.org/10.1038/nclimate2912>.
 2093
 2094 Galeotti, S., R.M. DeConto, T.R. Naish, P. Stocchi, F. Florindo, M. Pagani, P.J. Barrett, S.M. Bohaty, L. Lanci, D.
 2095 Pollard, Sandroni. Sonia and Talarico, Franco M. and Zachos, James C. (2016). Antarctic Ice Sheet variability
 2096 across the Eocene-Oligocene boundary climate transition. *Science*, 352:76-80,
<https://doi.org/10.1126/science.aab0669>.
 2097
 2098 Ganopolski, A., & Robinson, A. (2011). The past is not the future. *Nature Geoscience*, 4(10), 661-663.
 2099 <https://doi.org/10.1038/ngeo1268>.
 2100
 2101 Gasson, E., Lunt, D. J., DeConto, R., Goldner, A., Heinemann, M., Huber, M., ... & Winguth, A. (2014). Uncertainties
 2102 in the modelled CO₂ threshold for Antarctic glaciation. *Climate of the Past*. <https://doi.org/10.5194/cp-10-451-2014>.
 2103
 2104 Gasson, E., DeConto, R., & Pollard, D. (2015). Antarctic bedrock topography uncertainty and ice sheet stability.
 2105 *Geophysical Research Letters*, 42(13), 5372-5377.
 2106
 2107 Gasson, E., R.M. DeConto, and D. Pollard. (2016). Dynamic Antarctic ice sheet during the early to mid-Miocene.
 2108 *Proceedings of the National Academy of Sciences of the United States of America* 113(13):3,459–3,464,
<https://doi.org/10.1073/pnas.1516130113>.
 2109
 2110 Gasson, E.G.W., and B.A. Keisling (2020). The Antarctic Ice Sheet: A paleoclimate modeling perspective.
 2111 *Oceanography* 33(2), <https://doi.org/10.5670/oceanog.2020.208>.
 2112
 2113 Gersonde, R., Crosta, X., Abelmann, A., & Armand, L. (2005). Sea-surface temperature and sea ice distribution of
 2114 the Southern Ocean at the EPILOG Last Glacial Maximum—a circum-Antarctic view based on siliceous microfossil
 records. *Quaternary Science Reviews*, 24(7-9), 869-896.
 2115
 2116 Goelzer, H., Huybrechts, P., Loutre, M.-F., and Fichefet, T. (2016). Last Interglacial climate and sea-level evolution
 from a coupled ice sheet–climate model, *Clim. Past*, 12, 2195–2213, <https://doi.org/10.5194/cp-12-2195-2016>.
 2117
 2118 Goldner, A., Herold, N., & Huber, M. (2014). The Challenge of Simulating the Warmth of the Mid-Miocene Climatic
 Optimum in CESM1. *Climate of the Past*. <https://doi.org/10.5194/cp-10-523-2014>.
 2119
 2120 Gohl, K., Uenzelmann-Neben, G., Larer, R. D., Hillenbrand, C. D., Hochmuth, K., Kalberg, T., ... & Nitsche, F. O.
 2121 (2013). Seismic stratigraphic record of the Amundsen Sea Embayment shelf from pre-glacial to recent times:
 Evidence for a dynamic West Antarctic ice sheet. *Marine Geology*, 344, 115-131.
 2122 <https://doi.org/10.1016/j.margeo.2013.06.011>.
 2123
 2124 Gohl, K., Wellner, J.S., Klaus, A., and the Expedition 379 Scientists, 2019. *Expedition 379 Preliminary Report:*
 2125 *Amundsen Sea West Antarctic Ice Sheet History*. International Ocean Discovery Program.
 2126 <https://doi.org/10.14379/iodp.pr.379.2019>.

2127 Golledge, N.R., C.J. Fogwill, A.N. Mackintosh, and K.M. Buckley. 2012. Dynamics of the last glacial maximum
2128 Antarctic ice-sheet and its response to ocean forcing. *Proceedings of the National Academy of Sciences of the*
2129 *United States of America* 109:16,052–16,056, <https://doi.org/10.1073/pnas.1205385109>.

2130 Golledge, N. R., Levy, R. H., McKay, R. M., Fogwill, C. J., White, D. A., Graham, A. G., ... & Hall, B. L. (2013).
2131 Glaciology and geological signature of the Last Glacial Maximum Antarctic ice sheet. *Quaternary Science Reviews*,
2132 78, 225-247.

2133 Golledge, N. R., Menviel, L., Carter, L., Fogwill, C. J., England, M. H., Cortese, G., & Levy, R. H. (2014). Antarctic
2134 contribution to meltwater pulse 1A from reduced Southern Ocean overturning. *Nature communications*, 5, 5107.
2135 <https://doi.org/10.1038/ncomms6107>.

2136 Golledge, N. R., Kowalewski, D. E., Naish, T. R., Levy, R. H., Fogwill, C. J., & Gasson, E. G. (2015). The multi-
2137 millennial Antarctic commitment to future sea-level rise. *Nature*, 526(7573), 421-425.
2138 <https://doi.org/10.1038/nature15706>.

2139 Golledge, N. R., Thomas, Z. A., Levy, R. H., Gasson, E. G., Naish, T. R., McKay, R. M., ... & Fogwill, C. J. (2017a).
2140 Antarctic climate and ice-sheet configuration during the early Pliocene interglacial at 4.23 Ma. *Climate of the Past*,
2141 13(7). <https://doi.org/10.5194/cp-13-959-2017>.

2142 Golledge, N. R., Levy, R. H., McKay, R. M., & Naish, T. R. (2017b). East Antarctic ice sheet most vulnerable to
2143 Weddell Sea warming. *Geophysical Research Letters*, 44(5), 2343-2351.

2144 Golledge, N. R., Keller, E. D., Gomez, N., Naughten, K. A., Bernales, J., Trusel, L. D., & Edwards, T. L. (2019).
2145 Global environmental consequences of twenty-first-century ice-sheet melt. *Nature*, 566(7742), 65-72.
2146 <https://doi.org/10.1038/s41586-019-0889-9>.

2147 Golledge, N. R. (2020). Long-term projections of sea-level rise from ice sheets. *Wiley Interdisciplinary Reviews:*
2148 *Climate Change*, 11(2), e634.

2149 Gomez, N., Mitrovica, J.X., Huybers, P., Clark, P.U. (2010). Sea level as a stabilizing factor for marine-ice-sheet
2150 grounding lines. *Nat. Geosci.* 3, 850e853.

2151 Gomez, N., Pollard, D., & Mitrovica, J. X. (2013). A 3-D coupled ice sheet–sea level model applied to Antarctica
2152 through the last 40 ky. *Earth and Planetary Science Letters*, 384, 88-99. <https://doi.org/10.1016/j.epsl.2013.09.042>.

2153 Gomez, N., Pollard, D., & Holland, D. (2015). Sea-level feedback lowers projections of future Antarctic Ice-Sheet
2154 mass loss. *Nature communications*, 6(1), 1-8. <https://doi.org/10.1038/ncomms9798>.

2155 Gomez, N., Latychev, K., & Pollard, D. (2018). A coupled ice sheet–sea level model incorporating 3D earth
2156 structure: variations in Antarctica during the last deglacial retreat. *Journal of Climate*, 31(10), 4041-4054.

2157 Gomez, N., Weber, M. E., Clark, P. U., Mitrovica, J. X., & Han, H. K. (2020). Antarctic ice dynamics amplified by
2158 Northern Hemisphere sea-level forcing. *Nature*, 587(7835), 600-604.

2159 Graham, A. G., Dutrieux, P., Vaughan, D. G., Nitsche, F. O., Gyllencreutz, R., Greenwood, S. L., ... & Jenkins, A.
2160 (2013). Seabed corrugations beneath an Antarctic ice shelf revealed by autonomous underwater vehicle survey:
2161 origin and implications for the history of Pine Island Glacier. *Journal of Geophysical Research: Earth Surface*,
2162 118(3), 1356-1366.

2163 Grant, G. R., Naish, T. R., Dunbar, G. B., Stocchi, P., Kominz, M. A., Kamp, P. J., ... & Patterson, M. O. (2019).
2164 The amplitude and origin of sea-level variability during the Pliocene epoch. *Nature*, 574(7777), 237-241.
2165 <https://doi.org/10.1038/s41586-019-1619-z>.

2166 Grant G., Naish T, Pliocene sea-level revisited: Is there more than meets the eye? (2021). PAGES, in press,
2167 doi.org/10.22498/pages.29.1.4.

2168 Green, Ryan A., et al. "Evaluating seasonal sea-ice cover over the Southern Ocean from the Last Glacial
2169 Maximum." *Climate of the Past Discussions* (2020): 1-23.

2170 Greenop R, Foster GL, Wilson PA, Lear CH. 2014. Middle Miocene climate instability associated with high-
2171 amplitude CO2 variability. *Paleoceanography* 29. <https://doi.org/10.1002/2014PA002653>.

2172 Gulick, S. P., Shevenell, A. E., Montelli, A., Fernandez, R., Smith, C., Warny, S., ... & Blankenship, D. D. (2017).
2173 Initiation and long-term instability of the East Antarctic Ice Sheet. *Nature*, 552(7684), 225-229.
2174 <https://doi.org/10.1038/nature25026>.

2190 Hannah, M. J. (2006). The palynology of ODP site 1165, Prydz Bay, East Antarctica: a record of Miocene glacial
2191 advance and retreat. *Palaeogeography, Palaeoclimatology, Palaeoecology*, 231(1-2), 120-133.
2192 <https://doi.org/10.1016/j.palaeo.2005.07.029>.
2193
2194 Halberstadt, A. R. W., Simkins, L. M., Greenwood, S. L., & Anderson, J. B. (2016). Past ice-sheet behaviour: retreat
2195 scenarios and changing controls in the Ross Sea, Antarctica. *The Cryosphere*, 10, 1003-1020.
2196 <https://doi.org/10.5194/tc-10-1003-2016>.
2197
2198 Hambrey, M.J., W.U. Ehrmann, and B. Larsen. (1991). Cenozoic glacial record of the Prydz Bay continental shelf,
2199 East Antarctica. Pp. 77–132 in *Proceedings of the Ocean Drilling Program Scientific Results, Volume 119*. J.
2200 Barron, B. Larsen, et al., eds, College Station, TX, <https://doi.org/10.2973/odp.proc.sr.119.200.1991>.
2201
2202 Hannah, M. J. (2006). The palynology of ODP site 1165, Prydz Bay, East Antarctica: a record of Miocene glacial
2203 advance and retreat. *Palaeogeography, Palaeoclimatology, Palaeoecology*, 231(1-2), 120-133.
2204 <https://doi.org/10.1016/j.palaeo.2005.07.029>.
2205
2206 Hansen, M. A., Passchier, S., Khim, B.-K., Song, B., and Williams, T., 2015. Threshold behavior of a marine-based
2207 sector of the East Antarctic Ice Sheet in response to early Pliocene ocean warming, *Paleoceanography*, 30,
2208 doi:10.1002/2014PA002704.
2209
2210 Hansen, M.A. and Passchier, S., 2017. Oceanic circulation changes during early Pliocene marine ice-sheet
2211 instability in Wilkes Land, East Antarctica. *Geo-Mar Lett.*, doi:10.1007/s00367-016-0489-8
2212
2213 Hartman, J. D., Sangiorgi, F., Peterse, F., Barcena, M. A., Albertazzi, S., Asioli, A., ... & Trincardi, F. (2016).
2214 Phytoplankton assemblages and lipid biomarkers indicate sea-surface warming and sea-ice decline in the Ross
2215 Sea during Marine Isotope sub-Stage 5e. *EGUGA*, EPSC2016-2637.
2216
2217 Hartman, J. D., Sangiorgi, F., Salabarnada, A., Peterse, F., Houben, A. J., Schouten, S., ... & Bijl, P. K. (2018).
2218 Paleoceanography and ice sheet variability offshore Wilkes Land, Antarctica-Part 3: Insights from Oligocene-
2219 Miocene TEX86-based sea surface temperature reconstructions. *Climate of the Past*, 14(9), 1275-1297.
2220 <https://doi.org/10.5194/cp-14-1275-2018>.
2221
2222 Hauptvogel, D. W., & Passchier, S. (2012). Early–Middle Miocene (17–14 Ma) Antarctic ice dynamics reconstructed
2223 from the heavy mineral provenance in the AND-2A drill core, Ross Sea, Antarctica. *Global and Planetary Change*,
2224 82, 38-50. <https://doi.org/10.1016/j.gloplacha.2011.11.003>.
2225
2226 Haywood, A. M., Hill, D. J., Dolan, A. M., Otto-Bliesner, B. L., Bragg, F., Chan, W. L., ... & Zhang, Z. (2013).
2227 Large-scale features of Pliocene climate: results from the Pliocene Model Intercomparison Project. *Climate of the*
2228 *Past*, 9(1), 191-209.
2229
2230 Haywood, A. M., Dowsett, H. J., & Dolan, A. M. (2016). Integrating geological archives and climate models for the
2231 mid-Pliocene warm period. *Nature communications*, 7(1), 1-14. <https://doi.org/10.1038/ncomms10646>.
2232
2233 Haywood, A. M., Valdes, P. J., Aze, T., Barlow, N., Burke, A., Dolan, A. M., ... & Salzmann, U. (2019). What can
2234 Palaeoclimate Modelling do for you?. *Earth Systems and Environment*, 3(1), 1-18. <https://doi.org/10.1007/s41748-019-00093-1>.
2235
2236 Haywood, A. M., Tindall, J. C., Dowsett, H. J., Dolan, A. M., Foley, K. M., Hunter, S. J., Hill, D. J., Chan, W.-L.,
2237 Abe-Ouchi, A., Stepanek, C., Lohmann, G., Chandan, D., Peltier, W. R., Tan, N., Contoux, C., Ramstein, G., Li,
2238 X., Zhang, Z., Guo, C., Nisancioglu, K. H., Zhang, Q., Li, Q., Kamae, Y., Chandler, M. A., Sohl, L. E., Otto-Bliesner,
2239 B. L., Feng, R., Brady, E. C., von der Heydt, A. S., Baatsen, M. L. J., and Lunt, D. J.: A return to large-scale features
2240 of Pliocene climate: the Pliocene Model Intercomparison Project Phase 2, *Clim. Past Discuss.*,
2241 <https://doi.org/10.5194/cp-2019-145>, in review, 2020. <https://doi.org/10.5194/cp-2019-145>.
2242
2243 Hearty, P. J., Kindler, P., Cheng, H., & Edwards, R. L. (1999). A+ 20 m middle Pleistocene sea-level highstand
2244 (Bermuda and the Bahamas) due to partial collapse of Antarctic ice. *Geology*, 27(4), 375-378.
2245
2246 Hearty, P. J., Rovere, A., Sandstrom, M. R., O'Leary, M. J., Roberts, D., & Raymo, M. E. (2020). Pliocene-
2247 Pleistocene Stratigraphy and Sea-Level Estimates, Republic of South Africa With Implications for a 400 ppmv CO2
2248 World. *Paleoceanography and Paleoclimatology*, 35(7), e2019PA003835.
2249
2250 Herbert, T. D., Lawrence, K. T., Tzanova, A., Peterson, L. C., Caballero-Gill, R., & Kelly, C. S. (2016). Late Miocene
2251 global cooling and the rise of modern ecosystems. *Nature Geoscience*, 9(11), 843-847.
2252 <https://doi.org/10.1038/ngeo2813>.
2253
2254 Herold, N., Seton, M., Müller, R. D., You, Y., & Huber, M. (2008). Middle Miocene tectonic boundary conditions for
2255 use in climate models. *Geochemistry, Geophysics, Geosystems*, 9(10).

- 2257
2258 Hillenbrand, C. D., & Ehrmann, W. (2005). Late Neogene to Quaternary environmental changes in the Antarctic
2259 Peninsula region: evidence from drift sediments. *Global and Planetary Change*, 45(1-3), 165-191
- 2260 Hillenbrand, C. D., Kuhn, G., & Frederichs, T. (2009). Record of a Mid-Pleistocene depositional anomaly in West
2261 Antarctic continental margin sediments: an indicator for ice-sheet collapse?. *Quaternary Science Reviews*, 28(13-
2262 14), 1147-1159.
- 2263 Hillenbrand, C. D., Melles, M., Kuhn, G., & Larter, R. D. (2012). Marine geological constraints for the grounding-
2264 line position of the Antarctic Ice Sheet on the southern Weddell Sea shelf at the Last Glacial Maximum. *Quaternary
2265 Science Reviews*, 32, 25-47.
- 2266 Hillenbrand, C.-D., Bentley, M.J., Stollendorf, T.D., Hein, A.S., Kuhn, G., Graham, A.G.C., Fogwill, C.J., Kristoffersen,
2267 Y., Smith, J.A., Anderson, J.B., Larter, R.D., Melles, M., Hodgson, D.A., Mulvaney, R., Sugden, D.E., 2014.
2268 Reconstruction of changes in the Weddell Sea sector of the Antarctic Ice Sheet since the Last Glacial Maximum.
2269 *Quat. Sci. Rev.* 100, 111e136. <http://dx.doi.org/10.1016/j.quascirev.2013.07.020>.
- 2270 Hillenbrand, C. D., Smith, J. A., Hodell, D. A., Greaves, M., Poole, C. R., Kender, S., ... & Klages, J. P. (2017).
2271 West Antarctic Ice Sheet retreat driven by Holocene warm water incursions. *Nature*, 547(7661), 43-48.
2272 <https://doi.org/10.1038/nature22995>.
2273
- 2274 Hochmuth, Katharina, and Karsten Gohl (2019). "Seaward growth of Antarctic continental shelves since
2275 establishment of a continent-wide ice sheet: Patterns and mechanisms." *Palaeogeography, Palaeoclimatology,
2276 Palaeoecology* 520: 44-54. <https://doi.org/10.1016/j.palaeo.2019.01.025>.
2277
- 2278 Hochmuth, K., Gohl, K., Leitchenkov, G., Sauermilch, I., Whittaker, J. M., Uenzelmann-Neben, G., Davy B. & De
2279 Santis, L. (2020). The evolving paleobathymetry of the circum-Antarctic Southern Ocean since 34 Ma—a key to
2280 understanding past cryosphere-ocean developments. *Geochemistry, Geophysics, Geosystems*, e2020GC009122.
2281 <https://doi.org/10.1029/2020GC009122>.
2282
- 2283 Hodell, D. A., Charles, C. D., & Ninnemann, U. S. (2000). Comparison of interglacial stages in the South Atlantic
2284 sector of the southern ocean for the past 450 kyr: implications for Marine Isotope Stage (MIS) 11. *Global and
2285 Planetary Change*, 24(1), 7-26.
2286
- 2287 Hoffman, J. S., Clark, P. U., Parnell, A. C., & He, F. (2017). Regional and global sea-surface temperatures during
2288 the last interglaciation. *Science*, 355(6322), 276-279. <https://doi.org/10.1126/science.aai8464>.
2289
- 2290 Hodgson, D. A., Graham, A. G., Roberts, S. J., Bentley, M. J., Cofaigh, C. O., Verleyen, E., ... & Verfaillie, D.
2291 (2014). Terrestrial and submarine evidence for the extent and timing of the Last Glacial Maximum and the onset of
2292 deglaciation on the maritime-Antarctic and sub-Antarctic islands. *Quaternary Science Reviews*, 100, 137-158.
2293
- 2294 Holbourn, A., Kuhnt, W., Schulz, M., Flores, J. A., & Andersen, N. (2007). Orbitally-paced climate evolution during
2295 the middle Miocene "Monterey" carbon-isotope excursion. *Earth and Planetary Science Letters*, 261(3-4), 534-550.
2296
- 2297 Holbourn, A., Kuhnt, W., Clemens, S., Prell, W., & Andersen, N. (2013). Middle to late Miocene stepwise climate
2298 cooling: Evidence from a high-resolution deep water isotope curve spanning 8 million years. *Paleoceanography*,
2299 28(4), 688-699.
2300
- 2301 Holbourn, A., Kuhnt, W., Lyle, M., Schneider, L., Romero, O., & Andersen, N. (2014). Middle Miocene climate
2302 cooling linked to intensification of eastern equatorial Pacific upwelling. *Geology*, 42(1), 19-22.
2303 <https://doi.org/10.1130/G34890.1>.
2304
- 2305 Holden, P. B., Edwards, N. R., Wolff, E. W., Valdes, P. J., & Singarayer, J. S. (2011). The Mid-Brunhes event and
2306 West Antarctic ice sheet stability. *Journal of Quaternary Science*, 26(5), 474-477. <https://doi.org/10.1002/jqs.1525>.
2307
- 2308 Holloway, M. D., Sime, L. C., Singarayer, J. S., Tindall, J. C., Bunch, P., & Valdes, P. J. (2016). Antarctic last
2309 interglacial isotope peak in response to sea ice retreat not ice-sheet collapse. *Nature communications*, 7(1), 1-9.
2310 <https://doi.org/10.1038/ncomms12293>.
2311
- 2312 Honisch B, Hemming G, Archer D, Siddal M, McManus J. 2009. Atmospheric carbon dioxide concentration across
2313 the Mid-Pleistocene Transition. *Science* 324: 1551-4. <https://doi.org/10.1126/science.1171477>.
- 2314 Horgan, H. J., Christianson, K., Jacobel, R. W., Anandakrishnan, S., & Alley, R. B. (2013). Sediment deposition at
2315 the modern grounding zone of Whillans Ice Stream, West Antarctica. *Geophysical Research Letters*, 40(15), 3934-
2316 3939.
2317

- 2318 Huybrechts, P.: Sea-level changes at the LGM from ice-dynamic reconstructions of the Greenland and Antarctic
 2319 ice sheets during the glacial cycles, *Quaternary Sci. Rev.*, 21, 203–231, [https://doi.org/10.1016/S0277-](https://doi.org/10.1016/S0277-3791(01)00082-8)
 2320 [3791\(01\)00082-8](https://doi.org/10.1016/S0277-3791(01)00082-8), 2002.
- 2321 Huang, X., Gohl, K., & Jokat, W. (2014). Variability in Cenozoic sedimentation and paleo-water depths of the
 2322 Weddell Sea basin related to pre-glacial and glacial conditions of Antarctica. *Global and Planetary Change*, 118,
 2323 25-41. <https://doi.org/10.1016/j.gloplacha.2014.03.010>.
- 2324 Huang, X., & Jokat, W. (2016). Middle Miocene to present sediment transport and deposits in the Southeastern
 2325 Weddell Sea, Antarctica. *Global and Planetary Change*, 139, 211-225.
- 2326 Huang, X., Stürz, M., Gohl, K., Knorr, G., & Lohmann, G. (2017). Impact of Weddell Sea shelf progradation on
 2327 Antarctic bottom water formation during the Miocene. *Paleoceanography*, 32(3), 304-317.
 2328 <https://doi.org/10.1002/2016PA002987>.
- 2329 IPCC AR5, 2013. *Climate Change (2013): The Physical Science Basis. Contribution of Working Group I to the Fifth
 2330 Assessment Report of the Intergovernmental Panel on Climate Change*. T.F. Stocker, D. Qin, G.-K. Plattner, M.
 2331 Tignor, S.K. Allen, J. Boschung, A. Nauels, Y. Xia, V. Bex and P.M. Midgley, eds, Cambridge University Press,
 2332 Cambridge, United Kingdom, and New York, NY, USA, 1,535 pp, <https://doi.org/10.1017/CBO9781107415324>.
- 2333 IPCC, SROCC, 2019: IPCC Special Report on the Ocean and Cryosphere in a Changing Climate [H.-O. Pörtner,
 2334 D.C. Roberts, V. Masson-Delmotte, P. Zhai, M. Tignor, E. Poloczanska, K. Mintenbeck, A. Alegria, M. Nicolai, A.
 2335 Okem, J. Petzold, B. Rama, N.M. Weyer (eds.)]. In press.
- 2336 Imbrie J, Hays JD, Martinson DG, McIntyre A, Mix AC, Morely JJ, PisiasNG, Prell WL, Shackleton NJ. 1984. The
 2337 orbital theory of Pleistocene climate: support from a revised chronology of the marine $\delta^{18}O$ record. In *Milankovitch
 2338 and Climate*, Vol. 1, Berger AL(ed.). D. Reidel: Dordrecht; 269–305.
- 2339 Irali, N., Galaasen, E.V., Ninnemann, U.S., Rosenthal, Y., Born, A., Kleiven, H.F., 2020. A low climate threshold
 2340 for south Greenland Ice Sheet demise during the Late Pleistocene. *Proceedings of the National Academy of
 2341 Sciences* 117, 190-195.
- 2342 Ivins, E. R., & James, T. S. (2005). Antarctic glacial isostatic adjustment: a new assessment. *Antarctic Science*,
 2343 17(4), 541. <https://doi.org/10.1017/S0954102005002968>.
- 2344 Ivins, E. R., James, T. S., Wahr, J., O. Schrama, E. J., Landerer, F. W., & Simon, K. M. (2013). Antarctic contribution
 2345 to sea level rise observed by GRACE with improved GIA correction. *Journal of Geophysical Research: Solid Earth*,
 2346 118(6), 3126-3141. <https://doi.org/10.1002/jgrb.50208>.
- 2347 Jacobs, S.S., H.H. Hellmer, C.S.M. Doake, A. Jenkins, and R.M. Frolich. 1992. Melting of ice shelves and the mass
 2348 balance of Antarctica. *Journal of Glaciology* 38(130):375–387. <https://doi.org/10.3189/S002214300002252>.
- 2349 Jakob, K. A., Wilson, P. A., Pross, J., Ezard, T. H., Fiebig, J., Repschläger, J., & Friedrich, O. (2020). A new sea-
 2350 level record for the Neogene/Quaternary boundary reveals transition to a more stable East Antarctic Ice Sheet.
 2351 *Proceedings of the National Academy of Sciences*, 117(49), 30980-30987.
- 2352 Jakobsson, M., Anderson, J. B., Nitsche, F. O., Dowdeswell, J. A., Gyllencreutz, R., Kirchner, N., ... & Majewski,
 2353 W. (2011). Geological record of ice shelf break-up and grounding line retreat, Pine Island Bay, West Antarctica.
 2354 *Geology*, 39(7), 691-694.
- 2355 Jakobsson, M., Anderson, J. B., Nitsche, F. O., Gyllencreutz, R., Kirchner, A. E., Kirchner, N., ... & Eriksson, B.
 2356 (2012). Ice sheet retreat dynamics inferred from glacial morphology of the central Pine Island Bay Trough, West
 2357 Antarctica. *Quaternary Science Reviews*, 38, 1-10.
- 2358 Jamieson, S. S., Vieli, A., Livingstone, S. J., Cofaigh, C. Ó., Stokes, C., Hillenbrand, C. D., & Dowdeswell, J. A.
 2359 (2012). Ice-stream stability on a reverse bed slope. *Nature Geoscience*, 5(11), 799-802.
 2360 <https://doi.org/10.1038/ngeo1600>.
- 2361 Jamieson, S. S., Vieli, A., Cofaigh, C. Ó., Stokes, C. R., Livingstone, S. J., & Hillenbrand, C. D. (2014).
 2362 Understanding controls on rapid ice-stream retreat during the last deglaciation of Marguerite Bay, Antarctica, using
 2363 a numerical model. *Journal of Geophysical Research: Earth Surface*, 119(2), 247-263.
- 2364 Jansen, E., Fronval, T., Rack, F., & Channell, J. E. (2000). Pliocene-Pleistocene ice rafting history and cyclicity in
 2365 the Nordic Seas during the last 3.5 Myr. *Paleoceanography*, 15(6), 709-721.
- 2366 Jansen, E. et al. in *Climate Change 2007: The Physical Science Basis* (eds Solomon, S. D. et al.) 433–497
 2367 (Cambridge Univ. Press, 2007).

- 2384
2385 Johnson, J. S., Bentley, M. J., Smith, J. A., Finkel, R. C., Rood, D. H., Gohl, K., ... & Schaefer, J. M. (2014). Rapid
2386 thinning of Pine Island Glacier in the early Holocene. *Science*, 343(6174), 999-1001.
2387
- 2388 Jones, R. S., Mackintosh, A. N., Norton, K. P., Golledge, N. R., Fogwill, C. J., Kubik, P. W., ... & Greenwood, S. L.
2389 (2015). Rapid Holocene thinning of an East Antarctic outlet glacier driven by marine ice sheet instability. *Nature*
2390 *Communications*, 6(1), 1-9.
2391
- 2392 Joughin, I., & Alley, R. B. (2011). Stability of the West Antarctic ice sheet in a warming world. *Nature Geoscience*,
2393 4(8), 506-513. <https://doi.org/10.1038/ngeo1194>.
2394
- 2395 Jouzel, J., Masson-Delmotte, V., Cattani, O., Dreyfus, G., Falourd, S., Hoffmann, G., ... & Fischer, H. (2007). Orbital
2396 and millennial Antarctic climate variability over the past 800,000 years. *science*, 317(5839), 793-796.
2397 <https://doi.org/10.1126/science.1141038>.
2398
- 2399 Justino, F., Lindemann, D., Kucharski, F., Wilson, A., Bromwich, D., and Stordal, F. (2017). Oceanic response to
2400 changes in the WAIS and astronomical forcing during the MIS31 superinterglacial, *Clim. Past*, 13, 1081–1095,
2401 <https://doi.org/10.5194/cp-13-1081-2017>.
2402
- 2403 Justino, F., Kucharski, F., Lindemann, D., Wilson, A., & Stordal, F. (2019). A modified seasonal cycle during MIS31
2404 super-interglacial favors stronger interannual ENSO and monsoon variability. *Climate of the Past*, 15(2), 735-749.
2405 <https://doi.org/10.5194/cp-15-735-2019>.
2406
- 2407 Kageyama, M., Paul, A., Roche, D. M., & Van Meerbeek, C. J. (2010). Modelling glacial climatic millennial-scale
2408 variability related to changes in the Atlantic meridional overturning circulation: a review. *Quaternary Science*
2409 *Reviews*, 29(21-22), 2931-2956. <https://doi.org/10.1016/j.quascirev.2010.05.029>.
2410
- 2411 Kageyama, M., Braconnot, P., Harrison, S. P., Haywood, A. M., Jungclaus, J. H., Otto-Bliesner, B. L., ... & Zhou,
2412 T. (2018). The PMIP4 contribution to CMIP6—Part 1: Overview and over-arching analysis plan. *Geoscientific Model*
2413 *Development*, 11(3), 1033-1057.
2414
- 2415 Karas, C., Khélifi, N., Bahr, A., Naafs, B. D. A., Nürnberg, D., & Herrle, J. O. (2020). Did North Atlantic cooling and
2416 freshening from 3.65–3.5 Ma precondition Northern Hemisphere ice sheet growth?. *Global and Planetary Change*,
2417 185, 103085.
2418
- 2419 Katz, M. E., Miller, K. G., Wright, J. D., Wade, B. S., Browning, J. V., Cramer, B. S., & Rosenthal, Y. (2008).
2420 Stepwise transition from the Eocene greenhouse to the Oligocene icehouse. *Nature Geoscience*, 1(5), 329-334.
2421 <https://doi.org/10.1038/ngeo179>.
2422
- 2423 Kemp, A. E. S., Grigorov, I., Pearce, R. B., & Garabato, A. N. (2010). Migration of the Antarctic Polar Front through
2424 the mid-Pleistocene transition: evidence and climatic implications. *Quaternary Science Reviews*, 29(17-18), 1993-
2425 2009. <https://doi.org/10.1016/j.quascirev.2010.04.027>.
2426
- 2427 Kennedy A. T., Farnsworth A., Lunt D. J., Lear C. H., Markwick P. J. (2015). Atmospheric and oceanic impacts of
2428 Antarctic glaciation across the Eocene–Oligocene transition. *Phil. Trans. R. Soc. A*.37320140419.
<https://doi.org/10.1098/rsta.2014.0419>
- 2429 Kennett, J. P. (1977). Cenozoic evolution of Antarctic glaciation, the circum-Antarctic Ocean, and their impact on
2430 global paleoceanography. *Journal of geophysical research*, 82(27), 3843-3860.
2431
- 2432 Kirkham, J. D., Hogan, K. A., Larter, R. D., Arnold, N. S., Nitsche, F. O., Golledge, N. R., and Dowdeswell, J. A.:
2433 Past water flow beneath Pine Island and Thwaites glaciers, West Antarctica, *The Cryosphere*, 13, 1959–1981,
2434 <https://doi.org/10.5194/tc-13-1959-2019>, 2019.
- 2435 Kim, S., De Santis, L., Hong, J. K., Cottlerle, D., Petronio, L., Colizza, E., ... & Wardell, N. (2018). Seismic
2436 stratigraphy of the Central Basin in northwestern Ross Sea slope and rise, Antarctica: Clues to the late Cenozoic
2437 ice-sheet dynamics and bottom-current activity. *Marine Geology*, 395, 363-379.
2438 <https://doi.org/10.1016/j.margeo.2017.10.013>.
- 2439 Kindler, P., & Hearty, P. J. (2000). Elevated marine terraces from Eleuthera (Bahamas) and Bermuda:
2440 sedimentological, petrographic and geochronological evidence for important deglaciation events during the middle
2441 Pleistocene. *Global and Planetary Change*, 24(1), 41-58.
2442
- 2443 King, A. L., & Howard, W. R. (2000). Middle Pleistocene sea-surface temperature change in the southwest Pacific
2444 Ocean on orbital and suborbital time scales. *Geology*, 28(7), 659-662.
2445

- 2446 Kingslake, J., Scherer, R. P., Albrecht, T., Coenen, J., Powell, R. D., Reese, R., ... & Whitehouse, P. L. (2018).
 2447 Extensive retreat and re-advance of the West Antarctic Ice Sheet during the Holocene. *Nature*, 558(7710), 430-
 2448 434. <https://doi.org/10.1038/s41586-018-0208-x>.
 2449
- 2450 Klages, J. P., Kuhn, G., Graham, A. G., Hillenbrand, C. D., Smith, J. A., Nitsche, F. O., ... & Gohl, K. (2015). Palaeo-
 2451 ice stream pathways and retreat style in the easternmost Amundsen Sea Embayment, West Antarctica, revealed
 2452 by combined multibeam bathymetric and seismic data. *Geomorphology*, 245, 207-222.
 2453
- 2454 Klages, J. P., Kuhn, G., Hillenbrand, C. D., Smith, J. A., Graham, A. G., Nitsche, F. O., ... & Wacker, L. (2017).
 2455 Limited grounding-line advance onto the West Antarctic continental shelf in the easternmost Amundsen Sea
 2456 Embayment during the last glacial period. *Plos one*, 12(7), e0181593.
 2457
- 2458 Kohfeld, K. E., Graham, R. M., De Boer, A. M., Sime, L. C., Wolff, E. W., Le Quéré, C., & Bopp, L. (2013). Southern
 2459 Hemisphere westerly wind changes during the Last Glacial Maximum: paleo-data synthesis. *Quaternary Science
 2460 Reviews*, 68, 76-95.
 2461
- 2462 Kominz, M. A., Browning, J. V., Miller, K. G., Sugarman, P. J., Mizintseva, S., & Scotese, C. R. (2008). Late
 2463 Cretaceous to Miocene sea-level estimates from the New Jersey and Delaware coastal plain coreholes: An error
 2464 analysis. *Basin Research*, 20(2), 211-226. <https://doi.org/10.1111/j.1365-2117.2008.00354.x>.
 2465
- 2466 Konfirst, M. A., Scherer, R. P., Hillenbrand, C. D., & Kuhn, G. (2012). A marine diatom record from the Amundsen
 2467 Sea—Insights into oceanographic and climatic response to the Mid-Pleistocene Transition in the West Antarctic
 2468 sector of the Southern Ocean. *Marine Micropaleontology*, 92, 40-51.
 2469
- 2470 Konrad, H., Thoma, M., Sasgen, I., Klemann, V., Grosfeld, K., Barbi, D., Martinec, Z., (2014). The deformational
 2471 response of a viscoelastic solid earth model coupled to a thermomechanical ice sheet model. *Surv. Geophys.* 35,
 2472 1441e1458. <http://dx.doi.org/10.1007/s10712-013-9257-8>.
 2473
- 2474 Kristoffersen, Y., & Jokat, W. (2008). The Weddell Sea, In: Cooper et al., Cenozoic climate history from seismic-
 2475 reflection and drilling studies on the Antarctic continental margin,. In Fabio Florindo & M. Siegert (Eds.), *Antarctic
 2476 Climate Evolution* (Vol. 8, pp. 144–152). Elsevier.
 2477
- 2478 Kriwet, J., Engelbrecht, A., Mörs, T., Reguero, M., & Pfaff, C. (2016). Ultimate Eocene (Priabonian)
 2479 chondrichthyans (Holocephali, Elasmobranchii) of Antarctica. *Journal of Vertebrate Paleontology*, 36(4), e1160911.
 2480
- 2481 Kulpecz, A.A., Miller, K.G., Browning, J.V., Edwards, L.E., Powars, D.S., McLaughlin, P.P., Jr., Harris, A.D., and
 2482 Feigenson, M.D., 2009, Post-impact deposition in the Chesapeake Bay impact structure: Variations in eustasy,
 2483 compaction, sediment supply, and passive-aggressive tectonism, in Gohn, G.S., et al., eds., The ICDP-USGS deep
 2484 drilling project in the Chesapeake Bay impact structure: Results from the Eyreville core holes: Geological Society
 2485 of America Special Paper 458, p. 811–837, [https://doi.org/10.1130/2009.2458\(34\)](https://doi.org/10.1130/2009.2458(34)).
 2486
- 2487 Kuhn, G., Hillenbrand, C. D., Kasten, S., Smith, J. A., Nitsche, F. O., Frederichs, T., ... & Mogollón, J. M. (2017).
 2488 Evidence for a palaeo-subglacial lake on the Antarctic continental shelf. *Nature communications*, 8(1), 1-10.
 2489
- 2490 Kunz-Pirrung, M., Gersonde, R., & Hodell, D. A. (2002). Mid-Brunhes century-scale diatom sea surface temperature
 2491 and sea ice records from the Atlantic sector of the Southern Ocean (ODP Leg 177, sites 1093, 1094 and core
 2492 PS2089-2). *Palaeogeography, Palaeoclimatology, Palaeoecology*, 182(3-4), 305-328.
 2493 [https://doi.org/10.1016/S0031-0182\(01\)00501-6](https://doi.org/10.1016/S0031-0182(01)00501-6).
 2494
- 2495 Ladant, J. B., Donnadieu, Y., Lefebvre, V., & Dumas, C. (2014). The respective role of atmospheric carbon dioxide
 2496 and orbital parameters on ice sheet evolution at the Eocene-Oligocene transition. *Paleoceanography*, 29(8), 810-
 2497 823. <https://doi.org/10.1002/2013PA002593>.
 2498
- 2499 Lambeck, K., and J. Chappell (2001), Sea level change through the last glacial cycle, *Science*, 292, 679–686,
 2500 doi:10.1126/science.1059549.
 2501
- 2502 Lambeck, K., Yokoyama, and A. Purcell (2002), Into and out of the Last glacial Maximum sea level change
 2503 during Oxygen Isotope Stages 3–2, *Quat. Sci. Rev.*, 21, 343–360.
 2504
- 2505 Lambeck, K., Rouby, H., Purcell, A., Sun, Y., & Sambridge, M. (2014). Sea level and global ice volumes from the
 2506 Last Glacial Maximum to the Holocene. *Proceedings of the National Academy of Sciences*, 111(43), 15296-15303.
 2507 <https://doi.org/10.1073/pnas.1411762111>.
 2508
- 2509 Lamy, F., Gersonde, R., Winckler, G., Esper, O., Jaeschke, A., Kuhn, G., ... & Kilian, R. (2014). Increased dust
 2510 deposition in the Pacific Southern Ocean during glacial periods. *Science*, 343(6169), 403-407.
 2511

- 2512 Lamy F., Chiang J.C.H., Martínez-Méndez G., Thierens M., Arz H.W., Bosmans J., Hebbeln D., Lambert F.,
 2513 Lembke-Jene L., Stuuut J-B. (2019). Precession modulation of the South Pacific westerly wind belt over the past
 2514 million years. *Proceedings of the National Academy of Sciences*, 116 (47) 23455-23460;
 2515 <https://doi.org/10.1073/pnas.1905847116>.
 2516
- 2517 Lang, N., & Wolff, E. W. (2011). Interglacial and glacial variability from the last 800 ka in marine, ice and terrestrial
 2518 archives. *Climate of the Past*, 7(2), 361-380. <https://doi.org/10.5194/cp-7-361-2011>.
 2519
- 2520 Langebroek, P. M., Paul, A., & Schulz, M. (2009). Antarctic ice-sheet response to atmospheric CO₂ and insolation
 2521 in the Middle Miocene. *Climate of the Past*, 5(4). <https://doi.org/10.5194/cp-5-633-2009>.
 2522
- 2523 Larter, R. D., Rebesco, M., Vanneste, L. E., Gambôa, L. A. P., & Barker, P. F. (1997). Cenozoic Tectonic,
 2524 Sedimentary and Glacial History of the Continental Shelf West Of Graham Land, Antarctic Peninsula. In P. F.
 2525 Barker & A. K. Cooper (Eds.), *Geology and Seismic Stratigraphy of the Antarctic Margin*, 2 (pp. 1–27). American
 2526 Geophysical Union.
 2527
- 2528 Larter, R. D., Anderson, J. B., Graham, A. G., Gohl, K., Hillenbrand, C. D., Jakobsson, M., ... & Witus, A. E. (2014).
 2529 Reconstruction of changes in the Amundsen Sea and Bellingshausen sea sector of the West Antarctic ice sheet
 2530 since the last glacial maximum. *Quaternary Science Reviews*, 100, 55-86.
 2531
- 2532 Larter, R. D., Hogan, K. A., Hillenbrand, C. D., Smith, J. A., Batchelor, C. L., Cartigny, M., ... & Graham, A. G.
 2533 (2019). Subglacial hydrological control on flow of an Antarctic Peninsula palaeo-ice stream. *Cryosphere*, 13(6),
 2534 1583-1596. <https://doi.org/10.5194/tc-13-1583-2019>.
 2535
- 2536 Lear, C. H., T. R. Bailey, P. N. Pearson, H. K. Coxall, and Y. Rosenthal (2008), Cooling and ice growth across the
 2537 Eocene-Oligocene transition, *Geology*, 36(3), 251–254, <https://doi.org/10.1130/g24584a.1>.
 2538
- 2539 Lear, C. H., Coxall, H. K., Foster, G. L., Lunt, D. J., Mawbey, E. M., Rosenthal, Y., ... & Wilson, P. A. (2015).
 2540 Neogene ice volume and ocean temperatures: Insights from infaunal foraminiferal Mg/Ca paleothermometry.
 2541 *Paleoceanography*, 30(11), 1437-1454.
 2542
- 2543 Lee, J. I., McKay, R. M., Golledge, N. R., Yoon, H. I., Yoo, K. C., Kim, H. J., & Hong, J. K. (2017). Widespread
 2544 persistence of expanded East Antarctic glaciers in the southwest Ross Sea during the last deglaciation. *Geology*,
 2545 45(5), 403-406.
 2546
- 2547 Levy R., Harwood D., Florindo F., Sangiorgi F., Tripathi R., von Eynatten H., Gasson E., Kuhn G., Tripathi A., DeConto
 2548 R., Fielding C., Field B., Golledge N., McKay R., Naish T., Olney M., Pollard D., Schouten S., Talarico F., Warny
 2549 S., Willmott V., Acton G., Panter K., Paulsen T., Taviani M., SMS Science Team (2016). Early to mid-Miocene
 2550 Antarctic Ice Sheet dynamics. *Proceedings of the National Academy of Sciences* Mar 2016, 113 (13) 3453-3458;
 2551 <https://doi.org/10.1073/pnas.1516030113>.
- 2552 Levy, R.H., S.R. Meyers, T.R. Naish, N.R. Golledge, R.M. McKay, J.S. Crampton, R.M. DeConto, L. De Santis, F.
 2553 Florindo, E.G.W. Gasson, and others. (2019). Antarctic ice-sheet sensitivity to obliquity forcing enhanced through
 2554 ocean connections. *Nature Geosciences* 12:132–137, <https://doi.org/10.1038/s41561-018-0284-4>.
 2555
- 2555 Lewis, A. R., Marchant, D. R., Ashworth, A. C., Hedenäs, L., Hemming, S. R., Johnson, J. V., ... & Willenbring, J.
 2556 K. (2008). Mid-Miocene cooling and the extinction of tundra in continental Antarctica. *Proceedings of the National
 2557 Academy of Sciences*, 105(31), 10676-10680.
 2558
- 2559 Lewis, A. R., & Ashworth, A. C. (2016). An early to middle Miocene record of ice-sheet and landscape evolution
 2560 from the Friis Hills, Antarctica. *Bulletin*, 128(5-6), 719-738.
- 2561 Liakka, J., Colleoni, F., Ahrens, B., & Hickler, T. (2014). The impact of climate-vegetation interactions on the onset
 2562 of the Antarctic ice sheet. *Geophysical Research Letters*, 41(4), 1269-1276.
 2563 <https://doi.org/10.1002/2013GL058994>.
- 2564 Licht, K. J. (2004). The Ross Sea's contribution to eustatic sea level during meltwater pulse 1A. *Sedimentary
 2565 Geology*, 165(3-4), 343-353.
- 2566 Lindeque, A., Gohl, K., Henrys, S., Wobbe, F., & Davy, B. (2016). Seismic stratigraphy along the Amundsen Sea
 2567 to Ross Sea continental rise: A cross-regional record of pre-glacial to glacial processes of the West Antarctic
 2568 margin. *Palaeogeography, Palaeoclimatology, Palaeoecology*, 443, 183-202.
- 2569 Lisiecki, L. E., & Raymo, M. E. (2005). A Pliocene-Pleistocene stack of 57 globally distributed benthic $\delta^{18}O$ records.
 2570 *Paleoceanography*, 20(1). <https://doi.org/10.1029/2004PA001071>.

- 2571 Livingstone, S.J., O'Cofaigh, C., Stokes, C.R., Hillenbrand, C-D., Vieli, A. & Jamieson, S.S.R. (2013). Glacial
2572 geomorphology of Marguerite Bay Palaeo-Ice stream, western Antarctic Peninsula. *Journal of Maps*. 2013;9:558-
2573 572.
- 2574
2575 Liu, J., Milne, G. A., Kopp, R. E., Clark, P. U., & Shennan, I. (2016). Sea-level constraints on the amplitude and
2576 source distribution of Meltwater Pulse 1A. *Nature Geoscience*, 9(2), 130-134.
- 2577
2578 Liu, Z., Pagani, M., Zinniker, D., DeConto, R., Huber, M., Brinkhuis, H., Shah, S.R., Leckie, R.M., Pearson, A., 2009.
2579 Global cooling during the Eocene–Oligocene climate transition. *Science* 323, 1187–1190
- 2580
2581 Liu, Z., He, Y., Jiang, Y., Wang, H., Liu, W., Bohaty, S. M., & Wilson, P. A. (2018). Transient temperature asymmetry
2582 between hemispheres in the Palaeogene Atlantic Ocean. *Nature Geoscience*, 11(9), 656-660.
<https://doi.org/10.1038/s41561-018-0182-9>.
- 2583
2584 Loutre, M. F., & Berger, A. (2003). Marine Isotope Stage 11 as an analogue for the present interglacial. *Global and
planetary change*, 36(3), 209-217. [https://doi.org/10.1016/S0921-8181\(02\)00186-8](https://doi.org/10.1016/S0921-8181(02)00186-8).
- 2585
2586 Lowry, D. P., Golledge, N. R., Bertler, N. A., Jones, R. S., & McKay, R. (2019). Deglacial grounding-line retreat in
2587 the Ross Embayment, Antarctica, controlled by ocean and atmosphere forcing. *Science advances*, 5(8), eaav8754.
<https://doi.org/10.1126/sciadv.aav8754>.
- 2588
2589 Lunt, D. J., Haywood, A. M., Schmidt, G. A., Salzmann, U., Valdes, P. J., Dowsett, H. J., & Loptson, C. A. (2012).
2590 On the causes of mid-Pliocene warmth and polar amplification. *Earth and Planetary Science Letters*, 321, 128-138.
- 2591
2592 Lunt, D. J., Huber, M., Anagnostou, E., Baatsen, M. L., Caballero, R., DeConto, R., ... & Zeebe, R. E. (2017). The
2593 DeepMIP contribution to PMIP4: Experimental design for model simulations of the EECO, PETM, and pre-PETM
2594 (version 1.0). *Geoscientific Model Development*, 10(2), 889-901.
- 2595
2596 Lüthi, D., Le Floch, M., Bereiter, B., Blunier, T., Barnola, J. M., Siegenthaler, U., ... & Stocker, T. F. (2008). High-
2597 resolution carbon dioxide concentration record 650,000–800,000 years before present. *Nature*, 453(7193), 379-
2598 382.
- 2599
2600 Lythe, M. B., & Vaughan, D. G. (2001). BEDMAP: A new ice thickness and subglacial topographic model of
2601 Antarctica. *Journal of Geophysical Research: Solid Earth*, 106(B6), 11335-11351.
- 2602
2603 McKay, R., Browne, G., Carter, L., Cowan, E., Dunbar G., Krissek, L., Naish, T., Powell, R., Reed, J., Talarico, F.,
2604 Wilch, T. (2009). The stratigraphic signature of the late Cenozoic Antarctic Ice Sheets in the Ross Embayment.
GSA Bulletin, 121 (11-12): 1537–1561. doi: <https://doi.org/10.1130/B26540.1>
- 2605
2606 McKay, R.M., T. Naish, L. Carter, C. Riesselman, R. Dunbar, C. Sjunneskog, D. Winter, F. Sangiorgi, C. Warren,
2607 M. Pagani, and others. (2012a). Antarctic and Southern Ocean influences on Late Pliocene global cooling.
2608 *Proceedings of the National Academy of Sciences of the United States of America* 109(17):6,423–6,428,
<https://doi.org/10.1073/pnas.1112248109>
- 2609
2610 McKay, R.M., T. Naish, R. Powell, P. Barrett, F. Talarico, P. Kyle, D. Monien, G. Kuhn, C. Jackolski, and T. Williams.
2611 2012b. Pleistocene variability of Antarctic Ice Sheet extent in the Ross Embayment. *Quaternary Science Reviews*
34:93–112, <https://doi.org/10.1016/j.quascirev.2011.12.012>.
- 2612
2613 McKay, R., Golledge, N. R., Maas, S., Naish, T., Levy, R., Dunbar, G., & Kuhn, G. (2016). Antarctic marine ice-
sheet retreat in the Ross Sea during the early Holocene. *Geology*, 44(1), 7-10.
- 2614
2615 McKay, R.M., De Santis, L., Kulhanek, D.K., and the Expedition 374 Scientists, (2019). *Ross Sea West Antarctic
2616 Ice Sheet History*. Proceedings of the International Ocean Discovery Program, 374: College Station, TX
(International Ocean Discovery Program). <https://doi.org/10.14379/iodp.proc.374.2019>.
- 2617
2618 Mackintosh, A., Golledge, N., Domack, E., Dunbar, R., Leventer, A., White, D., ... & Gore, D. (2011). Retreat of the
2619 East Antarctic ice sheet during the last glacial termination. *Nature Geoscience*, 4(3), 195-202.
<https://doi.org/10.1038/ngeo1061>.
- 2620
2621 Mackintosh, A. N., Verleyen, E., O'Brien, P. E., White, D. A., Jones, R. S., McKay, R., ... & Miura, H. (2014). Retreat
history of the East Antarctic Ice Sheet since the last glacial maximum. *Quaternary Science Reviews*, 100, 10-30.
- 2622
2623 Marino, G., Rohling, E. J., Rodríguez-Sanz, L., Grant, K. M., Heslop, D., Roberts, A. P., ... & Yu, J. (2015). Bipolar
seesaw control on last interglacial sea level. *Nature*, 522(7555), 197-201. <https://doi.org/10.1038/nature14499>.

- 2624 Maris, M. N. A., De Boer, B., Ligtenberg, S. R. M., Crucifix, M., Van de Berg, W. J., & Oerlemans, J. (2014).
2625 Modelling the evolution of the Antarctic ice sheet since the last interglacial. *The Cryosphere*, 8(4), 1347-1360.
2626
- 2627 Martínez-Boti MA, Foster GL, Chalk TB, Rohling EJ, Sexton PF, et al. 2015. Plio-Pleistocene climate sensitivity
2628 evaluated using high-resolution CO2 records. *Nature* 518: 49-54. <https://doi.org/10.1038/nature14145>.
- 2629 Martín-Español, A., King, M. A., Zammit-Mangion, A., Andrews, S. B., Moore, P., & Bamber, J. L. (2016). An
2630 assessment of forward and inverse GIA solutions for Antarctica. *Journal of Geophysical Research: Solid Earth*,
2631 121(9), 6947-6965.
2632
- 2633 Mas e Braga, M., Bernales, J., Prange, M., Stroeven, A. P., & Rogozhina, I. (2021). Sensitivity of the Antarctic ice
2634 sheets to the peak warming of Marine Isotope Stage 11. *The Cryosphere*, 15, 459–478,
2635 <https://doi.org/10.5194/tc-2020-112>.
2636
- 2637 Masson-Delmotte, V., Buiron, D., Ekaykin, A., Frezzotti, M., Gallée, H., Jouzel, J., Krinner, G., Landais, A.,
2638 Motoyama, H., Oerter, H., Pol, K., Pollard, D., Ritz, C., Schlosser, E., Sime, L. C., Sodemann, H., Stenni, B.,
2639 Uemura, R., and Vimeux, F. (2011). A comparison of the present and last interglacial periods in six Antarctic ice
2640 cores, *Clim. Past*, 7, 397–423, <https://doi.org/10.5194/cp-7-397-2011>.
- 2641 Masson-Delmotte, V., Schulz, M., Abe-Ouchi, A., Beer, J., Ganopolski, A., González Rouco, JF, Jansen, E, Lambeck,
2642 K, Luterbacher, J, Naish, T, Osborn, T, Otto-Bliesner, B, Quinn, T, Ramesh, R, Rojas, M, Shao, X and
2643 Timmermann, A (2013) Information from Paleoclimate Archives. In: Stocker, TF, Qin, D, Plattner, GK, Tignor, M,
2644 Allen, SK, Boschung, J, Nauels, A, Xia, Y, Bex, V and Midgley, PM (eds.) *Climate Change 2013: The Physical
2645 Science Basis. Contribution of Working Group I to the Fifth Assessment Report of the Intergovernmental Panel on
2646 Climate Change*. Cambridge University Press, Cambridge, United Kingdom and New York, NY, USA.
2647
- 2648 Matsuoka, K., Hindmarsh, R. C., Moholdt, G., Bentley, M. J., Pritchard, H. D., Brown, J., ... & Hattermann, T. (2015).
2649 Antarctic ice rises and rumples: Their properties and significance for ice-sheet dynamics and evolution. *Earth-
2650 science reviews*, 150, 724-745.
- 2651 Melles, M., Brigham-Grette, J., Minyuk, P. S., Nowaczyk, N. R., Wennrich, V., DeConto, R. M., ... & Haltia-Hovi, E.
2652 (2012). 2.8 million years of Arctic climate change from Lake El'gygytyn, NE Russia. *science*, 337(6092), 315-320.
2653 <https://doi.org/10.1126/science.1222135>.
- 2654 Mengel, M., & Levermann, A. (2014). Ice plug prevents irreversible discharge from East Antarctica. *Nature Climate
2655 Change*, 4(6), 451-455. <https://doi.org/10.1038/nclimate2226>.
- 2656 Menviel, L., Timmermann, A., Timm, O. E., & Mouchet, A. (2011). Deconstructing the Last Glacial termination: the
2657 role of millennial and orbital-scale forcings. *Quaternary Science Reviews*, 30(9-10), 1155-1172.
- 2658 Milker, Y., Rachmayani, R., Weinkauff, M., Prange, M., Raitzsch, M., Schulz, M., & Kucera, M. (2013). Global and
2659 regional sea surface temperature trends during Marine Isotope Stage 11. *Climate of the Past*, 9(5), 2231-2252.
2660 <https://doi.org/10.5194/cp-9-2231-2013>.
- 2661 Miller, K.G., W.J. Schmelz, J.V. Browning, R.E. Kopp, G.S. Mountain, and J.D. Wright. 2020b. Ancient sea level
2662 as key to the future. *Oceanography* 33(2):32–41, <https://doi.org/10.5670/oceanog.2020.224>.
- 2663 Miller, K. G., Browning, J. V., Schmelz, W. J., Kopp, R. E., Mountain, G. S., & Wright, J. D. (2020a). Cenozoic sea-
2664 level and cryospheric evolution from deep-sea geochemical and continental margin records. *Science advances*,
2665 6(20), eaaz1346. <https://doi.org/10.1126/sciadv.aaz1346>.
- 2666 Miller, K. G., Wright, J. D., Browning, J. V., Kulpeck, A., Kominz, M., Naish, T. R., ... & Sosdian, S. (2012). High
2667 tide of the warm Pliocene: Implications of global sea level for Antarctic deglaciation. *Geology*, 40(5), 407-410.
2668 <https://doi.org/10.1130/G32869.1>.
- 2669 Miller, K. G., Mountain, G. S., Wright, J. D., & Browning, J. V. (2011). A 180-million-year record of sea level and
2670 ice volume variations from continental margin and deep-sea isotopic records. *Oceanography*, 24(2), 40-53.
2671 <https://www.jstor.org/stable/24861267>.
- 2672 Miller, K. G., J. D. Wright, M. E. Katz, B. S. Wade, J. V. Browning, B. S. Cramer, and Y. Rosenthal (2009), Climate
2673 threshold at the Eocene-Oligocene transition: Antarctic ice sheet influence on ocean circulation, *Geol. Soc. Am.
2674 Spec. Pap.*, 452, 169–178, [https://doi.org/10.1130/2009.2452\(11\)](https://doi.org/10.1130/2009.2452(11)).

- 2675 Miller, K. G., Wright, J. D., Katz, M. E., Browning, J. V., Cramer, B. S., Wade, B. S., & Mizintseva, S. F. (2008). A
2676 view of Antarctic ice-sheet evolution from sea-level and deep-sea isotope changes during the Late Cretaceous–
2677 Cenozoic. *Antarctica: a keystone in a changing world*, 55-70.
- 2678 Miller, K. G., Komazin, M. A., Browning, J. V., Wright, J. D., Mountain, G. S., Katz, M. E., ... & Pekar, S. F. (2005).
2679 The Phanerozoic record of global sea-level change. *science*, 310(5752), 1293-1298.
2680 <https://doi.org/10.1126/science.1116412>.
- 2681 Miller, K. G., Wright, J. D., & Fairbanks, R. G. (1991). Unlocking the ice house: Oligocene-Miocene oxygen
2682 isotopes, eustasy, and margin erosion. *Journal of Geophysical Research: Solid Earth*, 96(B4), 6829-6848.
2683 <https://doi.org/10.1029/90JB02015>.
- 2684 Miller, K. G., Fairbanks, R. G., & Mountain, G. S. (1987). Tertiary oxygen isotope synthesis, sea level history, and
2685 continental margin erosion. *Paleoceanography*, 2(1), 1-19. <https://doi.org/10.1029/PA002i001p00001>.
- 2686 Milne, G. A., & Mitrovica, J. X. (2008). Searching for eustasy in deglacial sea-level histories. *Quaternary Science
2687 Reviews*, 27(25-26), 2292-2302.
- 2688 Minzoni, R. T., Majewski, W., Anderson, J. B., Yokoyama, Y., Fernandez, R., & Jakobsson, M. (2017).
2689 Oceanographic influences on the stability of the Cosgrove Ice Shelf, Antarctica. *The Holocene*, 27(11), 1645-1658.
2690
- 2691 Morlighem, M., Rignot, E., Binder, T., Blankenship, D., Drews, R., Eagles, G., Eisen, O., Ferraccioli, F., Forsberg,
2692 R., Fretwell, P., Goel, V., Greenbaum, J. S., Gudmundsson, H., Guo, J., Helm, V., Hofstede, C., Howat, I., Humbert,
2693 A., Jokat, W., ... Young, D. A. (2020). Deep glacial troughs and stabilizing ridges unveiled beneath the margins of
2694 the Antarctic ice sheet. *Nature Geoscience*, 13(2), 132–137. <https://doi.org/10.1038/s41561-019-0510-8>.
2695
- 2696 Naish, T. R., et al. "Orbitally induced oscillations in the East Antarctic ice sheet at the Oligocene/Miocene
2697 boundary." *Nature* 413.6857 (2001): 719-723.
- 2698 Naish, T., R. Powell, R. Levy, G. Wilson, R. Scherer, F. Talarico, L. Krissek, F. Niessen, M. Pompilio, T. Wilson,
2699 and others. (2009a). Obliquity-paced Pliocene West Antarctic Ice Sheet oscillations. *Nature* 458:322–328,
2700 <https://doi.org/10.1038/nature07867>.
- 2701 Naish, T. R., & Wilson, G. S. (2009b). Constraints on the amplitude of Mid-Pliocene (3.6–2.4 Ma) eustatic sea-level
2702 fluctuations from the New Zealand shallow-marine sediment record. *Philosophical Transactions of the Royal
2703 Society A: Mathematical, Physical and Engineering Sciences*, 367(1886), 169-187.
2704 <https://doi.org/10.1098/rsta.2008.0223>.
- 2705 Naish, T., & Zwart, D. (2012). Looking back to the future. *Nature Climate Change*, 2(5), 317-318.
2706
- 2707 Nakada, M., Kimura, R., Okuno, J., Moriwaki, K., Miura, H., & Maemoku, H. (2000). Late Pleistocene and Holocene
2708 melting history of the Antarctic ice sheet derived from sea-level variations. *Marine Geology*, 167(1-2), 85-103.
2709
- 2710 Nichols, K. A., Goehring, B. M., Balco, G., Johnson, J. S., Hein, A. A., & Todd, C. (2019). New Last Glacial
2711 Maximum Ice Thickness constraints for the Weddell Sea sector, Antarctica. *The Cryosphere Discuss.*, <https://doi.org/10.5194/tc-2019-64>.
2712
- 2713 Nitsche, F. O., Gohl, K., Larter, R. D., Hillenbrand, C. D., Kuhn, G., Smith, J. A., ... & Jakobsson, M. (2013). Paleo
2714 ice flow and subglacial meltwater dynamics in Pine Island Bay, West Antarctica. *The Cryosphere*, 7, 249-262.
- 2715 Noble, T. L., Rohling, E. J., Aitken, A. R. A., Bostock, H. C., Chase, Z., Gomez, N., ... & McKay, R. M. (2020). The
2716 sensitivity of the Antarctic Ice Sheet to a changing climate: Past, present and future. *Reviews of Geophysics*,
2717 e2019RG000663.
- 2718 O'Brien, PE and Cooper, AK and Florindo, F and Handwerger, DA and Lavelle, M and Passchier, S and Pospichal,
2719 JJ and Quilty, PG and Richter, C and Theissen, KM and Whitehead, JM, (2004). Prydz channel fan and the history
2720 of extreme ice advances in Prydz Bay, Proceedings of the Ocean Drilling Program, Scientific Results, 188 pp. 1-
2721 32. ISSN 0884-5891.
- 2722 O'Brien, P. E., Goodwin, I., Forsberg, C. F., Cooper, A. K., & Whitehead, J. (2007). Late Neogene ice drainage
2723 changes in Prydz Bay, East Antarctica and the interaction of Antarctic ice sheet evolution and climate.
2724 *Palaeogeography, Palaeoclimatology, Palaeoecology*, 245(3-4), 390-410.
2725 <https://doi.org/10.1016/j.palaeo.2006.09.002>.
2726

- 2727 O'Brien, P., Opdyke, B., Post, A., & Armand, L. (2020). Sabrina Sea Floor Survey (IN2017-V01) Piston Core
2728 Images, Visual Logs and grain size DATA summaries IN2017-V01-A005-PC01.
2729
- 2730 O'Cofaigh, C., Davies, B. J., Livingstone, S. J., Smith, J. A., Johnson, J. S., Hocking, E. P., ... & Domack, E. (2014).
2731 Reconstruction of ice-sheet changes in the Antarctic Peninsula since the Last Glacial Maximum. *Quaternary*
2732 *Science Reviews*, 100, 87-110.
- 2733 Otto-Bliesner, B. L., Jahn, A., Feng, R., Brady, E. C., Hu, A., & Löffverström, M. (2017). Amplified North Atlantic
2734 warming in the late Pliocene by changes in Arctic gateways. *Geophysical Research Letters*, 44(2), 957-964.
2735 <https://doi.org/10.1002/2016GL071805>.
- 2736 Pagani M, Zachos JC, Freeman KH, Tipple B, Bohaty S. 2005. Carbon dioxide concentrations during the
2737 Paleogene. *Science* 309: 600-3. <https://doi.org/10.1126/science.1110063>.
- 2738 Pagani M, Liu Z, LaRiviere J, Ravelo AC. 2010. High Earth-system climate sensitivity determined from Pliocene
2739 carbon dioxide concentrations. *Nature Geoscience* 3: 27-30. <https://doi.org/10.1038/ngeo724>.
- 2740 Pagani M, Huber M, Liu Z, Bohaty S, Henderiks J, et al. 2011. The role of carbon dioxide during the onset of
2741 Antarctic Glaciation. *Science* 334: 1261-4. <https://doi.org/10.1126/science.1203909>.
- 2742 Pälike, H., Norris, R.D., Herrle, J.O., Wilson, P.A., Coxall, H.K., Lear, C.H., Shackleton, N.J., Tripathi, A., Wade,
2743 B.S., 2006. The heartbeat of the Oligocene climate system. *Science* 314, 1894-1897.
- 2744 Paolo, F. S., Fricker, H. A., & Padman, L. (2015). Volume loss from Antarctic ice shelves is accelerating. *Science*,
2745 348(6232), 327-331. <https://doi.org/10.1126/science.aaa0940>.
- 2746 Parrenin, F., Cavitte, M. G., Blankenship, D. D., Chappellaz, J., Fischer, H., Gagliardini, O., ... & Young, D. A.
2747 (2017). Is there 1.5-million-year-old ice near Dome C, Antarctica?. *The Cryosphere*, 11(6), 2427-2437.
- 2748 Passchier, S., Browne, G., Field, B., Fielding, C. R., Krissek, L. A., Panter, K., ... & ANDRILL-SMS Science Team.
2749 (2011). Early and middle Miocene Antarctic glacial history from the sedimentary facies distribution in the AND-2A
2750 drill hole, Ross Sea, Antarctica. *Bulletin*, 123(11-12), 2352-2365. <https://doi.org/10.1130/B30334.1>.
- 2751 Passchier, S. (2011). Linkages between East Antarctic Ice Sheet extent and Southern Ocean temperatures based
2752 on a Pliocene high-resolution record of ice-rafted debris off Prydz Bay, East Antarctica. *Paleoceanography*, 26(4).
2753 <https://doi.org/10.1029/2010PA002061>.
- 2754 Passchier, S., Bohaty, S.M., Jiménez-Espejo, F., Pross, J., Röhl, U., van de Flierdt, T., Escutia, C., Brinkhuis, H.,
2755 2013. Early Eocene – to – middle Miocene cooling and aridification of East Antarctica. *Geochemistry*,
2756 *Geophysics, Geosystems*, 14 (5), 1399-1410, doi:10.1002/ggge.20106.
2757
- 2758 Passchier, S., *Ciarletta, D., *Miriagos, T., Bijl, P., Bohaty, S., 2016. An Antarctic stratigraphic record of step-wise
2759 ice growth through the Eocene-Oligocene Transition. *Geological Society of America Bulletin*, v. 129, no. 3-4, 318-
2760 330, doi: 10.1130/B31482.
2761
- 2762 Passchier, S., Ciarletta, D. J., Miriagos, T. E., Bijl, P. K., & Bohaty, S. M. (2017). An Antarctic stratigraphic record
2763 of stepwise ice growth through the Eocene-Oligocene transition. *Bulletin*, 129(3-4), 318-330.
- 2764 Patterson, M.O., R. McKay, T. Naish, C. Escutia, F.J. Jimenez-Espejo, M.E. Raymo, S.R. Meyers, L. Tauxe, H.
2765 Brinkhuis, A. Klaus, and others. (2014). Orbital forcing of the East Antarctic ice sheet during the Pliocene and Early
2766 Pleistocene. *Nature Geoscience* 7:841–847, <https://doi.org/10.1038/ngeo2273>.
- 2767 Pattyn, F., Ritz, C., Hanna, E., Asay-Davis, X., DeConto, R., Durand, G., ... & Munneke, P. K. (2018). The
2768 Greenland and Antarctic ice sheets under 1.5 C global warming. *Nature Climate Change*, 8(12), 1053-1061.
2769 <https://doi.org/10.1038/s41558-018-0305-8>.
- 2770 Paxman, G. J., Jamieson, S. S., Hochmuth, K., Gohl, K., Bentley, M. J., Leitchenkov, G., & Ferraccioli, F. (2019).
2771 Reconstructions of Antarctic topography since the Eocene–Oligocene boundary. *Palaeogeography*,
2772 *palaeoclimatology, palaeoecology*, 535, 109346. <https://doi.org/10.1016/j.palaeo.2019.109346>.
- 2773 Paxman, G. J. G., Gasson, E. G. W., Jamieson, S. S. R., Bentley, M. J., & Ferraccioli, F. (2020). Long-term increase
2774 in Antarctic Ice Sheet vulnerability driven by bed topography evolution. *Geophysical Research Letters*, 47,
2775 e2020GL090003. <https://doi.org/10.1029/2020GL090003>.

- 2776 Pedro, J. B., Jochum, M., Buizert, C., He, F., Barker, S., & Rasmussen, S. O. (2018). Beyond the bipolar seesaw:
2777 Toward a process understanding of interhemispheric coupling. *Quaternary Science Reviews*, 192, 27-46.
2778 <https://doi.org/10.1016/j.quascirev.2018.05.005>.
- 2779 Peltier, W. R., & Fairbanks, R. G. (2006). Global glacial ice volume and Last Glacial Maximum duration from an
2780 extended Barbados sea level record. *Quaternary Science Reviews*, 25(23-24), 3322-3337.
- 2781 Peltier, W. R. (2004). Global glacial isostasy and the surface of the ice-age Earth: the ICE-5G (VM2) model and
2782 GRACE. *Annu. Rev. Earth Planet. Sci.*, 32, 111-149.
- 2783 Peltier, W. R. (2005). On the hemispheric origins of meltwater pulse 1a. *Quaternary Science Reviews*, 24(14-15),
2784 1655-1671.
- 2785 Peltier, W. R., Argus, D. F., & Drummond, R. (2015). Space geodesy constrains ice age terminal deglaciation: The
2786 global ICE-6G_C (VM5a) model. *Journal of Geophysical Research: Solid Earth*, 120(1), 450-487.
- 2787 Pekar, S. F., N. Christie-Blick, M. A. Kominz, and K. G. Miller (2002), Calibration between eustatic estimates from
2788 backstripping and oxygen isotopic records for the Oligocene, *Geology*, 30(10), 903-906,
2789 <https://doi.org/10.1130/0091-7613>.
- 2790 Pekar, S. F., and N. Christie-Blick (2008), Resolving apparent conflicts between oceanographic and Antarctic
2791 climate records and evidence for a decrease in pCO₂ during the Oligocene through early Miocene (34-16 Ma),
2792 *Palaeogeogr. Palaeoclimatol. Palaeoecol.*, 260(1-2), 41-49, <https://doi.org/10.1016/j.palaeo.2007.08.019>.
- 2793 Petit, J. R., Jouzel, J., Raynaud, D., Barkov, N. I., Barnola, J. M., Basile, I., ... & Delmotte, M. (1999). Climate and
2794 atmospheric history of the past 420,000 years from the Vostok ice core, Antarctica. *Nature*, 399(6735), 429.
2795 <https://doi.org/10.1038/20859>.
- 2796 Petri, M., Colleoni, F., Kirchner, N., Hughes, A. L., Camerlenghi, A., Rebesco, M., ... & Noormets, R. (2018).
2797 Interplay of grounding-line dynamics and sub-shelf melting during retreat of the Bjørnøyrenna Ice Stream. *Scientific*
2798 *reports*, 8(1), 1-9.
- 2800 Philippon, G., Ramstein, G., Charbit, S., Kageyama, M., Ritz, C., & Dumas, C. (2006). Evolution of the Antarctic
2801 ice sheet throughout the last deglaciation: A study with a new coupled climate—north and south hemisphere ice
2802 sheet model. *Earth and Planetary Science Letters*, 248(3-4), 750-758. <https://doi.org/10.1016/j.epsl.2006.06.017>.
- 2803 Pierce, E.L., van de Flierdt, T., Williams, T., Hemming, S.R., Cook, C.P., Passchier, S. (2017), Evidence for a
2804 dynamic East Antarctic ice sheet during the mid-Miocene climate transition. *Earth Planet. Sci. Lett.*, 478, 1-13.
- 2805 Pollard, D., & DeConto, R. M. (2003). Antarctic ice and sediment flux in the Oligocene simulated by a climate-ice
2806 sheet-sediment model. *Palaeogeography, Palaeoclimatology, Palaeoecology*, 198(1-2), 53-67.
2807 [https://doi.org/10.1016/S0031-0182\(03\)00394-8](https://doi.org/10.1016/S0031-0182(03)00394-8).
- 2808 Pollard, D., & DeConto, R. M. (2005). Hysteresis in Cenozoic Antarctic ice-sheet variations. *Global and Planetary*
2809 *Change*, 45(1-3), 9-21. <https://doi.org/10.1016/j.gloplacha.2004.09.011>.
- 2810 Pollard, D., and R.M. DeConto. (2009). Modelling West Antarctic ice sheet growth and collapse through the past
2811 five million years. *Nature* 458(7236):329-332, <https://doi.org/10.1038/nature07809>.
- 2812 Pollard, D., & DeConto, R. M. (2012). Description of a hybrid ice sheet-shelf model, and application to Antarctica.
2813 *Geoscientific Model Development*, 5(5), 1273-1295. <https://doi.org/10.5194/gmd-5-1273-2012>.
- 2814 Pollard, D., DeConto R. M., and Alley R. B. "Potential Antarctic Ice Sheet retreat driven by hydrofracturing and ice
2815 cliff failure." *Earth and Planetary Science Letters* 412 (2015): 112-121. <https://doi.org/10.1016/j.epsl.2014.12.035>.
- 2816 Pollard, D., Gomez, N., & Deconto, R. M. (2017). Variations of the Antarctic ice sheet in a coupled ice sheet-Earth-
2817 sea level model: sensitivity to viscoelastic Earth properties. *Journal of Geophysical Research: Earth Surface*,
2818 122(11), 2124-2138. <https://doi.org/10.1002/2017JF004371>.
- 2819 Pollard, D., & DeConto, R. M. (2020). Continuous simulations over the last 40 million years with a coupled Antarctic
2820 ice sheet-sediment model. *Palaeogeography, Palaeoclimatology, Palaeoecology*, 537, 109374.
2821 <https://doi.org/10.1016/j.palaeo.2019.109374>.
- 2822
2823
2824
2825
2826
2827

- 2828 Pollard, D., Chang, W., Haran, M., Applegate, P., & DeConto, R. (2016). Large ensemble modeling of the last
 2829 deglacial retreat of the West Antarctic Ice Sheet: comparison of simple and advanced statistical techniques.
 2830 <https://doi.org/10.5194/gmd-9-1697-2016>.
 2831
 2832 Peltier, W. R. (2004). Global glacial isostasy and the surface of the ice-age Earth: the ICE-5G (VM2) model and
 2833 GRACE. *Annu. Rev. Earth Planet. Sci.*, 32, 111-149. <https://doi.org/10.1146/annurev.earth.32.082503.144359>.
 2834
 2835 Presti, M., Barbara, L., Denis, D., Schmidt, S., De Santis, L., & Crosta, X. (2011). Sediment delivery and
 2836 depositional patterns off Adélie Land (East Antarctica) in relation to late Quaternary climatic cycles. *Marine*
 2837 *Geology*, 284(1-4), 96-113.
 2838
 2839 Pritchard, H., Ligtenberg, S. R., Fricker, H. A., Vaughan, D. G., van den Broeke, M. R., & Padman, L. (2012).
 2840 Antarctic ice-sheet loss driven by basal melting of ice shelves. *Nature*, 484(7395), 502-505.
 2841 <https://doi.org/10.1038/nature10968>.
 2842
 2843 Pross, J., Contreras, L., Bijl, P. K., Greenwood, D. R., Bohaty, S. M., Schouten, S., ... & Brinkhuis, H. (2012).
 2844 Persistent near-tropical warmth on the Antarctic continent during the early Eocene epoch. *Nature*, 488(7409), 73-
 2845 77.
 2846
 2847 Prothro, L. O., Simkins, L. M., Majewski, W., & Anderson, J. B. (2018). Glacial retreat patterns and processes
 2848 determined from integrated sedimentology and geomorphology records. *Marine Geology*, 395, 104-119.
 2849
 2850 Prothro, L. O., Majewski, W., Yokoyama, Y., Simkins, L. M., Anderson, J. B., Yamane, M., ... & Ohkouchi, N. (2020).
 2851 Timing and pathways of East Antarctic Ice Sheet retreat. *Quaternary Science Reviews*, 230, 106166.
 2852
 2853 Quiquet, A., Dumas, C., Ritz, C., Peyaud, V., & Roche, D. M. (2018). The GRISLI ice sheet model (version 2.0):
 2854 calibration and validation for multi-millennial changes of the Antarctic ice sheet. *Geoscientific Model Development*,
 2855 11(12), 5003. <https://doi.org/10.5194/gmd-11-5003-2018>.
 2856
 2857 Raymo, M. E., Lisiecki, L. E., & Nisancioglu, K. H. (2006). Plio-Pleistocene ice volume, Antarctic climate, and the
 2858 global $\delta^{18}O$ record. *Science*, 313(5786), 492-495. <https://doi.org/10.1126/science.1123296>.
 2859
 2860 Raymo, M. E., Mitrovica, J. X., O'Leary, M. J., DeConto, R. M., & Hearty, P. J. (2011). Departures from eustasy in
 2861 Pliocene sea-level records. *Nature Geoscience*, 4(5), 328-332.
 2862
 2863 Raymo, M. E., & Mitrovica, J. X. (2012). Collapse of polar ice sheets during the stage 11 interglacial. *Nature*,
 2864 483(7390), 453-456. <https://doi.org/10.1038/nature10891>.
 2865
 2866 Rayner, N., D. E. Parker, E. Horton, C. Folland, L. Alexander, D. Rowell, E. Kent, and A. Kaplan (2003), Global
 2867 analyses of sea surface temperature, sea ice, and night marine air temperature since the late nineteenth century,
J. Geophys. Res., 108(D14), 4407, <https://doi.org/10.1029/2002JD002670>.
 2868
 2869 Rebecco, M., Camerlenghi, A., Geletti, R., & Canals, M. (2006). Margin architecture reveals the transition to the
 2870 modern Antarctic ice sheet ca. 3 Ma. *Geology*, 34(4), 301-304. <https://doi.org/10.1130/G22000.1>.
 2871
 2872 Reinardy, B. T. I., Escutia, C., Iwai, M., Jimenez-Espejo, F. J., Cook, C., van de Flierdt, T., & Brinkhuis, H. (2015).
 2873 Repeated advance and retreat of the East Antarctic Ice Sheet on the continental shelf during the early Pliocene
 2874 warm period. *Palaeogeography, Palaeoclimatology, Palaeoecology*, 422, 65-84.
 2875
 2876 Retallack, G. J. (2009). Refining a pedogenic-carbonate CO₂ paleobarometer to quantify a middle Miocene
 2877 greenhouse spike. *Palaeogeography, Palaeoclimatology, Palaeoecology*, 281(1-2), 57-65.
 2878
 2879 Reyes, A. V., Carlson, A. E., Beard, B. L., Hatfield, R. G., Stoner, J. S., Winsor, K., ... & Ullman, D. J. (2014). South
 2880 Greenland ice-sheet collapse during marine isotope stage 11. *Nature*, 510(7506), 525-528.
 2881 <https://doi.org/10.1038/nature13456>.
 2882
 2883 Rignot, E., Mouginit, J., Scheuchl, B., van den Broeke, M., van Wessem, M. J., & Morlighem, M. (2019). Four
 2884 decades of Antarctic Ice Sheet mass balance from 1979–2017. *Proceedings of the National Academy of Sciences*,
 2885 116(4), 1095-1103. <https://doi.org/10.1073/pnas.1812883116>.
 2886
 2887 Rintoul, S. R., Silvano, A., Pena-Molino, B., van Wijk, E., Rosenberg, M., Greenbaum, J. S., & Blankenship, D. D.
 2888 (2016). Ocean heat drives rapid basal melt of the Totten Ice Shelf. *Science Advances*, 2(12), e1601610.
 2889
 2890 Roberts, D. L., Karkanias, P., Jacobs, Z., Marean, C. W., & Roberts, R. G. (2012). Melting ice sheets 400,000 yr
 2891 ago raised sea level by 13 m: Past analogue for future trends. *Earth and Planetary Science Letters*, 357, 226-237.
 2892 <https://doi.org/10.1016/j.epsl.2012.09.006>.

- 2893 Rohling, E. J., Grant, K., Bolshaw, M., Roberts, A. P., Siddall, M., Hemleben, C., & Kucera, M. (2009). Antarctic
2894 temperature and global sea level closely coupled over the past five glacial cycles. *Nature Geoscience*, 2(7), 500-
2895 504. <https://doi.org/10.1038/ngeo557>.
2896
2897 Rohling, E. J., Hibbert, F. D., Grant, K. M., Galaasen, E. V., Iralı, N., Kleiven, H. F., ... & Schulz, H. (2019).
2898 Asynchronous Antarctic and Greenland ice-volume contributions to the last interglacial sea-level highstand. *Nature*
2899 *communications*, 10(1), 1-9. <https://doi.org/10.1038/s41467-019-12874-3>.
2900
2901 Rovere, A., Raymo, M. E., Mitrovica, J. X., Hearty, P. J., O'Leary, M. J., & Inglis, J. D. (2014). The Mid-Pliocene
2902 sea-level conundrum: Glacial isostasy, eustasy and dynamic topography. *Earth and Planetary Science Letters*,
2903 387, 27-33.
2904
2905 Rovere, A., Antonioli, F., & Bianchi, C. N. (2015). Fixed biological indicators. *Handbook of Sea-Level Research*,
2906 268-280.
2907
2908 Roy, K. , and W.Peltier . 2018. Relative Sea Level in the Western Mediterranean Basin: A Regional Test of the
2909 ICE-7G NA (VM7) Model and a Constraint on Late Holocene Antarctic Deglaciation. *Quaternary Science Reviews*
2910 183: 76–87.
2911
2912 Roche, D. M., Paillard, D., Caley, T., & Waelbroeck, C. (2014). LGM hosing approach to Heinrich Event 1: results
2913 and perspectives from data–model integration using water isotopes. *Quaternary Science Reviews*, 106, 247-261.
2914 <https://doi.org/10.1016/j.quascirev.2014.07.020>.
2915
2916 Sadai, S., Condrón, A., DeConto, R., & Pollard, D. (2020). Future climate response to Antarctic Ice Sheet melt
2917 caused by anthropogenic warming. *Science advances*, 6(39), eaaz1169.
2918
2919 Salabarnada, A., Escutia, C., Röhl, U., Nelson, C. H., McKay, R., Jiménez-Espejo, F. J., Bijl, P. K., Hartman, J. D.,
2920 Strother, S. L., Salzmann, U., Evangelinos, D., López-Quirós, A., Flores, J. A., Sangiorgi, F., Ikehara, M., &
2921 Brinkhuis, H. (2018). Paleoceanography and ice sheet variability offshore Wilkes Land, Antarctica—Part 1: Insights
2922 from late Oligocene astronomically paced contourite sedimentation. *Climate of the Past*, 14(7), 991–1014. Scopus.
2923 <https://doi.org/10.5194/cp-14-991-2018>
2924
2925 Sandstrom, M. R., O'Leary, M. J., Barham, M., Cai, Y., Rasbury, E. T., Wootton, K. M., & Raymo, M. E. (2020). Age
2926 constraints on surface deformation recorded by fossil shorelines at Cape Range, Western Australia. *GSA Bulletin*.
2927
2928 Sangiorgi, F., Bijl, P. K., Passchier, S., Salzmann, U., Schouten, S., McKay, R., ... & Levy, R. (2018). Southern
2929 Ocean warming and Wilkes Land ice sheet retreat during the mid-Miocene. *Nature Communications*, 9(1), 1-11.
2930 <https://doi.org/10.1038/s41467-017-02609-7>.
2931
2932 Seki O, Foster GL, Schmidt DN, Mackensen A, Kawamura K, Pancost RD. 2010. Alkenone and boron based Plio-
2933 Pleistocene pCO2 records. *Earth and Planetary Science Letters* 292: 201-11.
2934 <https://doi.org/10.1016/j.epsl.2010.01.037>.
2935
2936 Shackleton, N.J., 2000. The 100,000-year Ice-Age cycle identified and found to lag temperature, carbon dioxide,
2937 and orbital eccentricity. *Science* 289, 1897–1902.
2938
2939 Shakun, J. D., Corbett, L. B., Bierman, P. R., Underwood, K., Rizzo, D. M., Zimmerman, S. R., ... & Hay, C. C.
2940 (2018). Minimal East Antarctic Ice Sheet retreat onto land during the past eight million years. *Nature*, 558(7709),
2941 284-287. <https://doi.org/10.1038/s41586-018-0155-6>.
2942
2943 Shepherd, A., Ivins, E., Rignot, E., Smith, B., Van Den Broeke, M., Velicogna, I., ... & Nowicki, S. (2018). Mass
2944 balance of the Antarctic Ice Sheet from 1992 to 2017. *Nature*, 558, 219-222. <https://doi.org/10.1038/s41586-018-0179-y>.
2945
2946 Scherer, R., Bohaty, S., Harwood, D., Roberts, A., & Taviani, M. (2003, April). Marine Isotope Stage 31 (1.07 Ma):
2947 an extreme interglacial in the Antarctic nearshore zone. In *Geophysical Research Abstracts* (Vol. 5, p. 11710).
2948
2949 Scherer, R. P., Bohaty, S. M., Dunbar, R. B., Esper, O., Flores, J. A., Gersonde, R., ... & Taviani, M. (2008).
2950 Antarctic records of precession-paced insolation-driven warming during early Pleistocene Marine Isotope Stage
2951 31. *Geophysical Research Letters*, 35(3).
2952
2953 Scherer, R. P., DeConto, R. M., Pollard, D., & Alley, R. B. (2016). Windblown Pliocene diatoms and East Antarctic
2954 Ice Sheet retreat. *Nature communications*, 7(1), 1-9. <https://doi.org/10.1038/ncomms12957>.
2955
2956 Shevenell, A. E., Kennett, J. P., & Lea, D. W. (2004). Middle Miocene southern ocean cooling and Antarctic
2957 cryosphere expansion. *Science*, 305(5691), 1766-1770.
2958

- 2959 Shevenell, A. E., Kennett, J. P., & Lea, D. W. (2008). Middle Miocene ice sheet dynamics, deep-sea temperatures,
2960 and carbon cycling: A Southern Ocean perspective. *Geochemistry, Geophysics, Geosystems*, 9(2).
- 2961
- 2962 Shevenell, A. E., Ingalls, A. E., Domack, E. W., & Kelly, C. (2011). Holocene Southern Ocean surface temperature
2963 variability west of the Antarctic Peninsula. *Nature*, 470(7333), 250-254.
- 2964
- 2965 Schmidtko, S., Heywood, K. J., Thompson, A. F., & Aoki, S. (2014). Multidecadal warming of Antarctic waters.
2966 *Science*, 346(6214), 1227-1231.
- 2967
- 2968 Schneider von Deimling, T., Ganopolski, A., Held, H., & Rahmstorf, S. (2006). How cold was the last glacial
2969 maximum?. *Geophysical Research Letters*, 33(14).
- 2970
- 2971 Schüpbach, S., Federer, U., Kaufmann, P., Albani, S., Barbante, C., Stocker, T., & Fischer, H. (2013). High-
2972 resolution mineral dust and sea ice proxy records from the Talos Dome ice core. *Climate of the Past*, 9(6), 2789-
2973 2807. <https://doi.org/10.5194/cp-9-2789-2013>.
- 2974
- 2975 Silvano, A., Rintoul, S. R., Kusahara, K., Peña-Molino, B., van Wijk, E., Gwyther, D. E., & Williams, G. D. (2019).
2976 Seasonality of warm water intrusions onto the continental shelf near the Totten Glacier. *Journal of Geophysical*
2977 *Research: Oceans*, 124(6), 4272-4289.
- 2978
- 2979 Sime, L. C., D. Hodgson, T. J. Bracegirdle, C. Allen, B. Perren, S. Roberts, and A. M. de Boer (2016), Sea ice led
2980 to poleward-shifted winds at the Last Glacial Maximum: The influence of state dependency on CMIP5 and PMIP3
2981 models, *Clim. Past*, 12(12), 2241–2253, doi:10.5194/cp-12-2241-2016.
- 2982
- 2983 Simkins, L. M., Anderson, J. B., Greenwood, S. L., Gonnermann, H. M., Prothro, L. O., Halberstadt, A. R. W., ... &
2984 DeConto, R. M. (2017). Anatomy of a meltwater drainage system beneath the ancestral East Antarctic ice sheet.
2985 *Nature Geoscience*, 10(9), 691-697. <https://doi.org/10.1038/ngeo3012>.
- 2986
- 2987 Simkins, Lauren M., Sarah L. Greenwood, and John B. Anderson. "Diagnosing ice sheet grounding line stability
2988 from landform morphology." *The Cryosphere* 12 (2018): 2707-2726. <https://doi.org/10.5194/tc-12-2707-2018>.
- 2989
- 2990 Simms, A. R., Lisiecki, L., Gebbie, G., Whitehouse, P. L., & Clark, J. F. (2019). Balancing the last glacial maximum
2991 (LGM) sea-level budget. *Quaternary Science Reviews*, 205, 143-153.
- 2992
- 2993 Small, D., Bentley, M. J., Jones, R. S., Pittard, M. L., & Whitehouse, P. L. (2019). Antarctic ice sheet palaeo-thinning
2994 rates from vertical transects of cosmogenic exposure ages. *Quaternary Science Reviews*, 206, 65-80.
- 2995
- 2996 Smith, J. A., Andersen, T. J., Shortt, M., Gaffney, A. M., Truffer, M., Stanton, T. P., ... & Vaughan, D. G. (2017).
2997 Sub-ice-shelf sediments record history of twentieth-century retreat of Pine Island Glacier. *Nature*, 541(7635), 77-
2998 80.
- 2999
- 3000 Smith, J. A., Graham, A. G., Post, A. L., Hillenbrand, C. D., Bart, P. J., & Powell, R. D. (2019). The marine geological
3001 imprint of Antarctic ice shelves. *Nature Communications*, 10(1), 1-16. [https://doi.org/10.1038/s41467-019-13496-](https://doi.org/10.1038/s41467-019-13496-5)
3002 [5](https://doi.org/10.1038/s41467-019-13496-5).
- 3003
- 3004 Smith, B., Fricker, H. A., Gardner, A. S., Medley, B., Nilsson, J., Paolo, F. S., ... & Harbeck, K. (2020). Pervasive
3005 ice sheet mass loss reflects competing ocean and atmosphere processes. *Science*, 368(6496), 1239-1242.
3006 <https://doi.org/10.1126/science.aaz5845>.
- 3007
- 3008 Sosdian, S., and Rosenthal, Y., 2009, Deep-sea temperature and ice volume changes across the Pliocene-
3009 Pleistocene climate transitions: *Science*, v. 325, p. 306–310, <https://doi.org/10.1126/science.1169938>.
- 3010
- 3011 Spector, P., Stone, J., Cowderly, S. G., Hall, B., Conway, H., & Bromley, G. (2017). Rapid early-Holocene
3012 deglaciation in the Ross Sea, Antarctica. *Geophysical Research Letters*, 44(15), 7817-7825.
- 3013
- 3014 Spector, P., Stone, J., Pollard, D., Hillebrand, T., Lewis, C., & Gombiner, J. (2018). West Antarctic sites for
3015 subglacial drilling to test for past ice-sheet collapse. *The Cryosphere*, 12(8), 2741-2757. [https://doi.org/10.5194/tc-](https://doi.org/10.5194/tc-12-2741-2018)
3016 [12-2741-2018](https://doi.org/10.5194/tc-12-2741-2018).
- 3017
- 3018 Stammer, D. (2008). Response of the global ocean to Greenland and Antarctic ice melting. *Journal of Geophysical*
3019 *Research: Oceans*, 113(C6). <https://doi.org/10.1029/2006JC004079>.
- 3020
- 3021 Stap, L. B., de Boer, B., Ziegler, M., Bintanja, R., Lourens, L. J., & van de Wal, R. S. (2016). CO2 over the past 5
3022 million years: Continuous simulation and new $\delta^{11}\text{B}$ -based proxy data. *Earth and Planetary Science Letters*, 439,
3023 1-10. <https://doi.org/10.1016/j.epsl.2016.01.022>.
- 3024

- 3025 Stap, L. B., Van De Wal, R. S., De Boer, B., Bintanja, R., & Lourens, L. J. (2017). The influence of ice sheets on
3026 temperature during the past 38 million years inferred from a one-dimensional ice sheet-climate model. *Climate of*
3027 *the Past*, 13(9), 1243-1257. <https://doi.org/10.5194/cp-13-1243-2017>.
3028
- 3029 Stap, L. B., Sutter, J., Knorr, G., Stürz, M., & Lohmann, G. (2019). Transient variability of the Miocene Antarctic ice
3030 sheet smaller than equilibrium differences. *Geophysical Research Letters*, 46(8), 4288-4298.
3031
- 3032 Stap, L. B., Knorr, G., & Lohmann, G. (2020). Anti-Phased Miocene Ice Volume and CO₂ Changes by Transient
3033 Antarctic Ice Sheet Variability. *Paleoceanography and Paleoclimatology*, 35(11), e2020PA003971.
3034
- 3035 Steinhorsdottir, M., Coxall, H. K., de Boer, A. M., Huber, M., Barbolini, N., Bradshaw, C. D., et al. (2020). The
3036 Miocene: the Future of the Past. *Paleoceanography and Paleoclimatology*, 35, e2020PA004037.
3037 <https://doi.org/10.1029/2020PA004037>
3038
- 3039 Steinhilber, D. Mark, and Peter-n. Webb. "Miocene foraminifera from DSDP site 272, Ross Sea (1987)." *Geology*
3040 11: 578-582.
3041
- 3042 Stenni, B., Buiron, D., Frezzotti, M., Albani, S., Barbante, C., Bard, E., ... & Capron, E. (2011). Expression of the
3043 bipolar see-saw in Antarctic climate records during the last deglaciation. *Nature Geoscience*, 4(1), 46-49.
3044 <https://doi.org/10.1038/ngeo1026>.
- 3045 Stocchi, P., et al. (2013), Relative sea-level rise around East Antarctica during Oligocene glaciation, *Nat. Geosci.*,
3046 6, 380–384, <https://doi.org/10.1038/ngeo1783>.
- 3047 Stocchi, P., Antonioli, F., Montagna, P., Pepe, F., Lo Presti, V., Caruso, A., Corradino, M., Dardanelli, G., Renda,
3048 P., Frank, N., Douville, E., Thil, F., De Boer, B., Ruggieri, R., Sciortino, S., and Pierre, C., (2017). A stalactite record
3049 of four relative sea-level highstands during the Middle Pleistocene Transition. *Quaternary Science Reviews*, 173,
3050 92-100.
3051
- 3052 Stocker, T. F. (1998). The seesaw effect. *Science*, 282(5386), 61-62.
3053
- 3054 Stocker, T. F. & Johnsen, S. J. A minimum thermodynamic model for the bipolar seesaw. *Paleoceanography* 18,
3055 1087 (2003). <https://doi.org/10.1029/2003PA000920>.
3056
- 3057 Stokes, C. R. (2018). Geomorphology under ice streams: Moving from form to process. *Earth Surface Processes*
3058 *and Landforms*, 43(1), 85-123. <https://doi.org/10.1002/esp.4259>.
3059
- 3060 Strugnell, J. M., Pedro, J. B., & Wilson, N. G. (2018). Dating Antarctic ice sheet collapse: Proposing a molecular
3061 genetic approach. *Quaternary Science Reviews*, 179, 153-157. <https://doi.org/10.1016/j.quascirev.2017.11.014>.
3062
- 3063 Struve, T., Pahnke, K., Lamy, F., Wengler, M., Böning, P., & Winckler, G. (2020). A circumpolar dust conveyor in
3064 the glacial Southern Ocean. *Nature communications*, 11(1), 1-11.
3065
- 3066 Sugden, D., & Denton, G. (2004). Cenozoic landscape evolution of the Convoy Range to Mackay Glacier area,
3067 Transantarctic Mountains: onshore to offshore synthesis. *Geological Society of America Bulletin*, 116(7-8), 840-
3068 857.
3069
- 3070 Super, J. R., Thomas, E., Pagani, M., Huber, M., O'Brien, C., & Hull, P. M. (2018). North Atlantic temperature and
3071 pCO₂ coupling in the early-middle Miocene. *Geology*, 46(6), 519-522. <https://doi.org/10.1130/G40228.1>.
3072
- 3073 Sutter, J., Gierz, P., Grosfeld, K., Thoma, M., & Lohmann, G. (2016). Ocean temperature thresholds for last
3074 interglacial West Antarctic Ice Sheet collapse. *Geophysical Research Letters*, 43(6), 2675-2682.
3075 <https://doi.org/10.1002/2016GL067818>.
3076
- 3077 Sutter, J., Fischer, H., Grosfeld, K., Karlsson, N. B., Kleiner, T., Van Liefferinge, B., & Eisen, O. (2019). Modelling
3078 the Antarctic Ice Sheet across the mid-Pleistocene transition—implications for Oldest Ice. *The Cryosphere*, 13(7),
3079 2023-2041. <https://doi.org/10.5194/tc-13-2023-2019>.
3080
- 3081 Tan, N., Ramstein, G., Dumas, C., Contoux, C., Ladant, J. B., Sepulchre, P., ... & De Schepper, S. (2017). Exploring
3082 the MIS M2 glaciation occurring during a warm and high atmospheric CO₂ Pliocene background climate. *Earth and*
3083 *Planetary Science Letters*, 472, 266-276. <https://doi.org/10.1016/j.epsl.2017.04.050>.
3084
- 3085 Tarasov, L., and W. R. Peltier (2002), Greenland glacial history and local geodynamic consequences, *Geophys. J.*
3086 *Int.*, 150, 198–229, doi:10.1046/j.1365-246X.2002.01702.x.
3087
- 3088 Tarasov, L., and W. R. Peltier (2003), Greenland glacial history, borehole constraints, and Eemian extent, *J.*
3089 *Geophys. Res.*, 108, 1–20, doi:10.1029/2001JB001731.

3090
3091 Taviani, M., Reid, D. E., & Anderson, J. B. (1993). Skeletal and isotopic composition and paleoclimatic significance
3092 of Late Pleistocene carbonates, Ross Sea, Antarctica. *Journal of Sedimentary Research*, 63(1), 84-90.
3093 <https://doi.org/10.1306/D4267A96-2B26-11D7-8648000102C1865D>.
3094
3095 Taylor-Silva, B. I., & Riesselman, C. R. (2018). Polar frontal migration in the warm late Pliocene: Diatom evidence
3096 from the Wilkes Land margin, East Antarctica. *Paleoceanography and Paleoclimatology*, 33(1), 76-92.
3097 <https://doi.org/10.1002/2017PA003225>.
3098
3099 Teitler, L., Florindo, F., Warnke, D. A., Filippelli, G. M., Kupp, G., & Taylor, B. (2015). Antarctic Ice Sheet response
3100 to a long warm interval across Marine Isotope Stage 31: A cross-latitudinal study of iceberg-rafted debris. *Earth
3101 and planetary science letters*, 409, 109-119.
3102
3103 Tigchelaar, M., Timmermann, A., Pollard, D., Friedrich, T., & Heinemann, M. (2018). Local insolation changes
3104 enhance Antarctic interglacials: Insights from an 800,000-year ice sheet simulation with transient climate forcing.
3105 *Earth and Planetary Science Letters*, 495, 69-78. <https://doi.org/10.1016/j.epsl.2018.05.004>.
3106
3107 Thiede, J., Jessen, C., Knutz, P., Kuijpers, A., Mikkelsen, N., & Spielhagen, R. F. (2011). Millions of years of
3108 Greenland Ice Sheet history recorded in ocean sediments. *Polarforschung*, 80(3), 141-159.
3109
3110 Tierney, J.E., Zhu, J., King, J., Malevich, S.B., Hakim, G.J., Poulsen, C.J., 2020. Glacial cooling and climate
3111 sensitivity revisited. *Nature* 584, 569-573.

3112
3113 The RAISED Consortium, Bentley, M. J., Cofaigh, C. O., Anderson, J. B., Conway, H., Davies, B., Graham, A. G.,
3114 ... & Mackintosh, A. (2014). A community-based geological reconstruction of Antarctic Ice Sheet deglaciation since
3115 the Last Glacial Maximum. *Quaternary Science Reviews*, 100, 1-9.
3116 <https://doi.org/10.1016/j.quascirev.2014.06.025>.
3117
3118 Tripathi, A., & Darby, D. (2018). Evidence for ephemeral middle Eocene to early Oligocene Greenland glacial ice
3119 and pan-Arctic sea ice. *Nature communications*, 9(1), 1-11.
3120
3121 Tzedakis, P. C., Wolff, E. W., Skinner, L. C., Brovkin, V., Hodell, D. A., McManus, J. F., and Raynaud, D.: Can we
3122 predict the duration of an interglacial?, *Clim. Past*, 8, 1473–1485, <https://doi.org/10.5194/cp-8-1473-2012>, 2012.
3123 <https://doi.org/10.5194/cp-8-1473-2012>.
3124
3125 Turney, C. S., & Jones, R. T. (2010). Does the Agulhas Current amplify global temperatures during super-
3126 interglacials?. *Journal of Quaternary Science*, 25(6), 839-843. <https://doi.org/10.1002/jqs.1423>.
3127
3128 Turney, C. S., Jones, R. T., Phipps, S. J., Thomas, Z., Hogg, A., Kershaw, A. P., Fogwill, C. J., Palmer, J., Bronk
3129 R. C. and Adolphi, F., Muscheler, R., Hughen, K. A., Staff, R. A., Grosvenor, M. and Golledge, N. R. and
3130 Rasmussen, S. O. and Hutchinson, D. K. and Haberle, S. and Lorrey, A. and Boswijk, G. and Cooper, A. (2017).
3131 Rapid global ocean-atmosphere response to Southern Ocean freshening during the last glacial. *Nature
3132 communications*, 8(1), 1-9. <https://doi.org/10.1038/s41467-017-00577-6>.
3133
3134 Turney, C. S., Fogwill, C. J., Golledge, N. R., McKay, N. P., van Sebille, E., Jones, R. T., ... & Ramsey, C. B.
3135 (2020). Early Last Interglacial ocean warming drove substantial ice mass loss from Antarctica. *Proceedings of the
3136 National Academy of Sciences*, 117(8), 3996-4006.
3137
3138 Uemura, R., Motoyama, H., Masson-Delmotte, V. *et al.* (2018). Asynchrony between Antarctic temperature and
3139 CO₂ associated with obliquity over the past 720,000 years. *Nat Commun* 9, 96. <https://doi.org/10.1038/s41467-018-03328-3>.
3140
3141 Uenzelmann-Neben, G. (2006). Depositional patterns at Drift 7, Antarctic Peninsula: Along-slope versus down-
3142 slope sediment transport as indicators for oceanic currents and climatic conditions. *Marine geology*, 233(1-4), 49-
3143 62.
3144
3145 Uenzelmann-Neben, G., Gohl, K., Larer, R., & Schlüter, P. (2007). Differences in ice retreat across Pine Island
3146 Bay, West Antarctica, since the Last Glacial Maximum: Indications from multichannel seismic reflection data. *US
3147 Geological Survey Open-File Report, 2007, srp084* {<http://pubs.usgs.gov/of/2007/1047/srp/srp084/>} {doi:
3148 10.3133/of.
3149
3150 Uenzelmann-Neben, G., & Gohl, K. (2012). Amundsen Sea sediment drifts: archives of modifications in
3151 oceanographic and climatic conditions. *Marine Geology*, 299, 51-62.
3152
3153

- 3154 Uenzelmann-Neben, G., & Gohl, K. (2014). Early glaciation already during the Early Miocene in the Amundsen
3155 Sea, Southern Pacific: indications from the distribution of sedimentary sequences. *Global and Planetary Change*,
3156 120, 92-104.
- 3157
3158 Uenzelmann-Neben, G. (2019). Variations in ice-sheet dynamics along the Amundsen Sea and Bellingshausen
3159 Sea West Antarctic Ice Sheet margin. *Bulletin*, 131(3-4), 479-498.
- 3160
3161 Vautravers, M. J., & Hillenbrand, C. D. (2008). Deposition of planktonic foraminifera on the Pacific margin of the
3162 Antarctic Peninsula (ODP Site 1101) during the last 1 Myr. In *Geophysical Research Abstracts* (Vol. 10).
- 3163
3164 Villa, G., Lupi, C., Cobianchi, M., Florindo, F., & Pekar, S. F. (2008). A Pleistocene warming event at 1 Ma in Prydz
3165 Bay, East Antarctica: evidence from ODP site 1165. *Palaeogeography, Palaeoclimatology, Palaeoecology*, 260(1-
3166 2), 230-244. <https://doi.org/10.1016/j.palaeo.2007.08.017>.
- 3167
3168 Villa, G., Persico, D., Wise, S. W., & Gadaleta, A. (2012). Calcareous nannofossil evidence for Marine Isotope
3169 Stage 31 (1 Ma) in core AND-1B, ANDRILL McMurdo ice shelf project (Antarctica). *Global and Planetary
3170 Change*, 96, 75-86.
- 3171
3172 von der Heydt, A.S., Dijkstra, H. A., van de Wal, R. S., Caballero, R., Crucifix, M., Foster, G. L., ... & Ashwin, P.
3173 (2016). Lessons on climate sensitivity from past climate changes. *Current Climate Change Reports*, 2(4), 148-158.
3174 <https://doi.org/10.1007/s40641-016-0049-3>.
- 3175
3176 Waelbroeck, C., Labeyrie, L., Michel, E., Duplessy, J. C., McManus, J. F., Lambeck, K., ... & Labracherie, M. (2002).
3177 Sea-level and deep water temperature changes derived from benthic foraminifera isotopic records. *Quaternary
3178 Science Reviews*, 21(1-3), 295-305. [https://doi.org/10.1016/S0277-3791\(01\)00101-9](https://doi.org/10.1016/S0277-3791(01)00101-9).
- 3179
3180 WAIS Divide Project Members. (2015). Precise inter-polar phasing of abrupt climate change during the last ice age.
3181 *Nature*, 520(7549), 661-665.
- 3182
3183 Wardlaw B.R., Quinn T.M., 1991, The record of Pliocene sea-level change at Enewetak atoll: *Quaternary Science
3184 Reviews*, v.10, p.247–258, [https://doi.org/10.1016/0277-3791\(91\)90023-N](https://doi.org/10.1016/0277-3791(91)90023-N).
- 3184
3185 Warny, S., Askin, R. A., Hannah, M. J., Mohr, B. A., Raine, J. I., Harwood, D. M., ... & SMS Science Team. (2009).
3186 Palynomorphs from a sediment core reveal a sudden remarkably warm Antarctica during the middle Miocene.
3187 *Geology*, 37(10), 955-958. <https://doi.org/10.1130/G30139A.1>.
- 3187
3188 Warrick, R. A., C. Le Provost, M. F. Meier, J. Oerlemans, and P. L. Woodworth (1996), Changes in sea level, in
3189 *Climate Change 1995: The Science of Climate Change*, edited by J. T. Houghton et al., pp. 361 – 405, Cambridge
3190 Univ. Press, New York.
- 3190
3191 Watanabe, O., Jouzel, J., Johnsen, S., Parrenin, F., Shoji, H., & Yoshida, N. (2003). Homogeneous climate
3192 variability across East Antarctica over the past three glacial cycles. *Nature*, 422(6931), 509-512.
3193 <https://doi.org/10.1038/nature01525>.
- 3194
3195 Weaver, A. J., Saenko, O. A., Clark, P. U., & Mitrovica, J. X. (2003). Meltwater pulse 1A from Antarctica as a trigger
3196 of the Bølling-Allerød warm interval. *Science*, 299(5613), 1709-1713.
- 3197
3198 Weber, M. E., Clark, P. U., Kuhn, G., Timmermann, A., Sprenk, D., Gladstone, R., ... & Friedrich, T. (2014).
3199 Millennial-scale variability in Antarctic ice-sheet discharge during the last deglaciation. *Nature*, 510(7503), 134-138.
3200 <https://doi.org/10.1038/nature13397>.
- 3201
3202 Werner, M., Jouzel, J., Masson-Delmotte, V., & Lohmann, G. (2018). Reconciling glacial Antarctic water stable
3203 isotopes with ice sheet topography and the isotopic paleothermometer. *Nature communications*, 9(1), 1-10.
- 3204
3205 Westerhold, T., Marwan, N., Drury, A.J., Liebrand, D., Agnini, C., Anagnostou, E., Barnett, J. SK, Bohaty, S. M., De
3206 Vleeschouwer, D., Florindo, F. and others (2020). An astronomically dated record of Earth's climate and its
3207 predictability over the last 66 million years. *Science*, 369(6509), 1383–1387.
3208 <http://doi.org/10.1126/science.aba6853>.
- 3209
3210 Whitehead, J. M., & Bohaty, S. M. (2003). Pliocene summer sea surface temperature reconstruction using
3211 silicoflagellates from Southern Ocean ODP Site 1165. *Paleoceanography*, 18(3).
- 3211
3212 Whitehead, J. M., Wotherspoon, S., & Bohaty, S. M. (2005). Minimal Antarctic sea ice during the Pliocene. *Geology*,
3213 33(2), 137-140. <https://doi.org/10.1130/G21013.1>.

- 3213 Whitehead, J. M., Quilty, P. G., McKelvey, B. C., & O'Brien, P. E. (2006). A review of the Cenozoic stratigraphy and
3214 glacial history of the Lambert Graben-Prydz Bay region, East Antarctica. *Antarctic Science*.
3215 <https://doi.org/10.1017/S0954102006000083>.
- 3216 Whitehouse, P. L., Bentley, M. J., Milne, G. A., King, M. A., & Thomas, I. D. (2012a). A new glacial isostatic
3217 adjustment model for Antarctica: calibrated and tested using observations of relative sea-level change and present-
3218 day uplift rates. *Geophysical Journal International*, 190(3), 1464-1482.
- 3219 Whitehouse, P. L., Bentley, M. J., & Le Brocq, A. M. (2012b). A deglacial model for Antarctica: geological
3220 constraints and glaciological modelling as a basis for a new model of Antarctic glacial isostatic adjustment.
3221 *Quaternary Science Reviews*, 32, 1-24. <https://doi.org/10.1016/j.quascirev.2011.11.016>.
- 3222 Whitehouse, P. L., Bentley, M. J., Vieli, A., Jamieson, S. S., Hein, A. S., & Sugden, D. E. (2017). Controls on last
3223 glacial maximum ice extent in the Weddell Sea embayment, Antarctica. *Journal of Geophysical Research: Earth*
3224 *Surface*, 122(1), 371-397. <https://doi.org/10.1002/2016JF004121>.
- 3225 Whitehouse, P. L. (2018). Glacial isostatic adjustment modelling: historical perspectives, recent advances, and
3226 future directions. *Earth surface dynamics*, 6(2), 401-429.
- 3227 Whitehouse, P. L., Gomez, N., King, M. A., & Wiens, D. A. (2019). Solid Earth change and the evolution of the
3228 Antarctic Ice Sheet. *Nature communications*, 10(1), 1-14. <https://doi.org/10.1038/s41467-018-08068-y>.
- 3229 Wilson, D. S., & Luyendyk, B. P. (2009). West Antarctic paleotopography estimated at the Eocene-Oligocene
3230 climate transition. *Geophysical Research Letters*, 36(16).
- 3231 Wilson, D. S., Jamieson, S. S., Barrett, P. J., Leitchenkov, G., Gohl, K., & Larter, R. D. (2012). Antarctic topography
3232 at the Eocene–Oligocene boundary. *Palaeogeography, Palaeoclimatology, Palaeoecology*, 335, 24-34.
3233 <https://doi.org/10.1016/j.palaeo.2011.05.028>.
- 3234 Wilson, D. S., Pollard, D., DeConto, R. M., Jamieson, S. S., & Luyendyk, B. P. (2013). Initiation of the West Antarctic
3235 Ice Sheet and estimates of total Antarctic ice volume in the earliest Oligocene. *Geophysical Research Letters*,
3236 40(16), 4305-4309. <https://doi.org/10.1002/grl.50797>.
- 3237 Wilson, D. J., Bertram, R. A., Needham, E. F., van de Flierdt, T., Welsh, K. J., McKay, R. M., ... & Escutia, C.
3238 (2018). Ice loss from the East Antarctic Ice Sheet during late Pleistocene interglacials. *Nature*, 561(7723), 383-
3239 386. <https://doi.org/10.1038/s41586-018-0501-8>.
- 3240 Winnick, M. J., & Caves, J. K. (2015). Oxygen isotope mass-balance constraints on Pliocene sea level and East
3241 Antarctic Ice Sheet stability. *Geology*, 43(10), 879-882. <https://doi.org/10.1130/G36999.1>.
- 3242 Wise, M. G., Dowdeswell, J. A., Jakobsson, M., & Larter, R. D. (2017). Evidence of marine ice-cliff instability in
3243 Pine Island Bay from iceberg-keel plough marks. *Nature*, 550(7677), 506-510.
3244 [Wise Jr. et al., 1992](#), Wise Jr., S.W., Schlich, R., et al., 1992. Proceedings of ODP, Science Results, Part 2, vol.
3245 120: College Station, TX (Ocean Drilling Program), pp. 451–1155.
3246
- 3247 Wolff, E. W., Fischer, H., Fundel, F., Ruth, U., Twarloh, B., Littot, G. C., ... & Hansson, M. (2006). Southern Ocean
3248 sea-ice extent, productivity and iron flux over the past eight glacial cycles. *Nature*, 440(7083), 491-496.
3249 <https://doi.org/10.1038/nature04614>.
- 3250 Wu, L., Wilson, D.J., Wang, R., Passchier, S., Krijgsman, W., Yu, X., Wen, T., Xiao, W., Liu, Z., 2021. Late
3251 Quaternary dynamics of the Lambert Glacier-Amery Ice Shelf system, East Antarctica. *Quat. Sci. Rev.*, 106738.
- 3252 Yan, Q., Zhang, Z., & Wang, H. (2016). Investigating uncertainty in the simulation of the Antarctic ice sheet during
3253 the mid-Piacenzian. *Journal of Geophysical Research: Atmospheres*, 121(4), 1559-1574.
3254 <https://doi.org/10.1002/2015JD023900>.
- 3255 Yokoyama, Y., Anderson, J. B., Yamane, M., Simkins, L. M., Miyairi, Y., Yamazaki, T., ... & Hasumi, H. (2016).
3256 Widespread collapse of the Ross Ice Shelf during the late Holocene. *Proceedings of the National Academy of*
3257 *Sciences*, 113(9), 2354-2359.
3258
- 3259 Zachos, J. C., Breza, J. R., & Wise, S. W. (1992). Early Oligocene ice-sheet expansion on Antarctica: Stable isotope
3260 and sedimentological evidence from Kerguelen Plateau, southern Indian Ocean. *Geology*, 20(6), 569-573.

- 3261 Zachos, J., M. Pagani, L. Sloan, E. Thomas, and K. Billups. (2001). Trends, rhythms, and aberrations in global
3262 climate 65 Ma to present. *Science* 292(5517):686–693, <https://doi.org/10.1126/science.1059412>.
- 3263 Zachos, J. C., & Kump, L. R. (2005). Carbon cycle feedbacks and the initiation of Antarctic glaciation in the earliest
3264 Oligocene. *Global and Planetary Change*, 47(1), 51-66.
- 3265 Zachos, J. C., Dickens, G. R., & Zeebe, R. E. (2008). An early Cenozoic perspective on greenhouse warming and
3266 carbon-cycle dynamics. *Nature*, 451(7176), 279-283. <https://doi.org/10.1038/nature06588>.
- 3267 Zecchin, M., Catuneanu, O., & Rebesco, M. (2015). High-resolution sequence stratigraphy of clastic shelves IV:
3268 high-latitude settings. *Marine and Petroleum Geology*, 68, 427-437.
3269 <https://doi.org/10.1016/j.marpetgeo.2015.09.004>.
- 3270 Zhang YG, Pagani M, Liu Z, Bohaty SM, DeConto RM. 2013. A 40-million-year history of atmospheric CO2.
3271 *Philosophical Transaction of the Royal Society A* 371: 20130096. <https://doi.org/10.1098/rsta.2013.0096>.
- 3272 Zhang, L., Hay, W. W., Wang, C., & Gu, X. (2019). The evolution of latitudinal temperature gradients from the latest
3273 Cretaceous through the Present. *Earth-Science Reviews*, 189, 147-158.
3274 <https://doi.org/10.1016/j.earscirev.2019.01.025>.